Design and Performance of a VOC Abatement System Using a Solid Oxide Fuel Cell

by

Dhananjai Sudhakar Borwankar

A thesis
presented to the University of Waterloo
in fulfillment of the
thesis requirement for the degree of
Master of Applied Science
in
Chemical Engineering

Waterloo, Ontario, Canada, 2009

AUTHOR'S DECLARATION

I hereby declare that I am the sole author of this thesis. This is a true copy of the thesis, including any required final revisions, as accepted by my examiners.

I understand that my thesis may be made electronically available to the public.

ABSTRACT

There has always been a desire to develop industrial processes that minimize the resources they use, and the wastes they generate. The problem is when new guidelines are forced upon long established processes, such as solvent based coating operations. This means instead of integrating an emission reduction technology into the original design of the process, it is added on after the fact. This significantly increases the costs associated with treating emissions.

In this work the ultimate goal is the design of an "add-on" abatement system to treat emissions from solvent based coating processes with high destruction efficiency, and lower costs than systems in current use. Since emissions from processes that utilize solvent based coatings are primarily comprised of volatile organic compounds (VOCs), the treatment of these compounds will be the focus.

VOCs themselves contain a significant amount of energy. If these compounds could be destroyed by simultaneously extracting the energy they release, operational costs could be substantially reduced. This thesis examines the use of model-based design to develop and optimize a VOC abatement technology that uses a Solid Oxide Fuel Cell (SOFC) for energy recovery. The model was built using existing *HYSYS* unit operation models, and was able to provide a detailed thermodynamic and parametric analysis of this technology.

The model was validated by comparison to published literature results and through the use of several Design of Experiment factorial analyses. The model itself illustrated that this type of system could achieve 95% destruction efficiency with performance that was superior to that of Thermal Oxidation, Biological Oxidation, or Adsorption VOC abatement technologies. This was based upon design criteria that included ten year lifecycle costs and operational flexibility, as well as the constraint of meeting (or exceeding) current regulatory thresholds.

ACKNOWLEDGEMENTS

I would like to thank my supervisors Professor William Anderson, and Professor Michael Fowler for their guidance and support during the production of this thesis. I am very lucky to have two individuals that have cared enough to provide guidance, not only for the thesis, but also for my overall career path.

I also want to thank my brother Paraag, and his family (Evelyne, Madhuri, and Amani), my mother Meera, my Father Sudhakar, and of course Marilyn and Jack for their love, support, and encouragement. There are no words sufficient for all the help these individuals have given me, and I hope they all know I appreciate all the things they have done to help me reach this goal (especially all the free good meals!).

Lastly, and most importantly, I must thank my love, Suzanne. Without her, I would have never had the courage to leave my profession and pursue this degree. I owe it to her for filling me with encouragement and confidence, and telling me over and over again that I can do this. Without her my life would be empty, and although my name is on the degree, to me, it will always belong to both of us.

Thank –you so much.

TABLE OF CONTENTS

LIST OF FIGURES

LIST OF TABLES

Chapter 1: INTRODUCTION

Development and optimization of industrial processes involve designs that balance production with resource use and waste generation. The problem is when new criteria are forced upon a process that has already been developed and in operation. Re-engineering of a developed process will result in a loss of production efficiency and will require a significant cost to be incurred. This is precisely what is happening to solvent based industrial coating operations. Over the last decade or more, governments around the world have been implementing reduction strategies targeted at volatile organic compounds (VOCs), which are the main component of solvent based coatings. These reduction strategies include limiting emission rates, mandatory emission reporting, and providing guidance through published best management practices.

For this reason, industries emitting VOCs are pressured to implement VOC reduction strategies. The ideal (and most effective) pollution treatment solutions normally involve removing the pollution source from the process. This would involve substitution of current VOC based coatings with low or no VOC based coatings. Secondary pollution abatement strategies involve alteration of the process itself to reduce the overall contaminant processed and released. An example of this would involve altering (updating) spray equipment to increase the transfer efficiency of the coating being applied onto the part. Unfortunately, due to very long and costly approval procedures for new processes and materials, these types of solutions tend to be prohibitive to implement, and therefore industries turn towards “end of pipe” or “add on” solutions.

There are many “end of pipe” technologies currently available that can effectively reduce VOC emissions, however, in many cases implementation of these technologies will substantially increase facility costs, downtime, and/or maintenance. The result is that facility management is required to implement a new process into their currently established operations that will drastically increase their operating budgets and complicate overall operations. For example, for a medium sized automotive parts painting facility that runs 60,000 cfm of air through the paint booths with an annual loading of 100 tonnes of VOCs, implementation of an abatement system

consisting of a Regenerative Thermal Oxidizer is calculated to require a capital investment of $1,699,600 and an annual investment of $1,832,800 to operate (costs calculated using the design principles outlined in the EPA Cost Control Air Pollution Handbook) [1].

Clearly these types of monetary investments are considered "non-value added processes" and will deter against the implementation of air pollution abatement systems. Therefore there is a need to develop VOC abatement technologies that have reduced operational costs without sacrificing VOC destruction efficiency.

In order to reduce these operational costs, either the system must become more cost-effective as a whole, or a secondary product of significant value must be generated from the process. By their nature, VOCs contain significant amounts of recoverable chemical energy, and if extracted with sufficient efficiency, operational costs could be offset. Therefore, the following simple design constraints could be established:

- VOC destruction with high efficiency to innocuous basic compounds that meet regulatory thresholds; and,
- Energy recovery with high overall efficiency.

To meet this energy recovery goal, there are two types of technology that could be employed: the Stirling Engine and a Fuel Cell (in particular the Solid Oxide Fuel Cell or SOFC). Both of these systems would generate high value electrical energy. The Stirling Engine is a well matured technology with relatively low capital investiture and predictable performance. The idealized system is limited by the well known Carnot efficiency and therefore is limited by temperature differences in the hot and cold reservoirs of the engine, and the requirement of having a combustible concentration of VOCs. Efficiency will then be limited to temperature differences that can realistically be maintained throughout the operation.

On the other hand, a fuel cell will recover energy through electrochemical reactions at constant temperature. These conditions mean the system is extracting the energy of reaction directly from the oxidation-reduction reactions and is not relying on physical changes in the system to provide the work. Therefore the fuel cell does not meet the definition of a heat engine, and will not be

limited by the Carnot efficiency. This also means that under similar operating conditions, the fuel cell will achieve higher electrical generating efficiency then the Stirling engine.

Furthermore, the conversion of hydrocarbon based fuels to energy using a fuel cell is a much cleaner method then by any combustion process. This is because the combustion reactions will produce nitrogen oxides, carbon monoxide and particulate matter if the oxygen concentration in the reaction is not at perfect stoichiometry. Since they operate a lower temperatures, and the anode and cathode streams are separated, electrochemical reactions do not produce these by-products, and therefore emit a cleaner final exhaust stream. As such, this work is focused on the use of fuel cell systems.

Although conceptually the idea of using a fuel cell for this application is valid, significant engineering considerations must be met to make the system function in a real world environment. Typical VOC emission streams from industrial solvent based coating operations have the characteristic of a high volume of air with a low concentration of contaminant (VOC). Dilution of the feed stream entering the fuel cell will cause significant in-efficiencies, and therefore for realistic operation the VOC stream will have to be pre-concentrated prior to being sent to the fuel cell. Furthermore, fuel cells cannot use hydrocarbon based fuels directly. These fuels must be at least partially converted to hydrogen (and/or carbon monoxide for high temperature fuel cells) before they can be utilized. This means after the pre-concentrator, the VOCs must be sent through a reforming operation to convert the VOCs into a usable fuel derivative.

The last consideration is the type of fuel cell that must be used. Low to moderate temperature (80^0C to 220^0C) fuel cells require specific noble metal catalysts to ensure the reaction rate is sufficient for practical application. These catalysts tend to be expensive to purchase and prone to carbon monoxide poisoning. For high temperature fuel cells (650^0C to 1100^0C), the catalyst requirements are relaxed because the elevated operating temperatures ensure a sufficient reaction rate [2]. The catalysts in high temperature cells are more robust, and instead of being poisoned by carbon monoxide, can actually use them as a fuel source, as high temperature operations allow

for internal reforming. For this reason, the choice of fuel cell in this project was the Solid Oxide Fuel Cell (SOFC).

Overall this means the system will need to consist of a VOC concentrator unit, followed by a reforming unit, and finally the SOFC. A schematic overview of the system flow is seen below in Figure 1.

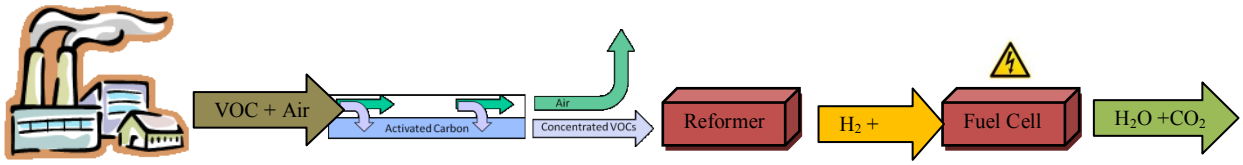

Figure 1: Schematic representation of the SOFC-VOC hybrid VOC abatement system.

1.1 Research Contributions

Currently, Ford has a program in place for the development of this technology. They have studied the use of various fuel cells (SOFC and MCFC), as well as the Stirling engine to perform the simultaneous VOC destruction and energy recovery. Although their system shows promise, no data is publicly available for review.

In this work, a new hybrid VOC abatement system with the dual purpose of destroying VOCs and generating energy for useful work or distribution was modelled; with the model being used to evaluate the system. During this model based design process the following has been done:

- Development of a VOC abatement technology rating tool to be used to compare and contrast the effectiveness of various VOC abatement technologies against one another;
- Lifecycle analysis performed on three mainstream VOC abatement systems (Regenerative Thermal Oxidizer, Carbon Adsorption System, and Biofilter) for a medium sized automotive part painting facility;
- A *HYSYS* steady-state model was created of a hybrid SOFC-VOC abatement system to complete a detailed thermodynamic and parametric analysis of the process, and to develop sizing and lifecycle cost parameters; and,

- Overall feasibility determined for the hybrid SOFC-VOC abatement system in comparison to current mainstream technologies using the technology assessment tool and lifecycle cost analysis.

1.2 Thesis Structure

This thesis is divided into six main sections. Chapter 2 provides a review of the issues associated with the release of VOC compounds into the atmosphere, beginning with associated health effects on human and plant life. Moreover, this chapter reviews legislation and guidelines that have been established in various countries around the world regarding the emission of VOCs from industrial coating operations. Next it provides an explanation of the mainstream technologies being currently utilized in add-on situations for industrial coating operations. Lastly, it describes fuel cell operations (specifically the Solid Oxide Fuel Cell).

Chapter 3 documents a Technology Assessment Tool that was developed to allow for the objective comparison of VOC abatement technologies against one another. The chapter also outlines a case study in which the Technology Assessment Tool can be used to provide an objective comparison of current VOC abatement technologies to the SOFC hybrid abatement system.

Chapter 4 outlines the model based design process used to develop the SOFC hybrid abatement system, and examines the considerations involved in creating this design.

Chapter 5 validates the model through comparison to published literature values, and by use of several Design of Experiment' Factorial Analysis. This chapter also uses the results of the factorial analyses to assist with the optimization of the model. Lastly, this model utilizes the techniques outlined in Chapter 3 to develop a lifecycle analysis of the SOFC abatement system, and to develop objective comparison criteria.

Chapter 6 summarizes the results of this work, and provides a direction for the next stage of research for this promising technology.

Chapter 2: BACKGROUND AND LITERATURE REVIEW

To justify the need to develop an abatement system that can simultaneously destroy volatile organic compounds and extract the energy contained within these compounds requires a fundamental understanding in following:

- Health effects of volatile organic compounds in the atmosphere, and their contribution to the impairment of local air quality;
- The political strategies being used by governments to regulate industrial emissions;
- The current status of VOC abatement systems, their operational principles, their overall efficiency; and,
- The general operation of fuel cells.

2.1 Volatile Organic Compound Structure and Health Effects

VOCs are compounds primarily composed of hydrogen and carbon that are found in products such as solvents, paints, inks, petroleum, oils, and fuels [3]. At ambient conditions these compounds are found in the liquid phase, but they have a characteristically high vapour pressure causing a significant percentage to be lost to vaporization [3]. For this reason, human activities are seen to be the major source of VOCs in the local atmosphere of urban centers.

This class of compounds is quite extensive, and as a result, their importance as ambient air pollutants has only recently been recognized [3]. For compounds specific to industrial coating operations (e.g. alkenes, ketones, acetates), the environmental issues are more readily quantified. There are two reasons for this:

- The main degradation pathway for these specific VOCs is through photochemical oxidation to ozone in presence of nitrogen oxides; and,
- The measurement of ground level ozone concentrations has come to the forefront of public concern [3].

At ground level, ozone is a substance that can cause significant harm to both plant and animal life. In humans, ozone has been proven to impair the function of the upper respiratory tract [3, 4]. In urban centers, this translates into detrimentally affecting the local populace while

simultaneously placing increased strain on healthcare systems. In plants, ozone has been seen to inhibit photosynthetic activity and weaken the overall health of plants [4, 5]. In rural environments, elevated ozone concentrations will have the ability to lower crop yields and negatively impact natural ecosystems [4, 5].

VOCs can also directly impact human health, as some compounds effect human senses through odour, some exert a narcotic effect when inhaled, and others may be toxic [3]. In particular, for industrial coating operations, it is the odour threshold which will cause the most problem. This is because odour is a difficult concern to objectively quantify. For a typical industrial coating plant using solvent based coatings in close proximity to residential or commercial sites, odour detection of the solvents can have major repercussions in regards to business operations. For example, if in Ontario Canada, if a resident were to detect a solvent odour, and complain about this odour to the local Ministry of Environment Office (MOE), the MOE would launch an investigation. If the investigation found that an industrial coating operation using solvent based coatings was in close proximity to the resident, the onus would be on the facility to prove the odour was not coming from their facility. Furthermore, if the facility was positively identified as the source of emission, the facility would likely have to implement an odour reduction strategy (regardless if their emissions were proven to be below the regulated emission thresholds for those particular VOCs). This would typically involve some sort of VOC abatement.

2.2 Regulatory Overview

In this section, the current status of regulatory/non-regulatory VOC emission control programs is explored. The scope of this section is to include legislation put in place in Canada and the United States with a focus relating to solvent based coating operations.

2.2.1 Canada

In Canada, VOC emission rates and limits are controlled at the provincial and federal levels. Federally, Environment Canada (EC) published proposed concentration limits for several sectors utilizing VOCs in significant amounts. The aim is to curb the overall use of VOCs. The sectors of concern were subdivided as follows:

- Architectural Coatings; and,
- Automotive Refinishing Products,

EC estimates that through the implementation of these VOC reduction guidelines, annual VOC emissions from automotive refinishing operations would reduce by 40% (reductions from the alterations in the architectural products have not been quantified). Table 1 below outlines Canadian regulatory and non-regulatory requirements.

Table 1: Regulatory and non-regulatory guidance applicable to Canadian jurisdictions.

Governing Body	Document Title	Implication
Canada (CCME)	PN 1318 - Recommended CCME Standards and Guidelines for the Reduction of VOC Emissions From Canadian Automotive Parts Coatings Operations	Guidance document recommending minimum VOC emission standards for Automotive Coating Operations.
Canada Federal (Environment Canada)	Proposed limits for the amount of VOCs allowed in various types of coatings (April 2008) http://www.ec.gc.ca/nopp/voc/EN/bkg.cfm[6] NPRI – mandatory annual reporting	NPRI - annual reporting of VOCs mandatory for industries meeting certain threshold size requirements. Information is made publicly available.
Canadian Provincially: Alberta	Ambient Air Quality Objectives and Guidelines	Sets out guidelines for various contaminants that all industrial facilities must remain below. Includes various VOCs.
Provincially: New Brunswick	Clean Air Act	Under this Act, facilities meeting certain size restrictions must apply for an approval to emit a contaminant. VOCs are included. Class 1 approvals require public consultation.
Provincially: Ontario	Ontario EPA, O. Reg. 419, O. Reg. 127	OEPA – Requires facilities to obtain approval prior to operating systems that will emit a contaminant (includes VOCs) O. Reg. 419 - Sets out threshold limits for individual compounds (includes VOCs) O. Reg. 127 – Mandatory annual reporting criteria
Provincially: Quebec	Environmental Quality Act Air Quality Regulation, Division V, Emission of Organic Compounds R.Q. c.Q-2,r.20 Articles 12, 13 and 15	Article 12 – outlines general emission rates allowable for substances baked or heated Article 13 – outlines incineration limits if the general limits cannot be met Article 15 – outlines specific emission rates to various types of coatings

Provincially, there are only four provinces that have specifically implemented guidance and/or regulatory requirements with regards to VOC emissions. Alberta, New Brunswick, and Ontario all have implemented mandatory emission limits that all industrial facilities must abide by. New Brunswick and Ontario in particular have permitting requirements that facilities must meet prior to beginning or altering a process. Quebec outlines the actual emission rate of processes specific to the operation taking place.

2.2.2 United States

In the United States, the Federal government instituted 40CFR63, to limit the emission of contaminants from various sectors. Each subpart of the regulation pertains to a specific sector. An example is Subpart PPPP which pertains to Surface Coating of Plastic Parts and Products. The plan limits the amount of VOC emission limits based upon what substrate the coating is being applied to. The rule applies to major sources that use more than 100 gallons of coating per year that contain HAPs, or greater than 10 tons of any individual HAP, or greater than 25 tons of total HAPs.

Furthermore, individual states, and groups of states have implemented their own regulations that go beyond those limitations imposed by the United States Federal Government. These include Illinois, Indiana, Michigan, New York, and California. Tables 2 and 3 outline the rules in place governing the emission of VOCs throughout the United States.

Table 2: Summary of the regulated requirements put in place by the Environmental Protection Agency (Federal) of the United States.

Governing Body	Document Title	Implication
United States Federal Government	40CFR63, National Emission Standards for Hazardous Air Pollutants (NESHAP) outlines limits for various sectors and various compounds. Subpart IIII – Auto and light duty truck surface coating Subpart T – Degreasing Organic Cleaners Subpart NNNN – Large Appliance Subpart EE – Magnetic Tape Surface Coating Subpart KKKK – Metal Can Surface Coating Subpart SSSS – Metal Coil Surface Coating Subpart RRRR – Metal Furniture Surface Coating Subpart HHHHH – Misc. Coating Mfg. Subpart FFFF – Misc. Organic Chemical Production and Process Subpart HHHHHH – Paint Stripping and Misc. Surface Coating Operations Subpart PPPP – Plastic Parts Surface Coating Subpart KK – Printing and Publishing Surface Coating Subpart QQQQ – Wood Building Products Surface Coating Subpart JJ – Wood Furniture Surface Coating	Each subpart is specific to the operation or sector involved. Example, Subpart PPPP sets out limits for the Plastic Parts Surface Coating Sector. In the guideline, the following limitations are placed: **Affects:** Facilities that are considered a major source, located at a major source, or part of a major source of a HAP, and uses ≥ 100 gallons of coatings annually. **Compliance Dates:** Initial start-up on or before Dec-04-2002, then considered existing source and must comply by April 19, 2007 Initial start-up after Dec-04-2002, then you are a new source and you must comply by April 19, 2004, or your initial start-up date. **Compliance Requirements:** General Coating Use 0.16kg HAP/kg of coating solid Auto Lamp Coating 0.26 or 0.45 kg HAP/kg of coating solid TPO 0.22 or 0.26 kg HAP/kg of coating solid New Assembled On-Road Vehicle 1.34 kg HAP/kg of coating solid http://www.epa.gov/ttn/atw/mactfnlalph.html[7]
	PSD/NSR http://www.epa.gov/nsr/[8]	Pre-construction permitting agreements for emissions. Also applies when modifying facilities or processes.

Table 3: Summary of the regulated requirements put in place by the individual States of the United States.

Governing Body	Document Title	Implication
California (LA area)	Rule 1122 – Solvent Degreasers Rule 1125 – Metal Container, Closure and Coil Coating Operations Rule 1132- Further Control of VOC Emissions from High-Emitting Spray Booth Facilities Rule 1141 – Control of VOC Emissions from Resin Coating Operations Rule 1145- Plastic, Rubber, Leather and Glass Coatings Rule 1171 – Solvent Cleaning Operations http://www.aqmd.gov/rules/index.html[9]	New and existing sources
California (San Francisco Area)	Regulation 8 outlines all volatile organic compounds rules http://www.baaqmd.gov/dst/regulations/index.htm[10]	New and existing sources
Illinois	Title 35: Environmental Protection – Parts 218 - 220Organic Material Emission Standards And Limitations	New and existing sources www.ipcb.state.il.us/SLR/IPCBandIEPAEnvironmentalRegulations-Title35.asp[11]
Indiana	Article 8, 326 IAC Volatile Organic Compound Rules http://www.in.gov/legislative/iac/T03260/A00080.PDF	New facilities as of January 1980
Michigan	Rule 336.1601 to Rule 336.1661 outline emission rules for existing sources of VOCs Rule 336.1707 to Rule 336.1710 outline emission rules for new sources of VOCs	Outlines emission limits and permit requirements. http://www.deq.state.mi.us/apcrats/toc_collapsible_2.shtml[12]
Minnesota	None beyond NESHAP	http://www.pca.state.mn.us/air/air_mnrules.html[13, 14]
New York	New York State Environmental Conservation Rules and Regulations (6NYCRR) Part 228 Surface Coating Processes http://www.dec.ny.gov/regs/4214.html[15]	Applies to all new permits issued after July 23, 2003 to: - all facilities in New York City Metropolitan Area - facilities emitting more than 25 tons/year VOCs Lower Orange County Metropolitan Area -facilities emitting more than 50 tons/year VOCs in other areas of the state
Ohio	None beyond NESHAP http://www.epa.state.oh.us/dapc/regs/3745-21/21_09.pdf[16]	
Pennsylvania	None beyond NESHAP http://www.pacode.com/secure/data/025/chapter129/chap129toc.html[13]	Outlines emission limits of weight of VOC per volume of coating for various types of coatings
Wisconsin	Chapter NR 419 Storage and NR 422.083 Plastic Parts Coating http://dnr.wi.gov/air/rules/NR400toc.htm[17]	New and existing sources

2.3 Mainstream VOC Abatement Systems

VOC abatement systems are divided into two main categories; destruction, and recovery [18]. Destruction technologies involve oxidation of the VOC substances to their most basic form; namely, carbon dioxide, and water (for hydrocarbons containing chlorine or sulphur, the exhaust will also include HCl and SO_2) [19]. Recovery technologies, simply remove the contaminant from the exhaust stream for recovery or further treatment. Figure 2 below outlines this division, and includes subcategories for each type of system.

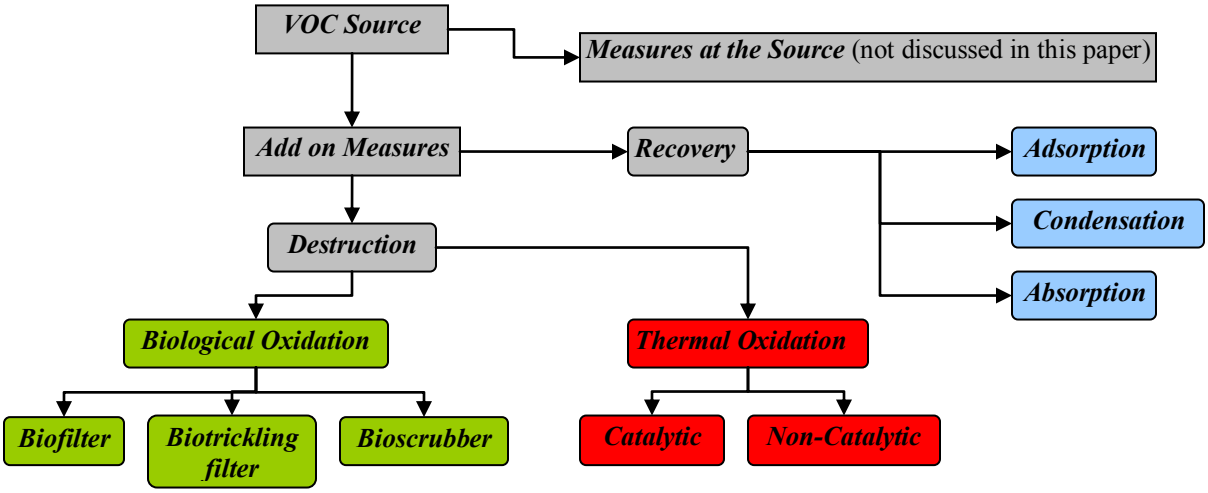

Figure 2: Categorization of VOC abatement technology systems.

2.3.1 Destructive Technologies

Destructive technologies use oxidative processes to break down complex VOC compounds to their most basic constituents. These technologies can be further sub-divided into thermal oxidation and biological oxidation.

2.3.1.1 Thermal Oxidation

Thermal oxidation (incineration) is the process of raising and maintaining the temperature of a combustible substance above its auto-ignition temperature in the presence of oxygen to complete its conversion to carbon dioxide and water [19, 20]. The process is quite effective, and virtually any gaseous organic stream may be safely incinerated given the proper design, engineering, and maintenance conditions [1].

Design parameters are a function of the feed stream composition, and consist of residence time, combustion chamber temperature, and turbulence [20, 21]. Knowledge of these parameters will provide enough information to develop a system lifecycle cost. To minimize capital and operational costs, it is always recommended that the designer attempt to lower the total volume of air that is being sent to the thermal oxidizer [21]. This could mean either concentrating the emission before it enters the thermal oxidizer, or incorporating some sort of air re-circulation system in the process to minimize clean air sent to the system[21]. There are practical upper limits to the level of concentration that can be achieved, as most municipal/regional fire prevention governing bodies and insurance companies limit the concentration of emission going through thermal oxidizers to below 25% of the lower explosive limit (LEL) [20-22]. This is a preventative measure used to minimize the risk of fires or explosions within the system, and can be considered part of the design constraint to meet current legislative requirements.

Another aspect of the design is the recovery of heat. Since these systems are operating between temperatures of 650^0C to $1{,}100^0$C it is standard practice to design the system to retain as much heat as possible [20, 21]. One method involves using heat exchangers to transfer heat from the exhaust side of the oxidizer to the feed stream. When this type of heat recovery is used the thermal oxidizer is called a Recuperative Thermal Oxidizer [21]. The second method of recovering heat involves the use of multiple beds packed with a ceramic type insulating material. Prior to entering the combustion chamber the feed stream is preheated as it is sent through one or more of these heated ceramic beds [21]. When the reaction is complete, the hot exhaust stream coming from the combustion chamber is sent through one of the cold ceramic beds exchanging heat with this bed to prepare it for the next volume of feed [20]. The bed packing normally has a very high rate of heat recovery, and can last between 5 to 10 years [19]. These systems are called Regenerative Thermal Oxidizers. Both the recuperative and regenerative thermal oxidizers can be referred to as RTO's. Figure 3 and 4 below illustrates both styles of RTO.

Cycle 1: 1.) Emission enters Bed 1, exchanges heat with it, causing Bed 1 to cool down and the emission stream to be preheated prior to combustion 2.) After combustion, the product exchanges heat with Bed 2, causing Bed 2 to heat up, and the emission stream to cool down.	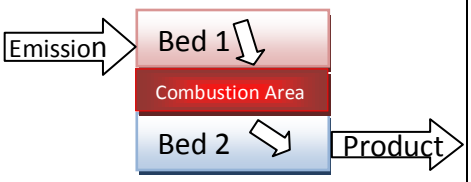
Cycle 2: 1.) Bed 1 is now the cool bed, and Bed 2 is now the hot bed. 2.) The emission now enters Bed 2, and exits from Bed 1. This preheats the emission stream prior to combustion, heats Bed 1, and cools Bed 2. It is now ready for the next cycle.	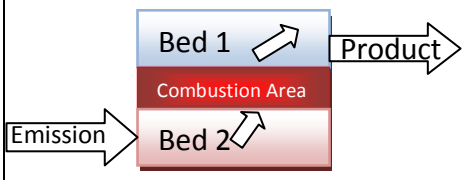

Figure 3: Illustration of the Regenerative type thermal oxidizer operating/heat exchange cycle.

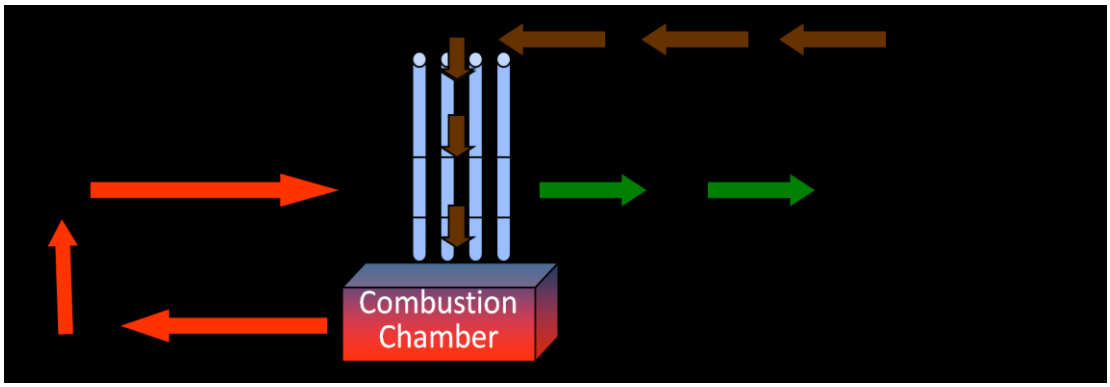

Figure 4: Recuperative type thermal oxidizer heat exchange cycle.

Catalytic thermal oxidation is essentially the same as thermal oxidation, except catalysts are used to modify the chemical kinetics of the reaction such that combustion can occur at a lower temperature. Limitations exist on which types of exhaust streams this process can be used, as certain combustion by-products from certain contaminants may poison the catalyst (e.g. when corrosive by-products are produced like HCl) [21].

Overall, thermal oxidation is an attractive VOC abatement option because it can be used for complex mixtures of compounds, and it can provide very high levels of control (destruction

efficiency range of 95% – 99.9%) [19, 21]. On the downside, once these systems are designed, they are set for a specific residence time which is very difficult to change[20]. Furthermore, thermal oxidizers are not well-suited to exhaust streams with highly variable flow rates, because the reduced residence time and poor mixing resulting from high flow rates decrease the completeness of combustion, which causes the combustion chamber temperature to fall and the destruction efficiency to drop[20]. For a typical hydrocarbon emission stream, a characteristic residence time would range between 0.5 sec to 2 sec, with temperatures between 650 ^{0}C to 1,100 ^{0}C (1,200 F - 2,000 F)[19, 21].

Often the VOC stream may not provide the appropriate concentration of VOCs to support combustion, and then there is the additional cost of adding fuel (e.g. natural gas) to the stream. Lastly, despite having substantially efficient heat recovery systems, auxiliary fuel costs, and electrical consumption arising from circulating air through the system add significantly to the operational costs.

2.3.1.2 Biological Oxidation

Biological oxidation processes work by making use of microbial populations that are able to utilize volatile organic compounds as the primary source for both their catabolic (respiration) and anabolic (growth) requirements [23]. The basic concept is to immobilize micro organisms (bacteria and fungi) in a packed porous bed or media through which nutrients and pollutants may flow [18, 24, 24]. Nutrients, nitrogen, and phosphorus, are supplied to the culture through a mixed solution, while the pollutants are allowed to flow through the media. The immobilized microbial population will utilize the pollutants as their primary carbon source for growth and metabolism, oxidizing the VOC components to their most basic form of carbon dioxide, water, salts and biomass [24].

The outcome is a relatively safe process that results in degradation of VOC compounds to carbon dioxide, water, nitrogen oxides, and salts. The main criteria to ensure successful operation lies in controlling the microbial population health and growth rates.
This can be done by ensuring the following are met:

1. Carbon, oxygen, water, and nutrient sources are provided to cells to meet their catabolic and anabolic requirements,
2. Carbon, oxygen and nutrient sources provided to the cells are able to reach the cells; and,
3. Biomass and wastes produced as a result of oxidation; do not accumulate in or around the microbial population [23].

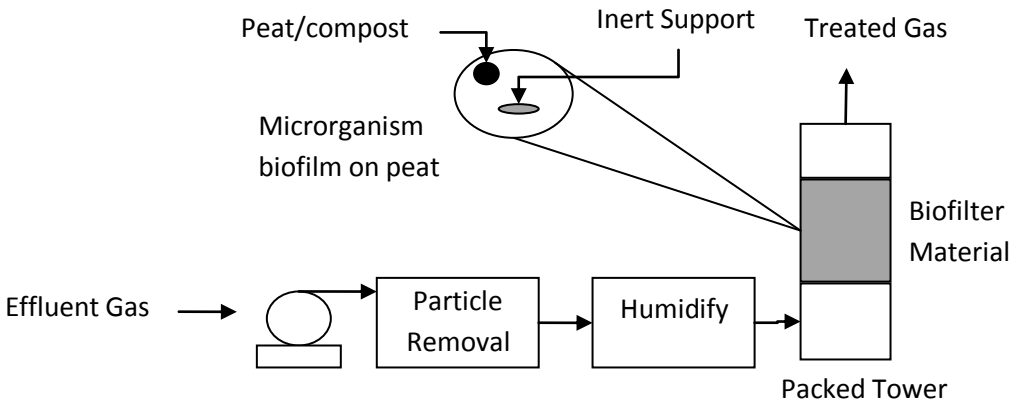

Figure 5: Illustrative depiction of a typical biofilter operation [18].

These three requirements can be met by understanding the contaminant type (and concentration), the substrate used to support cell growth, the physiochemical parameters of the system, and nutrient and moisture requirements of the bed [23].

The biodegradability of a pollutant type is dependent on the VOC transfer rate to the biofilm, and the VOC biodegradation rate of the microbial population [23]. The VOC transfer rate depends upon three basic processes: transport of the VOC and oxygen from the gas phase to the liquid phase, transport of the VOC, oxygen and nutrients from the liquid phase to the surface of the biofilm, and simultaneous diffusion and biotransformation of VOC, oxygen and nutrients within the biofilm [25]. Delhomnie and Heitz summarized the average time requirements for the completion of these main mechanisms within biofilters. Figure 6 below is a representation of this figure.

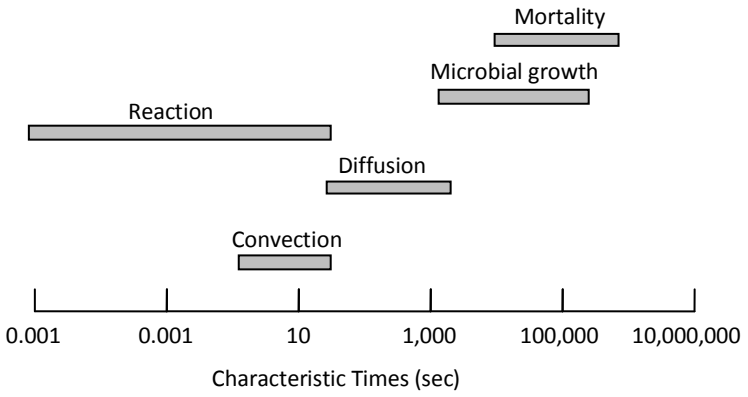

Figure 6: Average time taken for the main mechanisms in the biofilter [23].

Figure 6, illustrates that in comparison to the reaction within the cell, diffusion and convection can be on the order of 1000 times slower than the cellular reaction rate. This indicates that mass transport (diffusion & convection) activities in and around the microbial population could be the limiting factor for the overall biodegradation. For VOCs in particular, this occurs because industrial paint exhausts are composed of solvents with poor water solubility. This solubility relates to poor liquid-gas phase interactions, leading to poor pollutant-biofilm absorption rates, thereby potentially limiting overall degradation rates [23].

The substrate is one of the most integral parts of these systems because it provides a safe and habitable environment for microbial populations to grow. The ideal media would have the following characteristics:

1. Resistance to compaction (high tensile strength);
2. Moisture and nutrient holding capacity;
3. High surface area for bacterial attachment and improved VOC mass transfer;
4. Good for bacterial attachment (rough, porous, large surface area and hydrophilic); and,
5. pH buffering capacity [24].

Medias such as compost, peat, and soil have excellent water retention capacities, but may be prone to compaction events [23]. Compaction has a tendency to create fixed pathways throughout

the media, limiting gas and nutrient distribution resulting in inefficient conversions, or worse, cell death. Inorganic medias have high tensile strengths mitigating against compaction, however, microbial populations have trouble adhering to these surfaces (particularly metals and glasses), and can sometimes fall and block gas diffusion pathways [18, 25]. Furthermore, inorganic medias do not store/hold moisture near as well as organic media do, and therefore will require microbial inoculation and robust systems in place to ensure moisture and nutrient contents in the media remain suitable for the microbial population. Table 4 summarizes the most important properties for various biofilter media as outlined by Devinny et. al [24].

Table 4: Summary of important Properties of Common Biofilter Materials [24].

Characteristic	Compost	Peat	Soil	Inert Materials (i.e. activated carbon, perlite)	Synthetic Material
Indigenous microbial population	High	Medium-low	High	None	None
Surface Area	Medium	High	Low-medium	High	High
Air permeability	Medium	High	Low	Medium-High	Very High
Assimilable nutrient content	High	Medium-High	High	None	None
Pollutant Sorption Capacity	Medium	Medium	Medium	Low-High	None-High
Lifetime	2-4 years	2-4 years	> 30 years	> 5 years	> 15 years
Cost	Low	Low	Very Low	Medium-High	Very High
General Applicability	Easy, Cost effective	Medium, water control problems	Easy, low-activity biofilters	Needs nutrients, may be expensive	Prototype

Biological oxidation can be very cost effective provided the system has been designed properly. The main consideration for these systems is in understanding the properties of the emission stream and matching a biological system that can handle the requirements. Unfortunately, because of the complex processes that occur within the biofilter, the design process for these systems can be much more tedious than for other systems [24]. High residence times correlate to large bed sizes, or in economic terms, large facility space requirements. Lastly, because of the nature of these systems, increased operator training and effort is required to ensure smooth operation. Overall, these systems are only economical if a low level of control is required, and if a large area of land is available for installation.

2.3.2 Recovery Technologies

Adsorption, absorption, and condensation are among the leading recovery technologies used to separate VOC emissions from process exhaust streams. An added consideration for these

technologies is what to do with the captured contaminant once the process has been completed. In some cases, it is feasible to recover the pollutant with sufficient purity as a commodity for resale. In other cases, a final disposal step is required to complete the abatement process.

2.3.2.1 Adsorption

In nature, the attractive forces holding a solid together do not suddenly end at the surface of the solid. These forces can reach out beyond the surface and attract and retain molecules and ions of other substances in which it may come into contact with. This simply means that when a bulk fluid is in the presence of a solid surface, the solid surface will accumulate some of the molecules of the bulk fluid. This phenomenon is called adsorption, and the extent to which the process will occur depends upon the characteristics of the bulk fluid (adsorbate), and the solid (adsorbent) [26]. An important thing to realize is that if the bulk fluid contains a variety of molecules, each type of molecule will have a different affinity for the solid [26]. It is this difference in affinity that can be exploited to utilize adsorption as a separation or purification process.

Adsorption itself can be subdivided into two main categories which depend upon the actual interactions occurring between the adsorbate and the adsorbent. Physical adsorption is the process in which weak intermolecular forces such as dipole moments, polarization forces, dispersive forces, or short range repulsive forces interact with one another to form a weak connection [27]. Chemio-adsorption refers to adsorption where valence forces arising from the redistribution of electrons between the solid surface and the adsorbed atoms. This distinction is important, because with physical adsorption, the interactions holding the adsorbate to the adsorbent are weak and so the process is reversible[27]. This means the adsorbent can be reused by regenerating the adsorbent, allowing recovery of the adsorbate material. This is especially useful if an adsorbate-adsorbent system is chosen too preferentially adsorb one molecule from the bulk fluid over another (selectivity). In chemio-adsorption, the target molecules are strongly held therefore making the process difficult to reverse and the adsorbate difficult to recover. This means the adsorbent will now become a waste (depending on the adsorbed compound, it could be considered a hazardous waste) because it may only be able to be used for one cycle.

For the recovery of VOCs from airstreams, adsorption has become a feasible separation process, with the VOC molecules being the target adsorbates that are preferentially adsorbed to the appropriate adsorbent (normally activated carbon or zeolite). Design considerations require in depth knowledge of the emission stream and characteristics of available adsorbents [28].

For the emission stream, the important parameters tend to be the concentration of the target species in the carrier (normally as a partial pressure for gases), the overall system pressure, and physical characteristics like the molecular size and shape, polarity, bulk density, particle size, particle shape, size distribution, particle porosity, and pore size. For the adsorbent, there are numerous characteristics that must be taken into account, and these are listed and described in Table 5 below [29].

Table 5: Description of the main characteristics required of the adsorbent when developing an adsorption system design. [29]

Characteristic	Description	What does it tell you or how is it measured
Physical Considerations	1. Particle density 2. bulk density 3. pore volume 4. particle size	Allow determination of equipment size (volume of adsorber vessel), and pressure drop expected.
Capacity for Adsorbate	kg of adsorbate/kg of adsorbent	• Most important adsorbent characteristic • Allows for calculation of cost of adsorbent required • Allows for calculation of volume (when used with physical characteristics listed above • Determined using isotherms (fix temperature, and measure capacity vs. partial pressure of adsorbate) • Can be determined using isoteres or isobars (not normally)
Selectivity	Ratio of the capacity of one component to another in a given fluid	• Determines the purity obtainable for purification processes • Ratio approaches a constant value as concentration drops close to zero • Smaller selectivity means larger equipment is needed
Regenerability of adsorbent	The ability of a substance to be removed from an adsorbent	• Heat of adsorption provides a relative amount of energy required to perform regeneration (lower values are better) • Normally, the first couple regeneration cycles result in significant loss in capacity, then there is a gradual decay of capacity over the overall lifespan of the material • The working capacity is determined after this short term loss of capacity has been established
Kinetics of adsorption	Rate of adsorption	• Related to intraparticular mass transfer • Slow diffusion can be combated by decreasing particle size, but then this increases pressure drop, so a balance needs to be found • Helps determine cycle and residence times
Compatibility of adsorbent to adsorbate	Reactivity of adsorbate to adsorbent	• Adsorbent should be inert to carrier and adsorbate • Should not irreversibly react with any species in the emission (i.e., not chemio-adsorb to VOC or carrier) • Reaction conditions should not cause attrition of adsorbent
Cost	Basic capital cost	• Wide ranges, but can be between $0.30/ lbs to $50 / lbs

By far the most important characteristic of the adsorbent is the capacity [29]. The capacity is defined through the use of adsorption equilibrium data [28]. When a gas is exposed to a solid surface, gas molecules will strike the surface. Some of the molecules will stick to the surface and become adsorbed, and others will bounce off [28]. Initially, the rate of adsorption is high because the surface of the solid is bare, but over time, the rate will decrease. While this is

happening, molecules previously adsorbed to the surface will begin to leave (desorb). Over time, the decreasing rate of adsorption will equilibrate with the increasing rate of desorption. This will continue until the two rates are equal, meaning the surface of the solid is in adsorption equilibrium with the gas.

For a given adsorbent-adsorbate system, the equilibrium amount is a function of pressure and temperature as described by equation 1 below.

$$\frac{x}{m} = f(p, T) \qquad \textbf{Equation 1}$$

In this equation, x/m is the amount adsorbed (in mass) per unit mass of adsorbent at the equilibrium pressure and temperature.

The adsorption equilibrium amount can then be described in three ways:

1. Isotherm – hold temperature constant, and plot capacity vs. concentration;
2. Isobar – hold pressure constant, and plot capacity vs. temperature; or,
3. Isotere – hold capacity constant, and plot concentration vs. temperature.

The most convenient and typically most utilized form of the adsorption equilibrium is the isotherm. By developing an equilibrium relationship through the isotherm, one can also determine the other important adsorbent parameters. For instance, through development of the isotherm one also will determine:

- Kinetics of the adsorption process reaction;
- Heat of adsorption, which provides information on the regenerability;
- Selectivity of the adsorbent for specific compounds when compared to established standards; and,
- Cost because it is related to how much adsorbent is required.

The isotherm itself has been defined many times by many authors using kinetic, statistical, and thermodynamic methods, and empirically through experimentation[30, 31]. In many cases the

isotherms developed are only applicable under a very specific set of conditions. Nonetheless, the most common isotherm shapes have been categorized and identified with general performance predictions. These are depicted below:

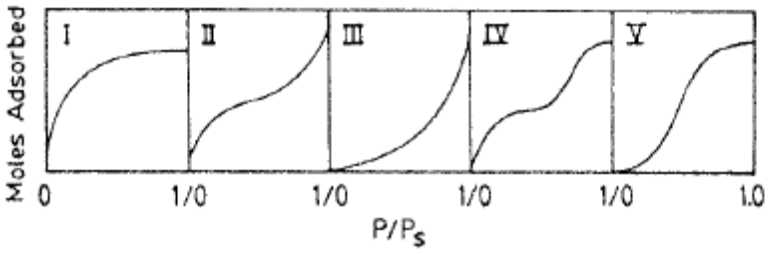

Figure 7: The five types of pure-component gas-adsorption isotherms in the classification of Bruanauer, Deming, Deming, and Teller. Also called the BET classification. [26].

Each isotherm shape depicts general operating characteristics which can be exploited during the adsorption/desorption process.

Overall, designing adsorption systems can become quite cumbersome, as many factors influence the actual performance of the technology. In industrial design situations, the isotherm relationship is the key, and therefore tends to be determined empirically. Once the empirical relationship between loading and pressure at various temperatures has been developed, operating criteria such as adsorption times, desorption times, overall cycle times, operating temperatures for each cycle, and the amount of purge gas can be predicted. This information can then be used to determine operational needs, and more importantly operational costs.

2.3.2.2 Absorption

Absorption involves the selective transfer of a gas to a specific solvent depending on the solubility of the gas in the liquid, and the mass transfer of the gas to the gas-liquid interface [32]. The diffusional component is made up of both molecular and turbulent diffusion, for which turbulent diffusion is orders of magnitude higher. For this reason, absorption systems are designed to maximize turbulence during absorption by flowing both the liquid solvent and gas contaminant through a randomly packed solid column [32]. The basic structure of the column and packing material is designed to increase the contact surface area increasing the overall mass

transfer of the absorbate to the solvent. A typical system operation would be to percolate the absorbent liquid through the top of the column down, and allow the contaminant gas to pass from the bottom of the column upwards.

2.3.2.3 Condensation

Separating VOCs by condensation is accomplished by one of two processes: holding the temperature constant and increasing the pressure (compression condensation), or holding the pressure constant and lowering the temperature (refrigeration condensation) [20]. Most condensation systems are refrigeration type condensation units [20]. For efficient operation these systems are limited to VOCs with boiling points above 100 F and relatively high concentrations above 5,000 ppm [33, 34].

2.4 Fuel Cell Operation and Considerations

The fuel cell is an energy conversion device used to transform chemical reaction energy into electricity. It was discovered in 1839 by Sir William Grove [35, 36]. Through experimentation, he was able to demonstrate that electricity could be produced via the reaction of hydrogen with oxygen over a catalyst [37].

The general reaction taking place is an oxidation-reduction reaction between a fuel and oxidant (typically hydrogen and oxygen). The orientation of the fuel cell is to have an electrolyte sandwiched between two electrodes [38]. Both electrodes serve the same general purpose, which is to provide a porous medium for the chemical reaction to take place, provide an interface between the electrolyte and the electrode, catalyze the respective reactions, and allow a path for electron transport to and from the external load [39]. The type of fuel cell denotes which electrode will form the ion, but in general, one electrode will form an ion, and the other will consume it [39]. During that process, electrons are formed and transported externally out of the fuel cell. The purpose of the electrolyte is to allow the selective transport of ions through it, facilitating the movement from one electrode to the other [39]. This ensures that the reactant and oxidant are physically separated, preventing direct combustion of the reactants. Figure 8 illustrates the general orientation of the Proton Exchange Membrane Fuel Cell (PEMFC), and Figure 9

illustrates the general orientation of the Solid Oxide Fuel Cell (SOFC). In comparing the figures you will note that in the PEMFC, the ion is generated at the anode (and has a positive charge), while in the SOFC, the ion is generated in the cathode (and has a negative charge).

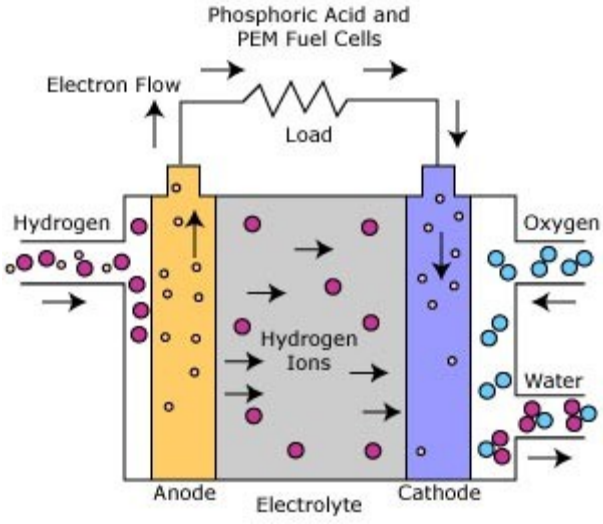

Figure 8: General schematic of a PEMFC and PAFC. Fuel (in this case hydrogen) moves into the anode, reacts to form a positive ion, which is then transferred through the electrolyte onto the cathode. At the cathode, these protons react with oxygen, releasing two electrons.

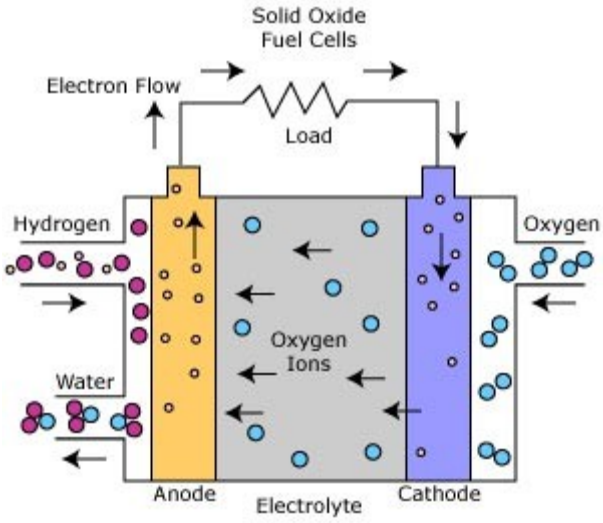

Figure 9: Schematic of an SOFC. Oxygen enters the anode, where it is reacted to form oxygen anions. These anions are transported across the electrolyte to the cathode. On the cathode, water (or carbon dioxide if carbon monoxide is used as a fuel) forms with the anion while losing two electrons.

As a summary, Table 6 outlines basic functions and components of the general fuel cell.

Table 6: Summarization of general fuel cell components, their functions, and requirements.

Component	Purpose	Requirements
Electrodes (anode –> fuel) (cathode -> air)	• Catalyze the reactions • Provides a site for the reaction occur • Allows for electron transport into and out of the cell	• Porous, conductive, and catalytic
Electrolyte	• Conducts the movement of ions • Physically separates the reactants preventing combustion	• Must promote the movement of ions • Must have similar thermal expansion properties as the electrodes (more important in high temperature fuel cells
Reactants	• Consist of Fuel and Air	• Is the source of electrons from which the current is developed
Supports	• Physical supporting structure.	• Materials must be compatible with the operating conditions (Temperatures and Pressures)

2.4.1 General Fuel Cell Performance

The promise of efficient and direct conversion of chemical to electrical energy makes fuel cells an attractive technology [40]. Although the same can be said for batteries, comparing the two technologies will highlight why such intense research is being focused on fuel cell technologies. In terms of similarities, they both have the same basic function (to generate power from electrochemical reactions), and both are considered galvanic cells which consist of two electrodes (anode and cathode), and an electrolyte [37]. Also, in both, the reactions that occur force electrons to move through the electrodes to and from an external load [37]. Lastly, individual batteries and fuel cells both produce small direct current (DC) voltages, which can be amplified to obtain useful power if the individual units are combined together in series or parallel configurations.

The major difference lies in the composition of the electrodes. In batteries, the anode and cathode are composed of materials, which are consumed during the reaction. This means the usable lifespan of a battery is dependent upon how long it takes for the reactions to consume the

electrodes [37]. Conversely, in a fuel cell, the consumable portion of the electrodes is supplied externally, meaning it will run as long as fuel and oxidant are supplied to it [37].

In this research, a fuel cell will be utilized in a stationary power generation application. For this particular use, the fuel cell is compared to a heat engine, because as mentioned previously, a Stirling Engine could be utilized as the energy generator. Fuel cells are superior to heat engines for several reasons. First, they have a higher thermodynamic efficiency, second, the electrochemical reactions taking place in fuel cells produce far less pollution then the combustion reactions associated with heat engines; and finally, fuel cells operate more efficiently at partial load [41].

The heat engine is a physical device that converts thermal energy to work [42]. It operates on a thermal cycle that exploits the temperature gradient between a hot source and cold sink [42]. In a heat engine, the following steps take place:

1. Receives heat from a high temperature source (combustion process like from a coal furnace or nuclear reactor);
2. Converts part of this heat to mechanical work (e.g. through a turbine, or moving piston on a crankshaft); and finally,
3. Rejects the remaining heat to a low temperature sink (typically the atmosphere)

The efficiency of both the heat engine and the fuel cell can be described using a first law of thermodynamics analysis. This means defining the efficiency as the difference between what is being used in comparison to what is being supplied. For the heat engine, French scientist Sadi Carnot proposed that theoretically, the most efficient heat engine would require all processes to occur reversibly[42]. This means expansion and compression steps would be both isothermal and adiabatic [42]. The ideal heat engine cycle is called the Carnot cycle, and its efficiency can be described by the Equation below:

$$\eta_{Carnot} = 1 - \frac{T_L}{T_H} \qquad \textbf{Equation 2}$$

In Equation 2, T_L refers to the temperature of the low temperature sink, T_H refers to the temperature of the high temperature sink, and η_{Carnot} refers to the Carnot efficiency [43]. T_L is usually limited by atmospheric conditions, and therefore the Carnot efficiency will depend upon the temperature of the high temperature sink (combustion chamber) [43].

For a fuel cell, the efficiency is determined by a comparison between the maximum work a cell will perform in comparison to the chemical energy input into the cell. The maximum work is equal to the change in Gibbs free energy between the products and reactants, which is equal to the work required to push electrons through a potential difference. Mathematically, this is described in Equations 3 and 4 [43].

$$W_{Max,cell} = -\Delta G = n_e F E^0 \qquad \textbf{Equation 3}$$

$$\eta_{cell} = \frac{W_{Max,cell}}{HHV} = \frac{n_e F E^0}{HHV} \qquad \textbf{Equation 4}$$

For equation 3, $W_{Max,cell}$ refers to the maximum work output, ΔG refers to the Gibbs free energy (or usable energy) of the reaction, n_e refers to the number of moles of electrons transferred per mole of fuel reacted, F refers to the Faraday constant, and E^0 refers to the reversible cell potential. In Equation 4, η_{cell} refers to the fuel cell efficiency, and HHV refers to the higher heating value of water.

With Equations 3 and 4, the efficiency of both systems can be compared. For a reversible fuel cell running on hydrogen as the fuel and oxygen as the oxidant, the maximum efficiency at 25^0C and 1 atm would be equal to [43].

$$\eta_{Cell} = \frac{n_e F E^0}{HHV} = \frac{2\ moles\ x\ 96485\ C/mole\ x\ 1.23\ V}{285,840\ kJ/mole} = 0.83$$

For a heat engine to reach an equivalent efficiency (0.83), the high temperature reservoir temperature can be calculated by rearranging Equation 2-1, and substituting in the appropriate values [2]:

$$T_H = \frac{T_L}{1 - \eta_{Carnot}} = \frac{298\ \mathrm{K}}{1 - 0.83} = 1753\ \mathrm{K}$$

Therefore in order for a reversible heat engine to reach the same efficiency as that of a reversible fuel cell operating on hydrogen and oxygen at 25^0C and 1 atm, the temperature of the high temperature reservoir would be very high (1480^0C). This temperature is significantly higher than would be seen in normal combustion style generation systems [2].

Practically speaking, the efficiency of a heat engine would be further limited because a portion of the heat being supplied via the fuel would have to be utilized to reach and maintain the combustion temperature of the reaction [2]. An example of this is in the utilization of methane. During the combustion reaction of methane, approximately 35% of the heat released in the combustion reaction is used to reach and maintain the combustion temperature [2].

For a fuel cell, this temperature relationship is not seen because fuel cells operate at one constant temperature. There is no thermal cycle, and the system is based on an electrochemical reaction (displacement and movement of electrons), not a combustion reaction. The overall result is a technology in which a greater amount of the input energy available can be utilized to do useful work.

This can be better observed by considering the overall processes taking place to transform the chemical energy into electricity for both the heat engine and the fuel cell. For a heat engine to transform chemical energy to electricity, there are three distinct steps [28]:

1. Chemical energy to heat;
2. Heat into mechanical work; and finally; and,
3. Mechanical work to electrical energy.

At each step of the process, a portion of the energy input will be lost as entropy. Conversely, for the fuel cell there is only one step - chemical energy converted to electrical energy. There is no heat transfer or mechanical work requirement, which in essence means there is much less opportunity to loose the inputted energy to entropy [37]. Figure 10 below illustrates this.

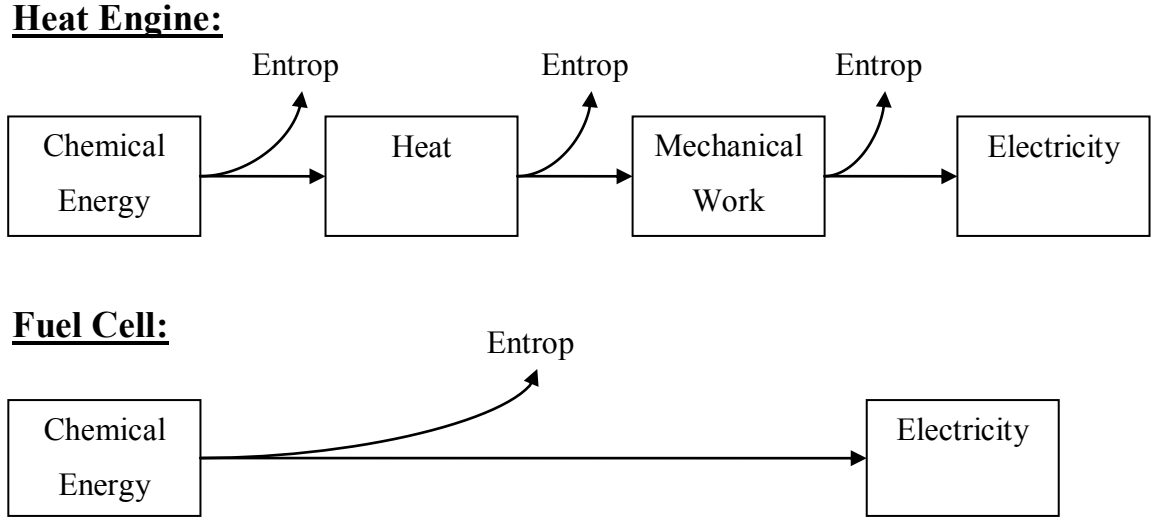

Figure 10: A comparison of the processes taking place to create electrical energy for the Heat Engine and the Fuel Cell. In the Heat Engine, there is more opportunity to lose input energy as entropy[41].

Basic combustion reactions for hydrocarbons involve the reaction of the hydrocarbon with oxygen to form carbon dioxide and water. This generic equation is depicted in Equation 5 below.

$$C_xH_yO_z + \left(x + \frac{y}{2} - 2z\right)O_2 \rightarrow xCO_2 + \frac{y}{2}H_2O \qquad \textbf{Equation 5}$$

As stated above, this equation does not tell the whole story, and is only valid for perfectly stoichiometric operations. In practical applications, it is difficult to achieve this ratio because the oxidant used is not pure oxygen (usually it is air), and the hydrocarbon source is rarely pure. Air

is composed of about 79% nitrogen, 20% oxygen, with trace components such as argon making up the remaining composition. To ensure complete combustion of the fuel, typical combustion reactions are undertaken using excess air. The excess oxygen reacts with nitrogen in air, and forms nitrogen oxides. Conversely, in situations where the oxygen stoichiometric ratio is too low, the product mixture of the combustion reaction will include carbon monoxide. Either way (burning with excess air, or sub-stoichiometric air), the heat engine will produce secondary pollutants (carbon monoxide and/or nitrogen oxides).

Fuel cell reactions are not combustion reactions. They are oxidation-reduction reactions which will only form water, and in some cases CO_2 (for high temperature cells that can utilize CO as a fuel). Therefore in comparison to other heat engine technologies, fuel cells do not produce secondary pollutants [40]. This is particularly important when trying to implement energy generation processes in air sheds heavily taxed with combustion related processes (resulting in increases in nitrogen oxide concentrations and thus smog). Although the process does form CO_2, the presence of CO and NO_X are severely decreased. In particular, it is these situations in which using fuel cells for the stationary generation of power would be environmentally beneficial.

Despite these benefits, there are also issues associated with utilizing fuel cells for this purpose. The primary issue is as a result of technology maturity. The long term performance of fuel cells, and degradation trends of fuel cell components are unknown, and thus provide much uncertainty in their ability to perform over long periods of time. Furthermore, because these systems are not being produced in mass numbers, capital production costs are much higher than other systems being able to generate comparable power.

That being said, these problems can be overcome provided appropriate research is undertaken. This is the first step in opening the door to this research.

2.4.2 Choosing the Appropriate Fuel Cell for VOC Abatement

The purpose of this research is to simultaneously destroy volatile organic compounds (VOCs) while generating energy. The idea is to develop a technology that will provide environmental and economical benefits. The main criteria will be the optimization of these two processes. This

means destroying the target compounds below regulatory thresholds, and extracting maximum energy from these compounds with minimal operational costs.

Fuel cells are an ideal technology for this purpose because they are thermodynamically efficient, environmentally unobtrusive, and in principle can operate utilizing any hydrogen rich hydrocarbon. For stationary power generation applications in particular, it has been found storage, delivery, and safety issues associated with hydrogen use can be alleviated if hydrogen is generated on demand from hydrocarbons in a process called reforming, which will be discussed in greater detail in Section 2.5 [44]. In fact, development of a fuel cell which can handle a variety of hydrocarbon fuels is actually a large field of active research.

Low temperature fuel cells such as the Polymer Exchange Membrane Fuel Cell (PEMFC), Alkaline Fuel Cell (AFC), and the Phosphoric Acid Fuel Cell (PAFC), have operating temperature maximums limited by their cellular components (usually the electrolyte). In order for these cells to show practical power production, noble metal catalysts must be used to speed up the reaction kinetics [41, 43]. However, these catalysts are very susceptible to carbon monoxide poisoning, and its presence in even very low concentrations will impede the function and lifespan of the fuel cell significantly [41]. Conversely, high temperature fuel cells, such as the Solid Oxide Fuel Cell (SOFC), and the Molten Carbonate Fuel Cell (MCFC), have operating temperatures which promote high reaction rates relaxing the catalytic requirements of the electrodes. Both the SOFC and MCFC can utilize carbon monoxide as a fuel – as opposed to be poisoned by it; and both can support internal reforming of hydrocarbons [41]. Furthermore, high temperature operation creates high grade waste heat [39, 40]. This heat can be utilized elsewhere in the plant, making the fuel cell's overall efficiency much higher (over 80%) [39]. Most importantly, these high temperatures can internally reform hydrocarbons (such as VOCs), thereby reducing the overall capital investiture required for implementation of these systems [39, 40, 44].

In this research, a mixture of volatile organic compounds will be utilized as the primary fuel source for the fuel cell. After considering reforming issues, and the need for higher efficiency, it is obvious that high temperature fuel cells are more suited to this research then low temperature fuel cells.

In particular, the high temperature fuel cell of choice for this research will be the SOFC. This is because it has the potential to be more robust then the MCFC. Although the MCFC shares the numerous advantages of high temperature operation with the SOFC, it has a tendency to form nickel oxide in the electrolyte after sustained use, thereby degrading fuel cell performance and lifespan [37, 41]. The MCFC is also more sensitive to sulphur compounds then the SOFC[41].

2.4.3 The Solid Oxide Fuel Cell: Fundamentals

The basic operation of the SOFC is outlined in the steps below:

1. At the cathode, oxygen from air is transformed into oxide ions by receiving electrons from the external load;
2. The oxide ion travels from the cathode, through the ceramic electrolyte, and onto the reaction site of the anode;
3. In the anode the oxide ion combines with the reformed fuel (hydrogen and carbon monoxide) to form water and carbon dioxide, releasing electrons to the external circuit, and venting gaseous water and carbon dioxide; and,
4. The electrons travel through the external circuit, through the load, and back to the cathode to begin the process again with fresh oxidant and fresh fuel.

The overall process is pictorially outlined in Figure 11 below:

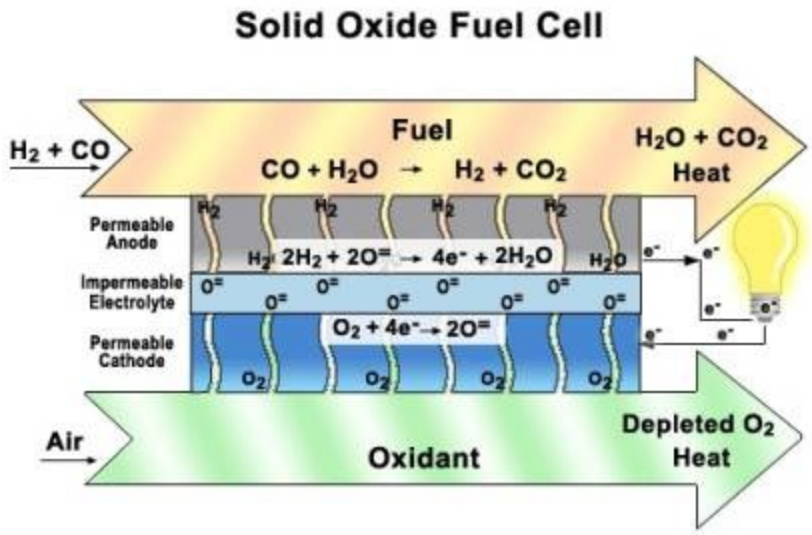

Figure 11: Pictorial representation of the operation of the solid oxide fuel cell [45].

The electrochemical reactions taking place are outlined in Equations 6 to 10

Anode Reactions

$$H_2 + O^{=} \rightarrow H_2O + 2e^{-} \qquad \textbf{Equation 6}$$

$$CO + O^{=} \rightarrow CO_2 + 2e^{-} \qquad \textbf{Equation 7}$$

Cathode Reactions

$$O_2 + 4e^{-} \rightarrow 2O^{=} \qquad \textbf{Equation 8}$$

Overall SOFC Reactions

$$H_2 + \frac{1}{2} O_2 \rightarrow H_2O \qquad \textbf{Equation 9}$$

$$CO + \frac{1}{2} O_2 \rightarrow CO_2 \qquad \textbf{Equation 10}$$

At 1000^0C, as displayed in Equation 2-6, carbon monoxide can be directly oxidized to carbon dioxide. In practice, the oxidation of carbon monoxide to carbon dioxide can actually follow

another pathway. This involves the water-gas shift (WGS) reaction which is displayed in Equation 11 below.

$$CO + H_2O \rightarrow H_2 + CO_2 \qquad \textbf{Equation 11}$$

Therefore the oxidation of carbon monoxide actually has two competing pathways, one which follows reaction 7, and one which involves reactions 11 followed by reaction 6. In reality reaction 11 (WGS reaction) is much faster than reaction 7 (direct oxidation of CO by oxygen) in an SOFC, meaning the majority of carbon monoxide is oxidized in this manner [41]. The significance of this is that cell performance calculations can be greatly simplified in an overall systems model such as the one used in this work. At the anode, reaction 7 no longer needs be considered provided that the equivalent amount of hydrogen produced from the WGS reaction is incorporated into reaction 6. This can be done by assuming that 1 mole of CO will produce 1 mole of H_2 (as is depicted in Equation 11).

2.4.4 The Solid Oxide Fuel Cell: Performance

To quantify the performance of a SOFC one must be able to determine what energy is coming into the fuel cell, how much energy is being converted to electricity, and how much energy is being converted to heat. The thermodynamic definition of the change in Gibbs free energy is presented in Equation 12 below.

$$\Delta G = \Delta H - T\Delta S \qquad \textbf{Equation 12}$$

In Equation 2-11, ΔG refers to the Gibbs free energy, ΔH refers to the enthalpy, T refers to the system temperature, and ΔS refers to the entropy. For fuel cell operations, a more practical relationship for the change in Gibbs free energy is that it also represents the maximum amount of electrical work that can be done at the standard state. This is presented below in Equation 13.

$$\Delta G^0 = -nF\Delta E^0 \qquad \textbf{Equation 13}$$

In this case, ΔG^0 is the change in Gibbs free energy, n refers to the number of electrons involved in the reaction, F is the Faraday constant (96,485 C/mole), and ΔE^0 is the potential difference of

the cell at equilibrium. This relationship can be further expanded to incorporate the calculation of the potential difference at different conditions other than the standard state. Equation 14 outlines this relationship.

$$\Delta G = \Delta G^0 + RT\ln Q \qquad \textbf{Equation 14}$$

In this Equation ΔG refers to the change in Gibbs energy at a non-standard pressure and temperature, with R representing the gas constant (8.314 J/moleK), and Q representing the reaction quotient. If the relationship in Equation 13 is inserted into Equation 14, the Equation that results is the general form of the Nernst Equation.

$$\Delta E = \Delta E^0 + \frac{RT}{nF}\ln Q \qquad \textbf{Equation 15}$$

With Equation 15, the potential difference for an ideal fuel cell operating reversibly can be calculated. The next step is to calculate the performance of a real fuel cell. Real fuel cells will experience loss as a result of differences in temperature, pressure, mass transfer, kinetic effects, fuel utilization, air utilization, and resistances of different components (anode, cathode, electrolyte, and interconnects) [43]. These can all be quantified.

Polarization

The polarization curve is the main tool in which to describe fuel cell performance; as this plot illustrates how voltage varies with current density. Current density is defined as the rate in which electrons are moving through the system per unit area. It is directly related to the rate of oxidation taking place. For this reason, the polarization curve also illustrates how the rate of chemical reaction affects fuel cell voltage. Furthermore, fuel cell voltage is an indication of fuel cell efficiency because in effect, it reflects the ideal amount of work that can be extracted from the fuel cell. The real fuel cell voltage deviates from the ideal voltage as a result of the various parameter considerations listed above (temperature, pressure, mass transfer, kinetic effects, fuel utilization, etc...), and is depicted by the curve in Figure 12.

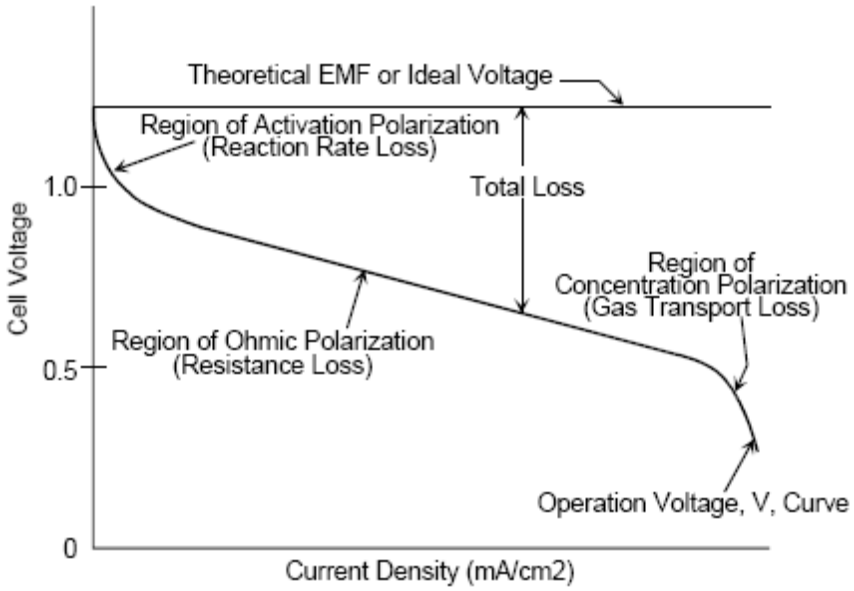

Figure 12: General polarization curve for a fuel cell. Describes the conditions that influence various regions of operation [43].

For a fuel cell running on pure hydrogen and oxygen, at 25^0C, and operating at atmospheric pressure, the ideal fuel cell voltage will be -1.23 V [43]. When no current is running through the cell this ideal potential difference is realized (on Figure 12, this is called the Theoretical EMF or ideal cell voltage). Once current begins to run through the cell, the actual work being extracted deviates from the ideal case as depicted by the curve in Figure 12. This curve experiences losses from three main sources, each of which exerts pronounced effects during different regions of the curve.

At low current densities, the reaction is slow, reflecting sluggish electrode kinetics [43]. At this point, the reaction is trying to overcome the activation energy of the reaction, which results in the pronounced drop in voltage as is outlined above. Stated another way, the activation potential is the extra potential required to overcome the kinetic barriers of the reaction. It can be quantified by using the Tafel Equation and is called Activation Polarization (Equation 16).

$$\eta_{Act} = \frac{RT}{\alpha n F} \ln\left(\frac{i}{i_0}\right) \qquad \textbf{Equation 16}$$

In Equation 16, η_{Act} is the drop in voltage due to Activation Polarization, α is the electron transfer co-efficient, i is the current density, and i_0 is the exchange current density. Higher exchange current densities reflect reactions with fast kinetics, meaning a smaller activation polarization needs to be used to overcome the kinetic barriers. Conversely, small exchange current densities result in larger activation polarization values.

On the extreme right of the curve, the reaction rate is very high, and reactants are being used much quicker than can be supplied to the reaction sites [43]. Essentially mass transfer of reactants is hindering the reaction, resulting in a severe drop in cell potential [43] The mathematical expression quantifying the contribution to voltage losses from this phenomenon is called Concentration Polarization and presented in Equation 17.

$$\eta_{Conc} = \frac{RT}{nF} \ln\left(1 - \frac{i}{i_L}\right) \qquad \textbf{Equation 17}$$

In Equation 17, η_{Conc} refers to the polarization effect on voltage as a result of mass transfer issues, and i_L refers to the limiting current density. The limiting current density is a measure of the maximum rate at which a reactant can be supplied to an electrode [2]. The term $\ln(1-i/i_L)$ actually represents the ratio of reactant in the surface of the electrode vs. reactant in the bulk solution, which allows the determination of how mass transfer will affect fuel cell efficiency (voltage) as the reactant gets depleted around the electrode surface.

In the intermediate regions, the drop in potential difference is related to the resistance of the various materials within the cell (electrodes, electrolytes, and interconnects) [2, 43]. The loss is linear because resistance of these materials is constant at constant temperatures. This is called Ohmic Polarization and is mathematically expressed as an Ohm's Law relationship in Equation 18 below.

$$\eta_{Ohm} = iR \qquad \textbf{Equation 18}$$

In Equation 18, η_{Ohm} refers to the voltage lost as a result of resistance within the fuel cells components, and R refers to the sum of the resistances of the various materials in the cell.

Overall, these effects can be summed up, and subtracted from the ideal voltage to determine the actual voltage.

$$E_{actual} = E_{ideal} - (\eta_{Act} + \eta_{Conc} + \eta_{Ohm}) \quad \textbf{Equation 19}$$

Overall, this allows for the development of a polarization curve for any system in consideration. The next step is to outline how temperature, pressure, fuel utilization and air utilization can affect the voltage of the fuel cell.

Temperature and Pressure

An examination of Equation 12 indicates that as temperature increases, the amount of energy lost to entropy will increase. This means that the ideal cell voltage or reversible potential will decrease. As an example, we can see that at atmospheric pressure, the oxidation of hydrogen by oxygen will have a reversible potential of -1.23 V at 25^0C, and -0.91 V at 1000^0C [43]. Conversely, the effect on the voltage performance of a fuel cell will actually increase with increasing temperature. This is because increasing temperature increases mass transfer rates, and kinetic reaction rates, while also decreasing resistance within the cell components. The effect is a decreasing influence in all types of polarization.

The effect of system pressure can also be analyzed by considering both the reversible and ideal potentials.

$$G_2 = G^0 + nRT \ln\left(\frac{P_{O_2}}{P^0}\right) \quad \textbf{Equation 20}$$

From Equation 20, when the system pressure increases, the Gibbs free energy increases. This allows more energy to be available for conversion into electrical work, meaning the ideal potential will increase with an increase in pressure. Furthermore, when the system pressure increases, reactant partial pressure, gas solubility and mass transfer rates will increase. As with increasing temperature, this means polarization effects will decrease, allowing for an overall increase in real cell potential. Figure 13 below summarizes these trends for the oxidation of hydrogen, carbon monoxide, and methane.

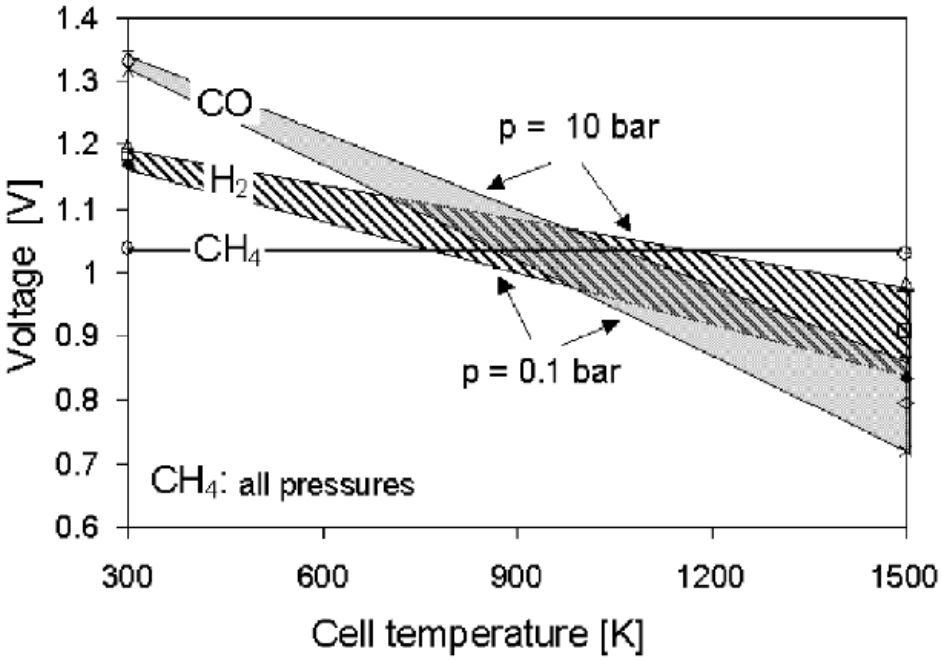

Figure 13: Representation of the effect of pressure and temperature on the ideal cell voltage for the oxidation of carbon monoxide, hydrogen, and methane [43].

Fuel and Air Utilization

The amount of fuel and air utilized is directly related to the magnitude of current flow. As more fuel is utilized, more electrons are moved, and thus a higher current is evolved. However, higher fuel or air utilization decreases the concentration of the reactant at the end of the flow path thus decreasing performance in this region of the cell. This is significant, because this develops a minimum potential. The cell voltage adjusts to this minimum potential because the electrodes are isopotential and good conductors. To quantify this effect, Equation 15, is rewritten with the reaction quotient being defined as the partial pressure of products over reactants at the outlet of the cell. This is seen in Equation 21 below.

$$E = E^0 + \frac{RT}{nF} \ln \left[\frac{X_{H_2OAnO}}{X_{H_2AnO} X_{O_2CaO}{}^{1/2} P_T{}^{1/2}} \right] \qquad \textbf{Equation 21}$$

In Equation 21, X_{H2OAnO} is the mole fraction of water at the anode outlet, X_{H2AnO} is the mole fraction of hydrogen at the anode outlet, X_{O2CaO} is the mole fraction of oxygen at the cathode

outlet, and P_T is the total pressure of the cell. Equation 21 can be further manipulated to obtain an expression that will yield a value for the ideal potential as function of fuel utilization. Equation 22, first defines fuel utilization (U_{fH2}), and Equations 23 and 24 define the respective mole fractions in terms of fuel utilization. Equation 26 combines Equations 21 to 25 to obtain the overall expression of the ideal potential of a fuel cell running on hydrogen and air.

$$U_{fH_2} = 1 - \frac{X_{H_2AnO}}{X_{H_2AnI}} \qquad \textbf{Equation 22}$$

$$X_{H_2AnO} = 1 - U_{fH_2} \qquad \textbf{Equation 23}$$

$$X_{H_2OAnO} = U_{fH_2} \qquad \textbf{Equation 24}$$

$$X_{O_2CaO} = \frac{\lambda - U_{fH_2}}{\frac{\lambda}{0.21} - U_{fH_2}} \qquad \textbf{Equation 25}$$

$$E_{ideal} = E^0 + \frac{RT}{nF} \ln \left[\frac{U_{fH_2}\left(\frac{\lambda}{0.21} - U_{fH_2}\right)^{\frac{1}{2}}}{\left(1 - U_{fH_2}\right)\left[\left(\lambda - U_{fH_2}\right)P_T\right]^{\frac{1}{2}}} \right] \qquad \textbf{Equation 26}$$

In Equations 25 and 26, λ refers to the ratio of excess air (not oxygen) being supplied to the cell. Equation 26 is an important one because it relates temperature, pressure, and fuel utilization together in one simplified relationship which will yield the ideal potential of the fuel cell. To obtain the polarization curve, the result of Equation 26 can be substituted into Equation 19.

Overall, Equations 19 and 26 can be used to quantify fuel cell performance.

2.4.5 Fuel Processing - Reforming

In principle, an SOFC can utilize any combustible fuel; as the high temperature operation supports internal reforming [40]. Internal reforming involves the conversion of the source fuel to a reformate mixture that is compatible with the internal electrochemical reactions of the fuel cell [39]. For the SOFC, this mixture is typically hydrogen and carbon monoxide.

The internal fuel reforming step utilizes the process of steam reforming to convert hydrocarbons into the reformate mixture. The overall chemical stoichiometry of the reaction is displayed in Equation 27 below.

$$C_xH_yO_z + (x-z)H_2O \xrightarrow{\Delta} xCO + \left(x - z + \frac{y}{2}\right)H_2 \qquad \textbf{Equation 27}$$

More specifically, steam reforming involves the reaction of hydrocarbons over catalysts to promote their conversion to carbon monoxide and hydrogen [46]. The breakdown of the original hydrocarbon itself is an endothermic reaction, and therefore requires a constant supply of energy to drive the reaction [47].

Overall, steam reforming is a well established process that can have high conversion efficiencies [36]. However, the process is not without problems, especially for higher hydrocarbons. Steam reforming of higher hydrocarbons occurs in two steps. First, there is an irreversible adsorption onto the catalyst, and second, a subsequent cleavage of C-C bonds one by one until finally only simple single carbon compounds are remaining [46]. Once cleavage begins, the reaction rates of individual hydrocarbons can vary substantially from compound to compound, and even though most higher hydrocarbons react faster than methane (and at lower temperatures), they are susceptible to non-catalytic thermal cracking [46]. At the high temperatures associated with fuel cells, thermal reactions begin competing with catalytic reactions, causing the formation of olefins (precursors to coke formation) from these higher hydrocarbons [46]. Coke deposits will inactivate the catalyst, causing irreversible harm, and deactivating the anode electrode [38]. In general, larger hydrocarbon molecules (more carbons), result in slower reaction rates, increasing the risk to thermal cracking [46].

To solve these problems, higher hydrocarbons can be pre-reformed prior to entering the vessel. This means transforming the hydrocarbon fuel into small or short chained carbon containing compounds (CH_4, CO, and/or CO_2) at lower temperatures, or completely reforming the hydrocarbon so it is immediately usable by the fuel cell. Pre-reforming can be performed

utilizing one of three different processes: steam reforming, partial oxidation, or autothermal reforming.

Steam reforming is the least expensive method of producing hydrogen and is used for most of the world's hydrogen supply [47]. It is basically the same process as internal reforming – which was described above. The main difference between the two processes is that by separating the process from the fuel cell, the reactor temperature can be controlled. This means lower temperatures can be used (approximately 250^0C – 300^0C) eliminating the risk of carbon formation [46]. The lower temperatures also permit the use of Group VIII metals – normally nickel [46].

The primary reaction involved in the steam reforming process is also highly endothermic [48]. For this reason, reactions tend to be limited by heat transfer, and not kinetics[48]. This means typical reactor designs are focused upon heat exchange, and thus tend to be large and heavy [48].

Partial Oxidation (POX) involves the reaction of the fuel hydrocarbon with a sub-stoichiometric ratio of oxygen to form a reformate mixture of carbon monoxide and hydrogen [48]. In principle, the low ratio of oxygen ensures the stoichiometry will not allow full combustion to occur; consuming all the oxygen but not all the fuel. One of the main attractions of this type of system is that the process is highly exothermic operating at approximately 800^0C to 1000^0C [48], thus no in-direct heat is required to sustain the system [49]. The general reaction is presented below as Equation 28.

$$C_xH_yO_z + \frac{1}{2}(x - z)O_2 \rightarrow xCO + \frac{y}{2}H_2 \qquad \textbf{Equation 28}$$

Issues occur when dealing with mixed hydrocarbons because the ideal stoichiometry is difficult to achieve. This means more oxygen is supplied then required leading to full combustion zones within the POX reactor [50]. The result is rapid temperature rise within the reactor, soot formation, and difficulties in controlling the actual reformate compositions [50]. Overall, although the process

is well studied, it is difficult to control, and on average has been found to have the lowest conversion efficiency in comparison to steam and autothermal reforming [50].

The last reforming technology is known as auto-thermal reforming (ATR). Auto-thermal reforming combines the steam reforming and POX reactions into one process. The idea is to exploit the benefits of each technology, lowering overall operational costs and increasing efficiencies. The POX reactions occur first, converting the higher hydrocarbons to lower molecular weights substances and generating energy to help drive the steam reforming reactions. The result is a self-sustaining reaction that does not need energy input.

The Autothermal Reactor (ATR) is a refractory lined vessel swaged with a smaller diameter at the top to provide a combustion zone [38]. The bottom of the reactor contains the catalyst. The feedstock and steam enter from one entry point, and are mixed with enriched air. They mix in the combustion zone. This is where the POX reactions take place. As the reaction mixture moves towards the outlet, steam reforming reactions begin to proceed. A diagram of this type of reactor is presented below in Figure 14.

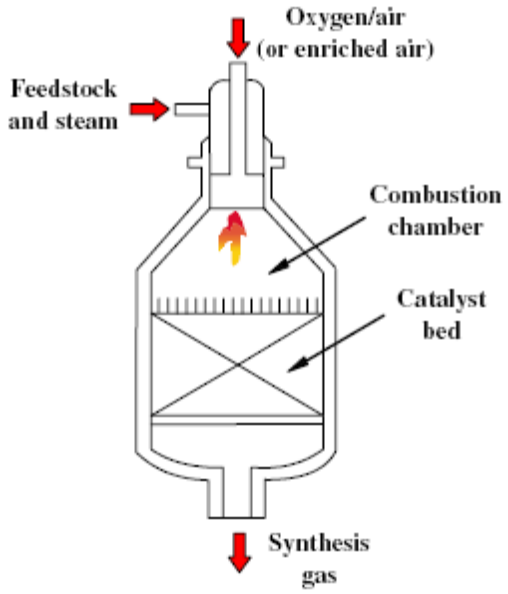

Figure 14: Autothermal Reactor [38].

In this system, the reaction is controlled by the amount of oxygen and steam being fed into each reactor. At the inlet, the oxygen content will be controlled to limit the reaction and more importantly the energy generated. The energy generated should balance that required by the endothermic steam reactions. In this way, the reactions are controlled and become self-sustaining.

The product from the POX reactions (mixture of single hydrocarbons and hydrogen) now becomes the feed to the steam reactions. Here, the steam content is controlled to drive the steam reforming reactions, and the water-gas shift reactions to the completion.

There are actually two general forms of Autothermal Reactors. In the first style, the POX and steam reforming reactions are separated into two separate reactors. The advantage of having separate reactors is that specific catalysts can be used for each reactor. The disadvantages are that two reactors are heavier, require more space, and there is less thermal integration than in just one reactor. The disadvantage of having both reactions in one reactor is that the different reaction rates cause a temperature gradient to form in the reaction vessel, resulting in in-efficient conversion.

Chapter 3: Problem Definition and System Baseline

To develop design criteria and constraints for the SOFC hybrid abatement system, the emission problem must be defined, and a rating system must be developed in order to provide baseline comparisons of the designed technology to those currently in use.

There is only one constraint for this system; the ability of the technology to lower compounds of concern to below current and foreseeable regulatory threshold limits. There are two criteria for this system; overall lifecycle costs must be within budgetary restrictions, and the system must be operationally flexible in order to ensure its operation will not hinder other facility processes. Since this technology is not being developed for a specific customer, instead of developing lifecycle costs that fit within budgetary restrictions, capital and operational costs will be developed as a method of comparing various technologies against one another.

In this chapter, a case study will be developed involving the treatment of VOCs from a moderately sized automotive parts coating facility located in the Greater Toronto Area (GTA). Section 3.1 develops the criteria and constraint rating system, by turning qualitative information into quantitative data. The idea is to use matrices with defined characteristics in which to rate the performance of possible current technologies that could be used to treat the problem in question. Section 3.2 defines the problem in terms of emission rate, composition, along with various other data. Sections 3.3 to 3.5 use the Technology Comparison Tool outlined in Section 3.1 to solve the problem presented in Section 3.2. It outlines possible technological options, and provides lifecycle analysis on each system. This will provide a baseline in which to compare the SOFC hybrid abatement system. The design of the SOFC hybrid system is presented in Chapter 4 of this thesis.

3.1 Technology Comparison Tool

The basic process flow used to determine which technologies can be utilized for VOC abatement is provided in Figure 15 below. It outlines what needs to be understood about the emission and process so that appropriate technologies are assessed for environmental problems.

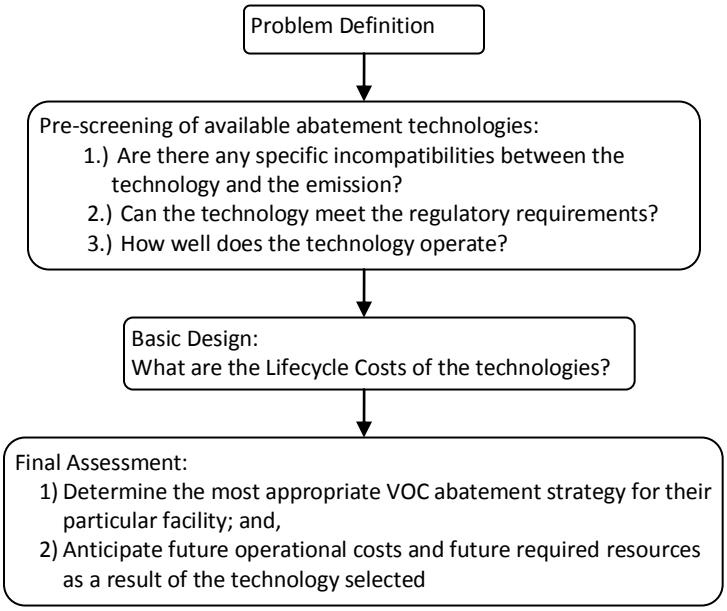

Figure 15: VOC abatement technology selection flow sheet.

3.1.1 Problem Definition

The problem definition is the step in which all preliminary data required to assess the issue is found. This means defining four key elements: the emission source, the emission itself, legal requirements that must be met, and any budgetary constraints. In almost all cases, these data are readily available at the facility, and can be compiled quickly provided the appropriate people are consulted.

3.1.2 Pre-screening

As outlined in Figure 15, the pre-screening step answers three questions:

1.) Are there any specific incompatibilities between the technology and the emission?
2.) Will the technology meet the current regulatory requirements?
3.) How well does the technology operate (technology robustness, and technology flexibility)?

The idea behind the pre-screening step is to compare the information compiled from the problem definition with all the limitations found in literature on the abatement technologies considered. This will allow facility management to discard technologies from consideration that don't meet their prescribed criteria, and thus shorten the number of technologies required to undergo the basic design step.

For instance, if it was found that the emission contained significant amounts of acidic gases (such as chlorine or sulphur compounds), certain regenerative catalytic thermal oxidation techniques may not be feasible (unless a scrubber step was implemented prior to the combustion chamber) as the catalysts would be poisoned [19].

Can Technology meet current regulatory requirements?

When referring to the Regulatory Requirements a facility must meet, the concern is specifically if the system can lower the current emission rate below the regulatory threshold, and if future regulatory requirements are identified, can the system maintain the facility's emission output below this future threshold. To avoid legislative issues, many facilities try to design systems to reduce emissions below 50% of the current threshold ensuring the technology will be able to be used for the entire lifespan of the system.

To obtain a quantitative measurement of how well each technology handles regulatory requirements, the matrix is outlined in Table 7.

Table 7: Matrix outlining regulatory scoring requirements.

Score	Description
3	Meets current and foreseeable future regulations and requirements
2	Meets current regulations and requirements
1	Does not meet current regulations and requirements

How well does the technology operate?

The ability of an abatement technology to smoothly incorporate process or facility changes in its operation is a function of how the basic technology works, and not the size of the facility or the emission composition used for the design phase. This is the Operational Flexibility of the technology, and can be assessed by examining the following factors:

1. Start-up times;
2. Continuous vs. Intermittent Operation; and,
3. Load Tolerance;
    a. Ability to handle fluctuations in emission concentration or emission types; and,
    b. Ability to handle fluctuations in total flow

The scoring matrices listed in Tables 8 through 10 outlines how each type of abatement technology will be quantifiably assessed for operational flexibility.

Table 8: Scoring system used to assess start-up timing for each type of abatement technology.

Score	Description
3	Start-up quicker then ½ production shift
2	Start-up quicker then 1 production shift
1	Start-up takes longer than 1 production shift

Table 9: Scoring system used to assess operational flexibility in terms of continuous vs. intermittent operation for the abatement technologies.

Score	Description
3	Intermittent Operation or cycling ok
2	Moderate Toleration to Intermittent operation
1	Does not tolerate intermittent operation

Table 10: Scoring system used to assess operational flexibility in terms of load tolerance for the abatement technologies.

Score	Description (fluctuations in flow)	Score	Description (fluctuations in concentration)
3	Tolerates fluctuations in flow	3	Tolerates fluctuations in concentration
2	Tolerates minor fluctuations in flow	2	Tolerates minor fluctuations in concentration
1	Does not tolerate fluctuations in flow	1	Does not tolerate fluctuations in concentration

3.1.3 Basic Design

Once the pre-screening step is complete, the list of feasible technologies for further investigation will be relatively small. A basic design for each of the technologies under consideration can now be completed. The purpose of the basic design is to determine the size and main operational requirements (utilities) of the system. The size will be used to obtain a good estimate of the capital costs, and the operational requirements will be used to determine the annual operating costs. Together, with the implementation of proper engineering economics, a lifecycle cost for the abatement system can be determined.

When determining lifecycle costs there are many things that need to be considered to ensure that a full assessment can be made. For this particular assessment the lifecycle cost calculation will include the following:

1. Capital costs (delivery costs are not included here);
2. Resource costs (natural gas, electricity, water);
3. Labour and maintenance costs;
4. Anticipated major maintenance costs (example: RTO bed replacement costs);
5. Land use costs; and,
6. Anticipated lifespan.

Once these factors are compiled, the lifecycle cost will be determined, providing a very effective technology comparison factor.

It is important to note that land use costs are very complex in nature and are highly dependent upon the geographic location, whether new land was required to be purchased, or existing land

could be used, and what type of construction would be required. For this reason, the land use costs calculated here are based on the data provided by the province of Ontario in their Site Development guide for the city of Toronto in terms of warehouse space[51].

3.1.4 Final Assessment

At this point in the analysis, a pre-screening assessment would have been completed to eliminate technologies not able to meet the minimum constraints defined by the facility. Furthermore, qualitative operational criteria and the ability of an abatement technology to meet legislative requirements have been quantified into numerical values for objective comparisons, and a basic lifecycle cost estimate has been created. At this stage the information is compiled into a meaningful way so abatement system decision makers will be able to make a clear and informed decision on the abatement strategy they wish to pursue. In this analysis, there is only one constraint and two criteria to base the decisions on. These scores can all be multiplied together to get an overall score assessing non-economic performance, and the lifecycle costs can be used to consider economic considerations.

For further clarity, a case study using this Technology Assessment Tool is presented in Section 3.2. The case study is based upon the general case of a moderately sized automotive parts painting facility in Southern Ontario.

3.2 Case Study - An Automotive Parts Painting Emission Problem.

In this particular case, the problem definition is presented in Table 11. It represents the emission characteristics of an automotive parts painting facility in Southern Ontario.

Table 11: Characteristics and composition of a typical emission stream being evolved from an automotive parts painting facility in Southern Ontario.

Definition	Process Data
Emission Definition	15% Xylene 35% Methyl Ethyl Ketone 40% Toluene 10% N-Butyl Acetate
Process Definition	1.) Process: Automotive trim parts painting 2.) Continuous process 3.) Annual Hours of Operation: 240 days @ 16 hrs/day annually Total Flow: 60,000 cfm Concentration: 100 tonnes VOCs
Legal Requirement Definition	Legal Requirements are based upon those defined in O. Reg. 419

**Note: Individual VOC concentrations are of the total VOCs, not of the total exhaust stream*

3.2.1 Pre-screening Assessment

The information in Table 11 illustrates the types of contaminants in the emission stream, the approximate concentration, the total flow rate, and the type of operation. Temperature for the coating preparation and spray application is typically between 20^0C and 25^0C. Humidity can vary depending on the operation, and system but we can assume the RH of the system is approximately 50%. It is assumed that the target emission load reduction is 50% of current levels.

Industrial coating operations using solvent based coatings are typically composed of high volume low concentration exhaust streams of components with relatively low boiling points. Condensation systems are limited to operations above 5,000 ppm in concentration and to solvents with boiling points above 5,000 ppm [33, 34]. The concentration of the emissions listed in Table 11 are all well below this 5,000 ppm threshold. Under these conditions condensation systems do not operate efficiently because the energy required to condense the component emissions would be substantial.

Furthermore, industrial coating operations emit highly variable and complex emission streams in which a suitable absorbing liquid is difficult to find. The result is that in this case, absorption systems will not operate efficiently either, therefore will not be discussed further.

In summary, under the conditions listed, only the following technologies will be reviewed for the sample facility in Table 11: RTO (Regenerative Type), RTO (Recuperative Type), RCO, Biological Oxidation, Carbon Adsorption, and the SOFC Abatement System.

3.3 Basic Design: Thermal Oxidation

3.3.1 Regulatory Requirements

Thermal oxidation systems are rated with destruction efficiencies that range between 95% - 99%. Properly designed, a thermal oxidation system will always be able to remove the contaminants below the prescribed emission limit. Even if regulatory threshold values were to decrease substantially, these rated destruction efficiencies ensure that the system would be able to maintain a consistent reduction. The only foreseeable problem is if regulatory thresholds were established for carbon dioxide, carbon monoxide, and/or nitrogen oxides. In this case, because the thermal reaction involves the transformation of VOCs to these specific contaminants, the facility would have to ensure that they are monitoring these emissions as well. In this case, the numerical value associated with this criterion is 3.

3.3.2 Lifecycle Costs

In order to determine the lifecycle costs for thermal oxidation abatement systems, the capital and operational costs must be established. For the three sample facilities, the operational costs were calculated using the EPA Handbook of Control Technologies for Hazardous Air Pollutants [1]. Capital costs were also obtained from tables contained in the EPA Handbook of Control Technologies for Hazardous Air Pollutants [1]. Finally, to transform these costs (capital costs as of 1999) to more current figures (2006 dollar values), the Vatavuk Air Pollution Control Cost Indices was used [52].

The capital and operational costs to purchase and operate the various thermal abatement systems outlined here are described below in Tables 12 through 14.

Table 12: Recuperative Type RTO cost analysis.

Purchased and installed equipment costs:					
Costs:				**Factor**	**Cost**	**Subtotals**
Incinerator (1994)					$197,400	
Incinerator (2006) factor is 138.8/100				1.388	$273,991	
Instrumentation				0.1	$19,740	
Taxes				0.15	$29,610	
Freight				0.03	$5,922	
Direct Installation Costs are included in purchase costs						
Subtotal Direct Installation Costs						$329,300
Indirect Costs						
Engineering				0.1	$27,399	
Construction and Field expense				0.05	$13,700	
Contractor fees				0.1	$27,399	
Start-up				0.02	$5,480	
Performance Testing				0.01	$2,740	
Contingencies				0.03	$8,220	
Subtotal Indirect Installation Costs						$84,900
Total Installation Costs						$414,200
Direct Annual Costs						
Utilities						
	Fuel				$1,755,772	
	Electricity				$267,196	
Labour		hours work	rate of pay			
	Supervisor	8/week	$20/hr		$5,440	
	Labour	8/week	$16/hr		$4,352	
Maintenance						
	Labour	8/week	$25/hr		$6,800	
	Material	same as labour			$4,352	
Land Lease costs		$5.75 per ft^2 - toronto			$8,500	
Subtotal Direct Costs						$2,052,400
Indirect Annual Costs						
Overhead	0.6 of			0.6	$164,395	
Administration						
	Property Taxes			0.01	$2,740	
	Insurance			0.01	$2,740	
	Capital Recovery			0.16	$44,606	
Subtotal Indirect Costs						$21,500
Total Annual Costs						$2,073,900

Notes: a.) The operational costs calculated here do not include the cost to keep the systems hot during non-production working times (8 hours per day).

b.) All costs have been rounded to the nearest $100 to reflect the accuracy of the numbers.

Table 13: Regenerative Type RTO cost analysis.

Purchased and installed equipment costs:					
Costs:				**Factor**	**Cost**	**Subtotals**
Incinerator (1994)					$810,000	
Incinerator (2006) factor is 138.8/100				1.388	$1,124,280	
Instrumentation				0.1	$81,000	
Taxes				0.15	$121,500	
Freight				0.03	$24,300	
Direct Installation Costs are included in purchase costs						
Subtotal Direct Installation Costs						$1,351,100
Indirect Costs						
Engineering				0.1	$112,428	
Construction and Field expense				0.05	$56,214	
Contractor fees				0.1	$112,428	
Start-up				0.02	$22,486	
Performance Testing				0.01	$11,243	
Contingencies				0.03	$33,728	
Subtotal Indirect Installation Costs						$348,500
Total Installation Costs						$1,699,600
Direct Annual Costs						
Utilities						
	Fuel				$658,532	
	Electricity				$264,737	
Labour		hours work	rate of pay			
	Supervisor	8/week	$20/hr		$5,440	
	Labour	8/week	$16/hr		$4,352	
Maintenance						
	Labour	8/week	$25/hr		$6,800	
	Material	same as labour			$4,352	
Land Lease costs ($5.75/ft^2 - toronto)					$8,500	
Subtotal Indirect Costs						$952,700
Indirect Annual Costs						
Overhead	0.6 of			0.6	$674,568	
Administration						
	Property Taxes			0.01	$11,243	
	Insurance			0.01	$11,243	
	Capital Recovery			0.16	$183,033	
Subtotal Indirect Costs						$880,100
Total Annual Costs						$1,832,800

Notes: a.) The operational costs calculated here do not include the cost to keep the systems hot during non-production working times (8 hours per day).

b.) All costs have been rounded to the nearest $100 to reflect the accuracy of the numbers.

Table 14: Recuperative Catalytic (RCO) thermal oxidizer cost analysis.

Purchased and installed equipment costs:					
Costs:			Factor	Cost	Subtotals
Incinerator (1994)				$662,474	
Incinerator (2006) factor is 138.8/100			1.388	$919,514	
Instrumentation			0.1	$91,951	
Taxes			0.15	$137,927	
Freight			0.03	$27,585	
Direct Installation Costs are included in purchase costs					
Subtotal Direct Installation Costs					$1,177,000
Indirect Costs					
Engineering			0.1	$91,951	
Construction and Field expense			0.05	$45,976	
Contractor fees			0.1	$91,951	
Start-up			0.02	$18,390	
Performance Testing			0.01	$9,195	
Contingencies			0.03	$27,585	
Subtotal Indirect Installation Costs					$285,000
Total Installation Costs					$1,462,100
Direct Annual Costs					
Utilities					
	Fuel			$348,015	
	Electricity			$238,478	
Labour		hours work	rate of pay		
	Supervisor	8/week	$20/hr	$5,440	
	Labour	8/week	$16/hr	$4,352	
Maintenance					
	Labour	8/week	$25/hr	$6,800	
	Material	same as labour		$4,352	
Land Lease Costs ($5.75/ft^2 - toronto)				$8,500	
Subtotal Indirect Costs					$616,000
Indirect Annual Costs					
Overhead	0.6 of		0.6	$551,708	
Administration					
	Property Taxes		0.01	$9,195	
	Insurance		0.01	$9,195	
	Capital Recovery		0.16	$149,697	
Subtotal Indirect Costs					$719,800
Total Annual Costs					$1,335,800

Notes: a.) The operational costs calculated here do not include the cost to keep the systems hot during non-production working times (8 hours per day).

b.) All costs have been rounded to the nearest $100 to reflect the accuracy of the numbers.

All three thermal oxidation systems work on the same basic principles and perform similarly in terms of Regulatory Compliance and Operational Flexibility. The only real difference between

the three systems would be cost. Therefore, the only way in which to differentiate between each system is through cost.

A preliminary analysis of the costs of each of these systems indicates that the Recuperative type of thermal oxidizer is a much cheaper capital investment. However, the lower price also means a substantially reduced level of performance. The Regenerative system has substantially lower natural gas costs because of the heat exchange efficiency, while the Catalytic system has lower operational costs due to the lower reaction temperatures needed.

By performing a lifecycle analysis on these systems the true costs become apparent. This was done by using a discount rate of 3% which is outlined in the NIST Handbook 135 Life-cycle costing Manual for the Federal Energy Management Program [53]. Cost factors for energy requirements were determined from references found within the NIST Handbook [53]. Table 15 summarizes the results of these efforts, and the calculation methodology is presented in Appendices A for the capital and operational cost assessments of each thermal oxidation system, and Appendices E for guidance on how the lifecycle assessment was completed.

Table 15: Lifecycle costs for Regenerative and Recuperative RTO systems over a 10 year lifespan.

RTO Type	Case Study Cost
Recuperative	$14,319,941
Regenerative	$8,794,107
Catalytic	$6,192,087

As would be expected, the cheapest system to purchase is also the most expensive system to operate. This is primarily because of the heat exchange efficiency. Both the initial purchase cost of the RCO and the Regenerative type RTO are quite similar, having a difference of less than $200,000. However, operationally, the RCO is by far the most efficient to operate. This is because the reaction is run at a substantially lower temperature (meaning less natural gas is required to reach this operational temperature).

3.3.3 Operational Flexibility

The operational flexibility of thermal oxidation systems is moderate. Start-up times are dependent upon the time it takes to get the combustion chamber to reach the combustion temperature. From a dormant state, thermal systems typically take 4 to 6 hours to reach combustion temperatures.

In terms of load tolerance, thermal oxidative systems are generally good because they can destroy virtually all VOC compounds provided the combustion temperature is above the auto-ignition temperature of all species in the mixture. The problem comes when varying the emission concentration or total flow rate. In practice, some VOC mixtures have enough energy to sustain combustion, provided heat recovery of the system is at a sufficient level. Kohl and Nielsen provide a figure outlining this relationship, and from it, one can interpolate that at a heat recovery percentage of 95%, the VOC concentration would need to be approximately 3% of the LEL to sustain combustion [34]. This means, in theory no supplementary natural gas is required, thereby lowering operational costs. For example, if the VOC mixture was initially at a concentration of 3% of the LEL, and was lowered due to production changes, large amounts of supplementary natural gas will be required, and operational costs could become prohibitive (this is the case for the three sample facilities described here).

On the other hand, if emission concentrations are raised significantly due to production variations (above 25% LEL), dilute air may be required to be added to the system. This would increase the overall flow rate, changing design requirements, which will result in an in-efficient destruction of the VOC compounds.

Therefore, in terms of concentration changes, the system has a fairly wide range of tolerance. Conversely, as previously mentioned, thermal oxidation systems are not suited to highly variable flow rates. The design of the system incorporates the flow rate to establish appropriate residence times and mixing of the exhaust stream. As a result, changing the flow rate may result in the incomplete combustion of the emission. Simply put, thermal oxidation systems are intolerant to flow rate changes and tolerant to changes in concentration.

Lastly, thermal oxidation systems are limited to processes that continually operate. If continuous operation is not possible, systems can be run intermittently if the system is kept hot during off hours. This is accomplished by continuously combusting natural gas in the oxidation chamber. This prevents the bed cycling between hot and cold temperatures, which will prevent cracking of the heat exchanger beds.

Overall, operational flexibility scores for thermal technologies have been outlined in Table 16.

Table 16: Overall operational flexibility scores for thermal oxidation abatement technologies.

Abatement System	Start-up times	Continuous vs. intermittent operation	Flexibility: Flow tolerance	Flexibility: Conc. tolerance
RTO (Recup.)	2	2	1	3
RTO (Reg.)	2	2	1	3
RCO	2	2	1	3

3.4 Basic Design: Biological Oxidation

3.4.1 Regulatory Requirements

For the sample facility in this analysis the removal efficiency (termed destruction efficiency for RTO's) for biological oxidation processes is substantially lower than that of thermal oxidation and adsorption abatement techniques. Despite this, biological oxidation systems can meet regulatory thresholds. Meeting regulatory thresholds only refers to reducing the given facility's emission output for a specific contaminant below the prescribed limit. If the facility in question was emitting pollutants barely above the facility limits, then the level of reduction required would be quite small. For this reason, a removal efficiency of 50% or lower may be satisfactory. The only issue this may present is if regulatory thresholds are substantially lowered in the future. If this is the case, the biological system may not be able to meet future limits, causing the possibility of non-compliance and extra cost.

3.4.2 Lifecycle Costs

Operational costs are normally quite low for these systems because the temperature and pressure will remain close to ambient conditions. The largest energy input is the power required to circulate the emission through the bed. Therefore, provided the bed is maintained appropriately,

the operational cost should not be high. The problem comes when assessing the overall space requirement for these systems. Mass transfer limitations require that contact areas (bed surface areas) are large. After associating the required space with an appropriate monetary value (lease or purchase cost), the lifecycle cost of this system can become prohibitive. Tables 17 and 18 summarize the capital and operational costs, while Table 19 summarizes the calculated 10 year lifecycle cost. The costing process used to calculate the biofilter capital and operational costs were referenced from Devinny, Webster, and Dehusses's book entitled: "*Biofiltration for Air Pollution Control*" [24]. Furthermore, the lifecycle analysis was determined using a discount rate of 3% which is outlined in the "*NIST Handbook 135 Life-cycle costing Manual for the Federal Energy Management Program"* [53]. Cost factors for energy requirements were also determined from within the NIST Handbook[53].

Table 17: Open Bed Biofilter Capital Cost Summary

Capital Costs	
Site Costs	
Airflow (Q) m^3/hr:	101940.65
EBRT (assume 60 seconds = 60 sec/3600 sec/hr) (hr)	0.0139
Volume (m^3):	1415.84
Assume 20% safety factor (increase V by 20%)	1699.01
Height (m)	1.061881747
Length x Width (m)	40x40
Area (ft^2)	17222.25667
Gravel Requirements height (m):	0.30
Gravel Requirements Volume (m^3) (varying dimensions)	480.00
Total Volume Required	2179.01
Total Site Cost(based on equipment, labour, overhead/profit)	$15,500
Media Costs	
Assume $37/m^3 for compost	$80,623
Assume $33/m^3 for gravel	$71,907
Assume $2.5/m^3 installation costs	$5,448
Total Media Costs	$158,000
Equipment Costs	
Assume one blower:	$7,500
Assume one bed tower humidifier:	$6,000
Piping (10% of capital Costs):	$17,350
Electrical (4% of Capital Costs):	$6,940
Equipment Install (4% of Capital Costs):	$6,940
Engineering Design (10% of Capital Costs):	$17,350
Liner Cost (Area + L x H x 2 + W x H x 2)	$193,965
Total Equipment Costs	$256,045
Total Equipment + Site + Media Costs	$429,545
Land Cost (5.75 per ft^2 - industrial land cost for toronto)	$1,188,336
Total Capital Costs	$1,617,800

Note: All costs have been rounded to the nearest $100 to reflect the accuracy of the numbers.

Table 18: Annual Biofilter (Open Bed) Operational Costs.

Operating Costs	
Electricity	
Superficial Velocity (flowrate / area) (m/s)	1.20
Pressure drop (P=au^b) (Pa/m)	7597.68
Pressure drop (Convert from Pa/m to inches water)	22.43
Blower horsepower (0.00025 x flowrate x pressure drop)	351.42
Blower (Hp x 0.75 kW x operation hours (240 days)) (kWh)	1012083.53
Annual Pump Electrical (assume 2 HP) (kWh)	7200.00
Total Cost (kWh x price per kWh - $0.08):	$81,543
Water	
Assume inlet air is 50% saturated, estimated that 72 m^3 required	
Total Water used: 72m^3/week x 52 weeks	3744.00
Cost of water $0.7/m^3	$2,621
Miscellaneous	
Labour (assume 2 hours per day @ $20/hr)	$12,000
Overhead (25% of Labour)	$3,000
Total Miscellaneous Cost:	$15,000
Total Operating Costs:	**$99,163**

Table 19: Biofilter (Open Bed) 10 year Lifecycle Costs.

Abatement System	Case Study Costs
Biofilter	$11,644,813

3.4.3 Operational Flexibility

The key to understanding biological oxidative technologies is in performing complete and thorough literature search to determine experimental parameters such as the removal efficiencies for specific contaminant and media configurations. These experimental parameters are then used to create a pilot design for testing. Once the pilot system is tested a better understanding of the overall performance can be established. In this analysis, the cost of performing trials is not explicitly outlined, however, it is considered as part of the engineering design fees. Operational considerations, like how robust the system is, start-up times, and load tolerance can be tested and evaluated before the implementation of a full scale system is undertaken.

That being said, biological systems are not quite as robust as other systems. Times required to achieve steady state performance may vary between several days to several months [24]. This is specifically due to the kinetics associated with biological processes and start-up conditions.

Biofilters are not very tolerant of load variations either. In biofilters, the main source of energy for the microbial population's anabolic and metabolic processes comes from the VOC that is fed to the biofilter[23]. Therefore if there is a large decrease in VOC loading, the microbial population may begin to starve. If the microbial population does die, the entire bed would require replacement or re-inoculation. This in effect, would cause a significant disruption in production and could be a very expensive endeavour.

If the VOC load is increased one of two problems may occur:

1. The microbial population cannot destroy enough of the VOC emission to maintain the regulatory limit because they have reached their maximum destruction capability; and/or,
2. The microbial population's growth rate rapidly increases, substantially increasing microbial wastes in the media, potentially creating a toxic environment for the microbial population.

Both situations would result in significant issues that would require considerable resources to remedy.

Biofilters can be somewhat resilient to intermittent operation, provided some contaminant has been absorbed into the media. This adsorbed contaminant can be utilized by the microbial population during downtime, or off shift periods. The actual level of resilience cannot be quantified unless pilot studies are completed. The table below outlines the Biofilter's operational flexibility scores.

Table 20: Operational flexibility scores for the biofilter.

Abatement System	Start-up times	Continuous vs. intermittent operation	Flexibility: Flow tolerance	Flexibility: Conc. tolerance
Biofilter	1	3	1	1

3.5 Basic Design: Adsorption System

3.5.1 Regulatory Requirements

Similar to the thermal oxidation systems, removal efficiencies can be quite high and provided the system is sized appropriately, it should always be able to reduce the contaminant loading well below the regulatory threshold. Realistically, because this system will have removal efficiencies close to 95%, there should not be a problem in meeting future regulatory thresholds that are more stringent then current thresholds.

3.5.2 Lifecycle Costs

The principal operation of this system is solvent recovery. For the purposes of the sample facilities described, solvent recovery will not be considered possible because the quality of the product will likely be poor. However, this system may still be economically competitive with other abatement systems once the true lifecycle costs for the system have been established.

As with the thermal abatement systems, the lifecycle costs can only be established after capital and operating costs are determined. In this case, capital costs were established using the *EPA Air Pollution Control Cost Manual* [1], and the operational costs were established using the procedures outlined in *Air Pollution Control: A Design Approach* [32].

Lifecycle costs were then established using a discount rate of 3% which is outlined in the NIST Handbook 135 Life-cycle costing Manual for the Federal Energy Management Program [53]. Cost factors for energy requirements were determined from within the NIST Handbook [53]. Table 21 below describes the calculated capital and operational costs, whereas Table 22 outlines the lifecycle costs associated with adding an adsorption system to the three sample facilities described in this work.

Table 21: Adsorption system cost analysis

Purchased and installed equipment costs:					
			Factor	Cost	Subtotals
Vessel Cost				$99,500	
Carbon Cost				$22,700	
Equipment Cost (1994 Costs)				$166,948	
Equipment Cost (2006 Costs) - factor:			1.621	$270,623	
Taxes			0.15	$40,593	
Freight			0.03	$8,119	
Foundations and Support			0.08	$21,650	
Handling and Erection			0.14	$37,887	
Electrical			0.04	$10,825	
Piping, Painting and Installation			0.04	$10,825	
Subtotal Direct Installation Costs					$400,522
Indirect Costs					
Engineering			0.1	$27,062	
Construction and Field expense			0.15	$40,593	
Start-up and Performance testing			0.03	$8,119	
Contingencies			0.03	$8,119	
Subtotal Indirect Installation Costs					$83,893
Total Installation Costs					$484,415
Direct Annual Costs					
Utilities					
	Steam (Gas Cost)			$4,363	
	Water Cost			$7,001	
	Electricity (system fan + cooling fan)			$40,851	
Labour		hours work	rate of pay		
	Supervisor	8/week	$20/hr	$5,486	
	Labour	15% of labour		$823	
Maintenance					
	Labour	8/week	$25/hr	$6,857	
	Material	same as labour		$823	
Solvent Disposal		$300/drum		$166,300	
Subtotal Direct Costs					$232,504
Indirect Annual Costs					
Overhead	0.6 of		0.6	$162,374	
Administration					
	Property Taxes		0.01	$2,706	
	Insurance		0.01	$2,706	
	Capital Recovery		0.16	$44,057	
Subtotal Indirect Costs					$211,843
Total Annual Costs					$444,300

Note: The total cost has been rounded to the nearest $100 to reflect the accuracy of the numbers

Table 22: Lifecycle costs for adsorption abatement systems.

Abatement System	Case Study Costs
Adsorption	$3,060,874

3.5.3 Operational Flexibility

The adsorption process takes place at near ambient pressure and temperature meaning there is no need for a preheating or pre-pressurizing step before the system can be put into operation. Therefore as long as enough carbon beds are available for operation, start-up times will be fast.

The design of adsorption systems is quite specific. The carbon requirement dictates the overall load that can be treated, and once the system is sized it is very difficult to make alterations for different loading levels or different flow rates. Therefore if the load is increased substantially, the system will not be able to handle the increase in load unless the overall configuration of the system is changed. More carbon would have to be added (new bed added), cycling and regeneration times would have to be re-calculated, and in extreme cases these changes may not be feasible. On the other hand, if the load was reduced substantially, the system would simply last longer per cycle – essentially taking up more facility space then required.

Moreover, changes in load composition pose other unique problems. The original design of these systems relies on the adsorption characteristics between the most difficult species to adsorb. If a new compound was included into the emission mixture, and this new compound was more difficult to adsorb than the assumptions used in the original design, a breakthrough situation may occur during operation. This simply means the system would have to be redesigned according to the new compound's adsorption characteristics.

Conversely, this system can operate both continuously and intermittently. This offers the advantage of not using extra energy to operate the system when production is down, or to start-up the systems when production times fluctuate substantially.

Overall, adsorption systems are moderately tolerant to flow rate variations, fairly intolerant to changes in emission composition, and very tolerant to intermittent vs. continuous operational strategies. Table 23 outlines the operational flexibility scores for adsorption based VOC abatement technologies.

Table 23: Operational flexibility scores for adsorption abatement systems.

Abatement System	Start-up times	Continuous vs. intermittent operation	Flexibility: Flow tolerance	Flexibility: Conc. Tolerance
Adsorption	3	3	2	1

Chapter 4: SOFC Integrated VOC Abatement System

Solvent based coating operations emit substantial amounts of volatile organic compounds. These compounds detrimentally affect the health of both plant and animal life, and negatively impact local air quality. For this reason, governments have been consistently increasing regulatory pressure on these facilities to handle their emissions more responsibly. Although current VOC abatement technologies have proven to be effective, they require significant monetary and operational investments. Therefore, it is particularly important to develop VOC abatement systems that have reduced operational costs while providing emission reductions comparable or better than current technologies.

4.1 Overall System Configuration

In this research, the development of a hybrid SOFC abatement technology is investigated. The basic processes occurring are:

1. Isolation and concentration of VOC compounds from a solvent based coating process emission using adsorption recovery technologies,
2. Reforming of the VOC compounds to form a mixture primarily consisting of hydrogen and carbon monoxide; and,
3. Oxidation of hydrogen and carbon monoxide to water and carbon dioxide by air through a solid oxide fuel cell.

The overall process flow was presented as Figure 1 in Chapter 1 of this thesis. It is reproduced here in the figure below.

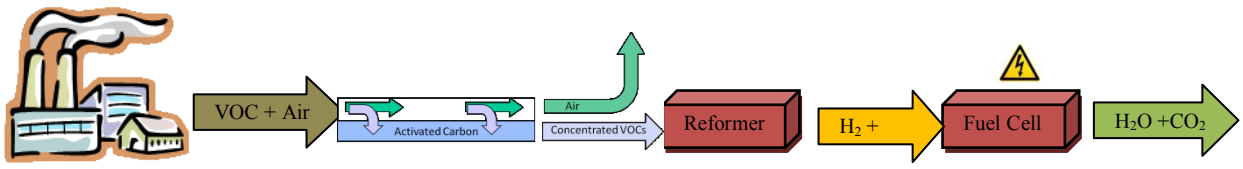

Figure 16: Schematic representation of the SOFC-VOC hybrid VOC abatement system.

Each of the process steps require in-depth analysis to ensure the processes can be integrated together as a single functioning technology.

4.1.1 Problem Definition

As previously mentioned, the design of this system will be based upon the facility profile presented in Section 3.2. In this manner, the SOFC hybrid abatement system can be compared to other more commonly used technologies.

To re-iterate, the main constraint of this system is to ensure VOC concentrations will be maintained below the current and foreseeable regulatory thresholds. The two criteria of this system is lifecycle cost, and operational flexibility (both of which have been defined in Section 3.1).

4.2 Model Based Design of the Hybrid SOFC Abatement System:

Model based design methodologies are used because they can rapidly examine system parameters of chemical processes to provide detailed information about process performance. In the end, these types of analysis will facilitate pilot project development, and allow for rapid development of full scale production facilities. The software package being used for the model design of the Hybrid SOFC Abatement System under development in this project is *Aspentech HYSYS.*

HYSYS is a commercial process simulator that contains a rigorous thermodynamic and physical property database. It also provides comprehensive built-in process models that address a wide range of steady-state and dynamic operations. Overall, it offers a convenient and time saving means for system modeling, integration, and optimization.

The challenge in the development of this particular model in *HYSYS* is that it does not contain separate models for the SOFC, reformer, or the adsorption system. In particular, the SOFC system provides its own challenges. This is because *HYSYS* does not account for ion movement across a membrane, nor does it include electrochemical reactions. In the literature, the most

common approach to modelling SOFC systems is to develop an SOFC stack model in a programming language such as FORTRAN, C++, or Visual Basic, then integrate these proprietary models into a well known flowsheeting software package such as Aspen Plus, or *HYSYS* [54]. The purpose of linking these models to the flowsheeting software is to allow integration with the balance of plant components such as heat exchangers, condensers, and turbines. Using proprietary models for SOFC development limits the accessibility to those researchers building and testing such systems, and more importantly, will not allow for alteration of the model, if validation of the model is unsuccessful with the given researcher's experimental results.

The method developed here is to fully utilize the functions within *HYSYS* to create all system components. There is no use of user defined code, and the system will run using only the *HYSYS* models. The advantage of this methodology is a reduction in computation times, ease of use, and the ability to perform rapid parametric, thermodynamic, and statistical analysis on the overall system. Overall, the result of this work will be a very simple model that can provide a holistic analysis of VOC abatement by a SOFC hybrid abatement system.

4.2.1 Model Structure

The Hybrid SOFC model is constructed of one main model, separated into four separate flowsheets. The Subflowsheets, or Subsystems, are listed below:

1. Adsorber Subsystem (Figure 18);
2. Heat Exchanger Subsystem (Figure 24);
3. Reformer Subsystem (Figure 25) ; and,
4. SOFC Stack Subsystem (Figure26).

The main flowsheet is presented below in Figure 17. The flowsheets representing each sub-system are discussed separately.

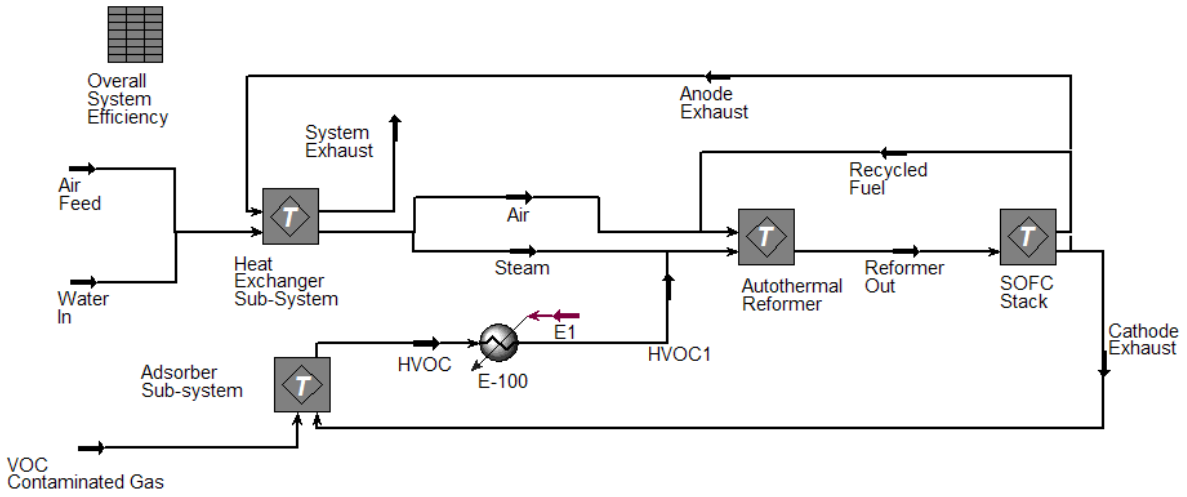

Figure 17: Main Flowsheet for the Hybrid SOFC Abatement System Model.

The overall process is as follows:

1. Contaminated gas enters the Adsorber Sub-System:
    a. Contaminated gas is separated into VOCs and air;
    b. Decontaminated air is exhausted to the atmosphere, and the VOC stream becomes humidified because it is purged from the adsorber using hot steam.
2. Heat Exchanger Sub-System:
    a. The *Humidified VOC Stream* is sent to the Heat Exchanger Sub-System for preheating by the hot anode exhaust gases coming off the SOFC;
    b. Heat from the *Anode Exhaust Stream* is used to preheat air and water streams.
3. The *Humidified VOC Stream*, *Recycled Fuel Stream*, *Preheated Air Stream*, and *Preheated Steam Streams* enter the Auto-Thermal Reformer Subsystem:
    a. The Auto-thermal reformer consists of one POX reactor and one Steam Reformer;
    b. The *Air Stream*, *VOC Stream*, and the *Recycled Fuel Stream* are all sent to the POX reactor;
    c. The reformate (rich in H_2 and CO), energy from the POX reactor, and steam, sent to the Steam Reformer for complete conversion;
    d. The final reformate consists of carbon monoxide, hydrogen, trace VOCs, steam, and excess air.

4. The Reformate enters the SOFC stack:
    a. The Reformate is sent to the SOFC stack;
    b. Pre-heated air is sent to the cathode;
    c. SOFC stack calculations are completed in two worksheets – one to calculate the required air ratio, and one to calculate SOFC performance;
    d. Anode exhaust is sent to the Heat Exchanger Sub-System for heat recovery;
    e. Cathode exhaust is sent to the adsorber for heat recovery.

4.2.2 Modeling the Adsorber Sub-System

Modeling an adsorption system in *HYSYS* presents interesting complexities. To begin, there are interphase transport issues, uncertainty in equilibrium effects, and uncertainty in the effect that each component may play upon one another during multi-component adsorption. These are only a few of the issues, without even considering the dynamic aspects of the process.

For this reason, much of the background rigor was simplified and calculated outside of *HYSYS*, with the results of these analyses being plugged into simple *HYSYS* system models made to represent the overall steady-state adsorption-desorption system.

In the figure below, the *HYSYS Component Splitter* represents the steady-state adsorption cycle, and is used to separate the air stream from the VOC stream. The concentrated VOC stream is then sent to a *Mixer* model which combines steam to the concentrated VOC stream. This simulates the anticipated desorption stream. A *HYSYS Condenser* model is then used to remove the excess water from the desorption stream. This minimizes the flow rate of feed to the Reformer Subsystem, but more importantly, increases the VOC concentration to represent approximately 40% of the feed.

In this particular case, the painting operation cycle is 16 hours per day, whereas the SOFC should be operated continuously (24 hrs per day). This will prevent having to thermally cycle the SOFC, which could cause damage to the many of the components such as the ceramic electrolyte or interconnect materials. For this reason, a *HYSYS Tee* model will be used to simulate the

removal of some VOC for storage (and use during shutdown periods), while the rest of the desorption flow is sent to the Reformer Subsystem.

The overall *HYSYS* model is presented in the figure below. The theoretical background and justification for the inputs are presented in the following discussion.

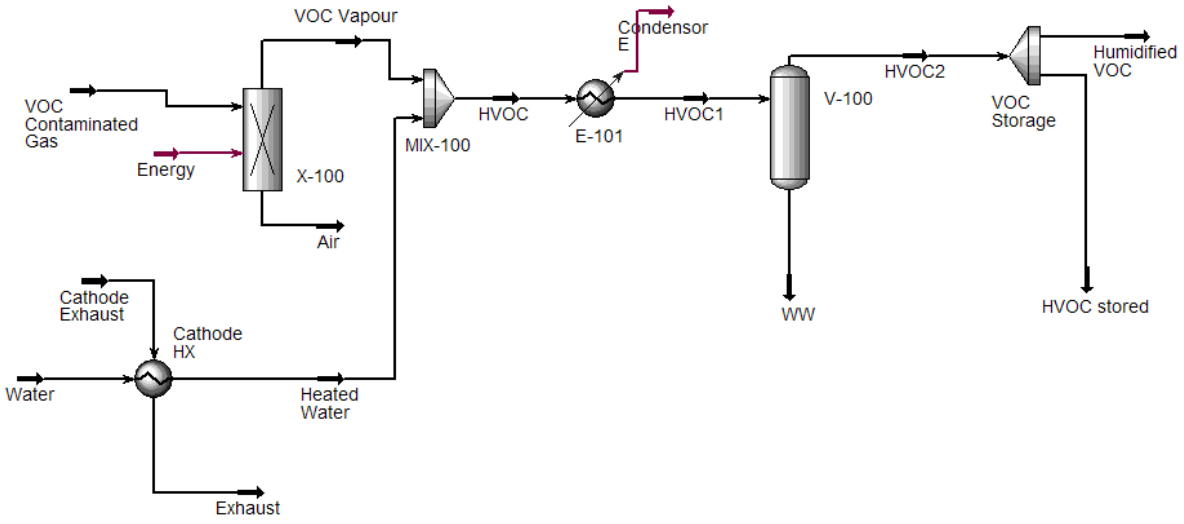

Figure 18: *HYSYS* flowsheet of the adsorption system.

In order to pre-concentrate the VOC emission stream, an adsorption system will be used. To develop adsorption and desorption parameters, the isotherm relationships for the target molecule and adsorption material must be reviewed. The simplest and still most useful adsorption isotherm equation is the Langmuir Equation [26, 31]. This Equation is of the following form:

$$q = \frac{aP_i}{1+bP_i} \qquad \textbf{Equation 29}$$

In Equation 29, q refers to the adsorbent loading (kg adsorbate/kg adsorbent), P_i refers to the partial pressure of the adsorbate, and a and b are both the Langmuir parameters. In normal situations, experimental determination of the isotherm on appropriate adsorbents would be

performed. With isotherms developed, a prediction of capital and operational requirements could be made for each adsorbent. Once selected, the adsorption system would be optimized and put into use. For this study the Langmuir isotherm parameters were obtained from literature, and these were used to calculate the adsorption isotherms for each of these compounds on activated carbon. The characteristics of the activated carbon are listed in the table below.

Table 24: Solid Adsorbent Physical Characteristics [55].

Parameter	Value
Surface Area (m^2/g)	1,100 – 1,200
Particle Density (kg/m^3)	720
Bulk Density (kg/m^3)	400
Particle Porosity	0.67
Bed void Fraction	0.44

Table 25 summarizes the Langmuir parameters for the MEK, Toluene, and Xylene on for the adsorbent material noted in Table 24.

Table 25: Langmuir isotherm parameters from various sources [55, 56].

Compound	Parameter a	Parameter b	Reference [55, 56]
Methyl Ethyl Ketone	1,301,120	402,450	Takeuchi and Shigeta, 1990[55]
Toluene	50,557	12,014	Yun, Choi, and Kim, 1999[56]
Xylene	263,817	72,384	Yun, Choi, and Kim, 1999[56]

As stated above, the Langmuir parameters allow for determination of an adsorption isotherm, which itself will be used to establish the operational parameters of the system. The adsorption isotherms for the compounds of concern (Toluene, Xylene, and MEK) in the emission stream are presented in three figures below.

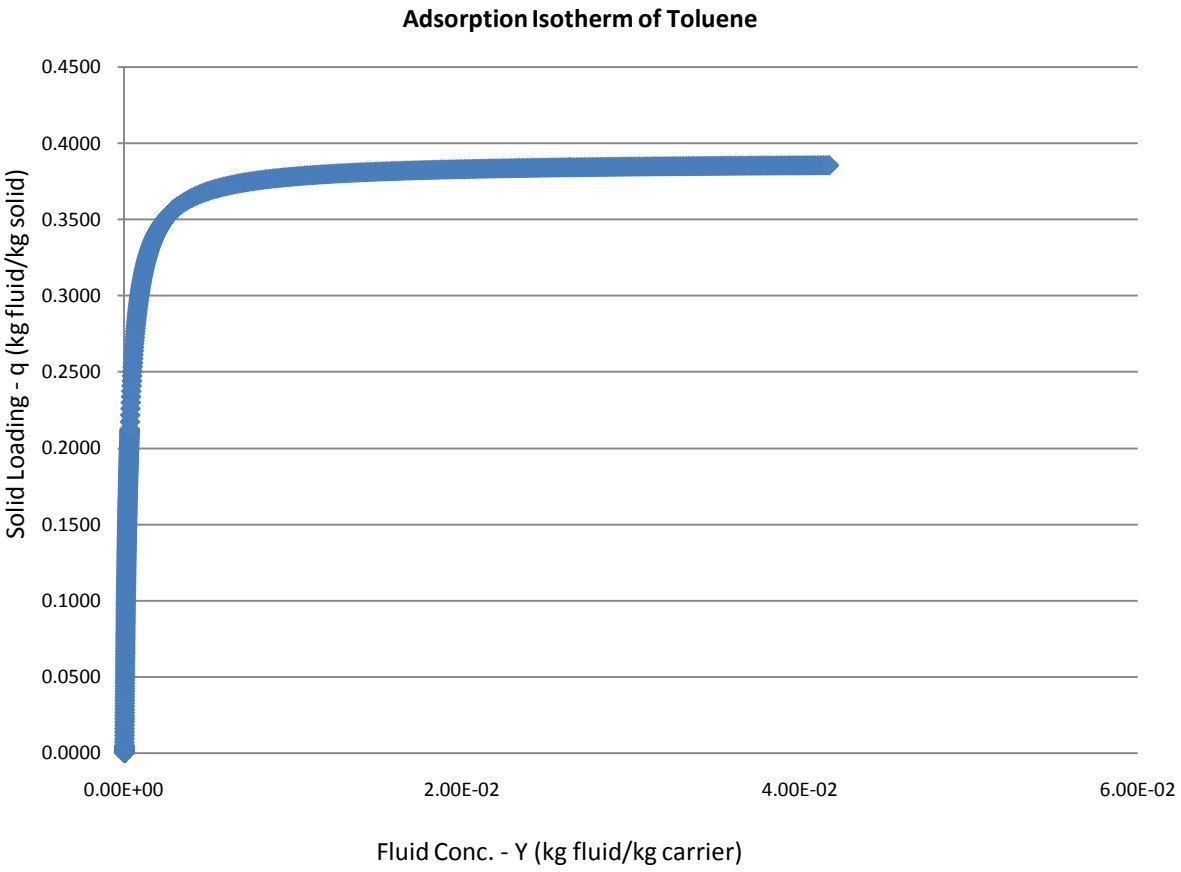

Figure 19: Calculated Adsorption Isotherm for Toluene.

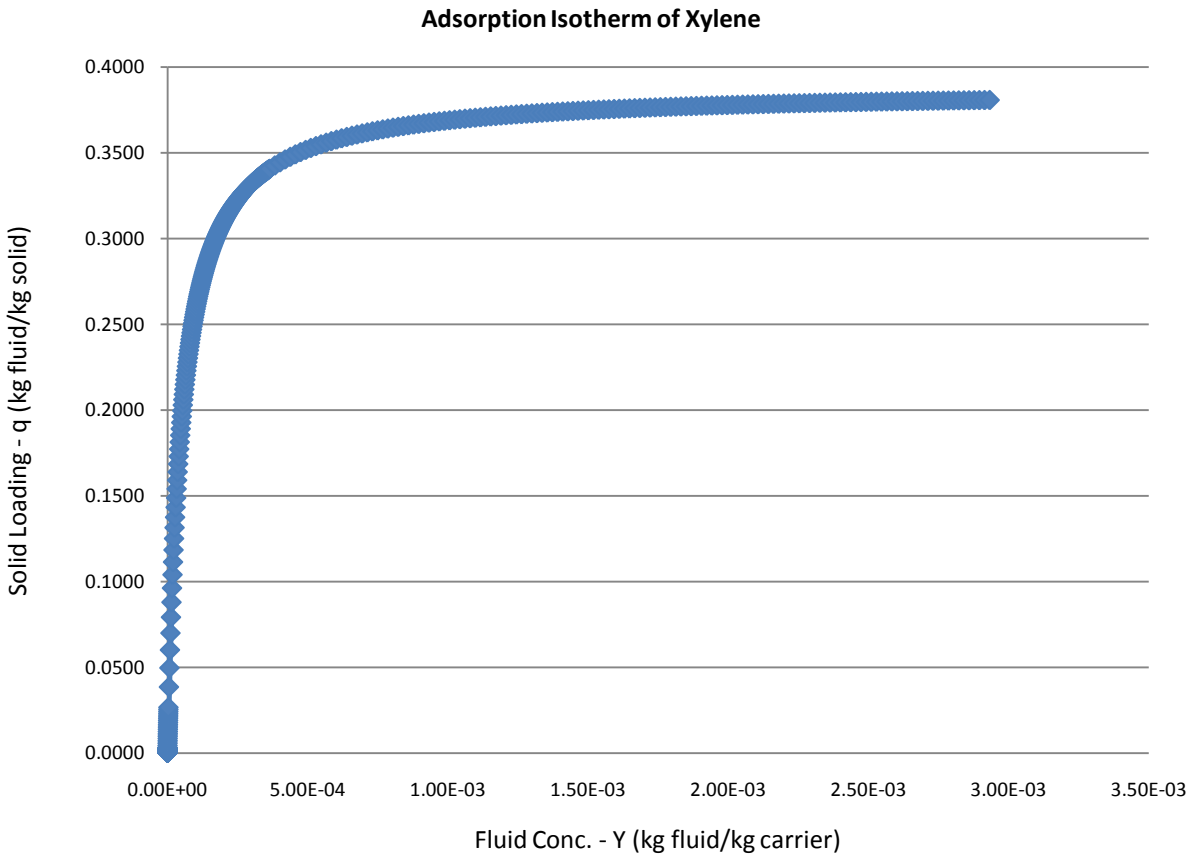

Figure 20: Calculated Adsorption Isotherm for Xylene.

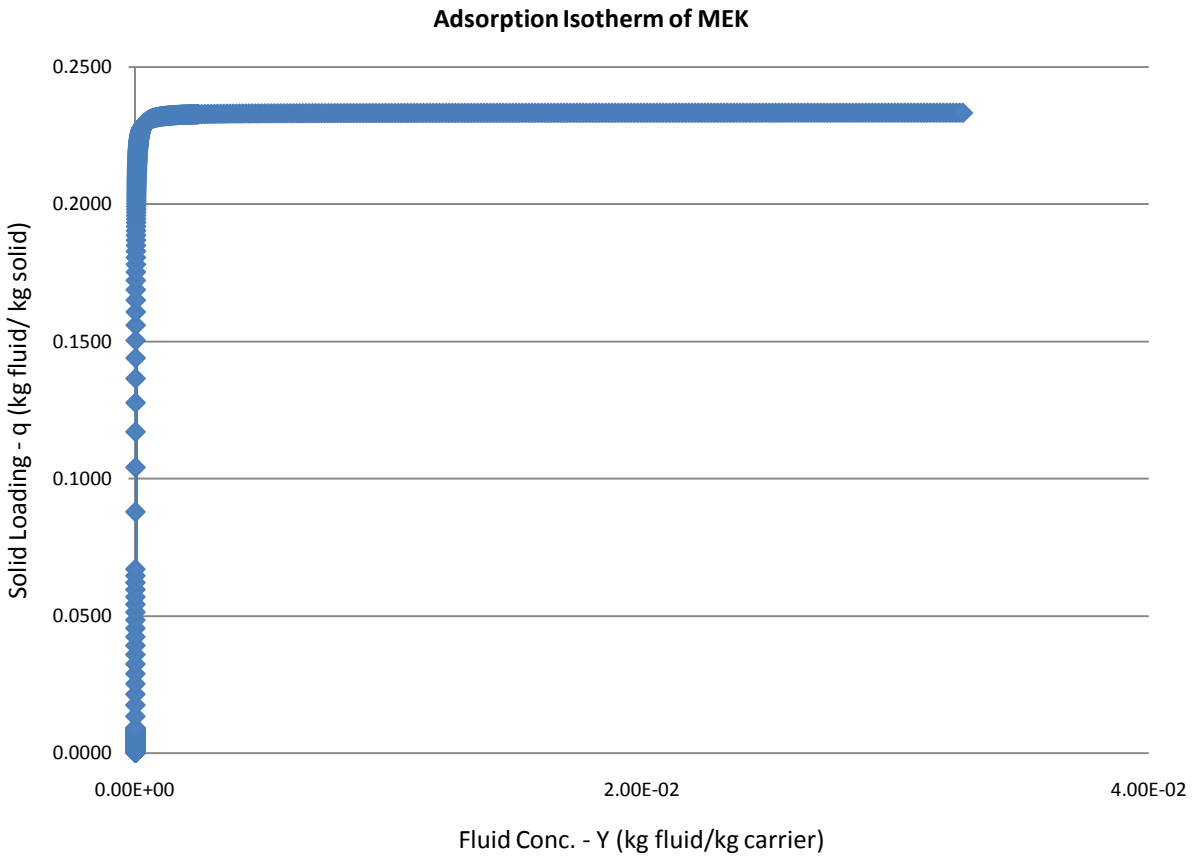

Figure 21: Calculated Adsorption Isotherm for MEK.

Here the adsorption isotherms can inevitably lead to insight regarding both the adsorption and desorption characteristics of the adsorption system. If one wanted to determine an actual mass balance for an adsorption operation, the result would lead to partial differential equations in the dependant variables q (mass loading kg adsorbate/kg solid) and Y (gas phase concentration – kg adsorbate/kg carrier), and the independent variables t (adsorption time) and z (distance down the adsorber) [57]. This can become cumbersome and complicated. It is actually much faster to develop operational relationships based upon experimental isotherms to predict adsorption system performance. In this research, the method outlined by Basmadjian, in which operational diagrams are developed from the adsorption isotherms to develop simple algebraic and differential relationships to predict various process parameters is used [57]. Although somewhat limiting, these expressions can estimate very useful information about the performance of the adsorption system. Furthermore, the accuracy of this information can be extended if it is used in

conjunction with mass transfer correlations. In the following discussion, adsorption parameters will be developed for the emission stream described in Table 8. These parameters are listed below:

1. Adsorbent requirement:
    a. Overall mass and volume of adsorbent required; and,
    b. Preliminary Development of bed dimension requirements.
2. Adsorption Parameters:
    a. Adsorption time – breakthrough time;
    b. Estimated Length of the Mass Transfer Zone;
    c. Final Dimension of beds; and,
    d. Number of adsorption beds.
3. Desorption Parameters:
    a. Desorption time;
    b. Desorption temperature; and,
    c. Purge requirements.

Adsorbent Requirements

The adsorption isotherm can be used to determine the adsorbent capacity. This in turn will determine how much total adsorbent (what weight and volume) will be required to adsorb the total emission stream. For this particular case, the emission stream is seen to contain a total of 100 annual tonnes of a mixture of toluene, xylene, and MEK. This annual amount can be broken down into a daily (or hourly) mass of adsorbate by knowing what the operational cycle of the emitting facility is. In Table 7, the operating cycle for the case study facility is 240 days (16 hours per day) and the daily mass of adsorbate emitted is calculated below:

Total mass of adsorbate per annum	100 (tonnes/year)
Emission rate of VOCs per day	100 (tonnes/year) x 1/240 (year/days) x 1000 (kg/tonne) = 417 kg/day of VOCs
Emission rate of VOCs per hour	417 kg/day of VOCs x 16 hrs/day = 26 kg/hr

To determine the mass of adsorbent needed to completely remove 417 kg VOC /day from the emission stream, the loading value from the adsorption isotherm needs to be utilized. This value (q) denotes the amount of adsorbate that can be adsorbed on the adsorbent at a given component concentration at a fixed temperature. In our case, we will be using the pure component isotherm for each compound, and assume that each particular compound is the only substance in the emission stream. For example, to calculate the required adsorbent for xylene, it will be assumed that the VOC emission stream is composed of 100 tonnes of xylene. This calculation is repeated for each compound separately. The amount of adsorbent for each compound is then compared, and the highest value will be the one used for the adsorption system design. The only issue with this calculation is that over time, and after repeated adsorption-desorption cycles, the capacity of the adsorbent will decrease. This is because some of the adsorbate from the initial cycles will be very difficult to remove, and in essence be considered permanently adsorbed onto the adsorbent. Therefore a best practice in the design of adsorption systems is to add a safety factor of two to the calculated amount of adsorbent required [1]. These calculations are summarized in the table below.

Table 26: Calculated mass and volume of adsorbent required.

Compound	Loading (kg fluid/kg solid)	Adsorbent Density (kg/m^3)	Total Adsorbent required (kg)	Actual Adsorbent Required (kg)	Volume Adsorbent (m^3)
Toluene	0.161	400	2,613	5,228	13.07
Xylene	0.334	400	1,251	2,502	6.26
MEK	0.225	400	1,854	3,709	9.28

Table 26 summarizes the total mass of adsorbent required to adsorb 100 tonnes of an emission composition matching that in Table 7. In this particular case the value for Toluene would be use, which is 5,228 kg. This mass corresponds to a volume of approximately 14 m^3. This volume allows for determination of the overall adsorption system dimensions. For this particular application, several orientations are plausible, and can be determined by considering the bed thickness and diameter comparison to the volume flow of emission being treated (60,000 cfm from Table 7). The normal recommendation is to keep the bed thickness small, between 1 and 2 m or smaller, and the superficial velocity around 1 m/s [1, 32, 57]. This will minimize the pressure drop through the bed and ensure appropriate residence time in the adsorbing bed.

The calculations used to determine the preliminary bed orientations and dimensions are presented below.

Required Volume of Bed	14 m^3
Given Volume Flow	60,000 cfm = 101,940 m^3/hr = 28.4 m^3/s
Area Required to have a superficial velocity of 1 m/s	28.4 m^2
The required radius for 1 adsorption bed	$(28.4m^2/ \pi)^{0.5}$ = 3.01 m
The required radius for 2 adsorption beds	$(28.4m^2/(2\pi))^{0.5}$ = 2.13 m
The required radius for 3 adsorption beds	$(28.4m^2/(3 \pi))^{0.5}$ = 1.74 m
Calculated bed thickness	14 $m^3/28.4m^2$ = 0.49 m

The calculations above illustrate that different numbers and orientations of adsorption beds are feasible, provided that the overall adsorbable area of the bed is fixed. The decision of which orientation to use will fall upon the end user, but typically, if higher pressure operations are desired, adsorption beds of smaller diameters are preferred. For this project, the system will be run at atmospheric pressure, and therefore only one adsorbing bed will be used.

Adsorption Times and Operational Diagrams

Adsorption cycle times are normally calculated by developing breakthrough curves. A breakthrough curve refers to the amount of time needed for a given concentration of fluid to escape the outlet of the adsorption bed [58]. In ideal conditions, the adsorbate molecules will fill up the sites one by one, until the entire adsorption bed is saturated. Once that happens, the total feed concentration will suddenly emerge from the outlet of the bed at one time. Unfortunately, this does not happen in practice, and some portion of the adsorbate will be seen at the adsorption bed outlet before the entire bed has been saturated. This occurs because there is a finite resistance to mass transfer between the adsorbate gas and the solid [58]. Therefore a finite amount of time is needed for each particle to be loaded with adsorbate [58]. This infers that mass transfer must somehow be incorporated into actual isotherm determination.

Another issue is in regards to the effect that temperature has on the adsorption-desorption processes. For adsorption, increasing temperature will decrease adsorption capacity. In practice,

adsorption is known as an exothermic process, and therefore, a temperature rise would be expected during operation. Therefore, before adsorption breakthrough times can be established, the temperature rise expected must be estimated so realistic inferences can be made whether the process will operate under isothermal or adiabatic conditions. Basmadjian developed a very simple relationship to predict the maximum temperature rise expected from the adsorption process [57]. This expression is presented below:

$$\Delta T = \frac{q\Delta H/C_{pb}}{(q/Y)_F - C_{ps}/C_{pb}} \qquad \textbf{Equation 30}$$

In Equation 30, ΔT refers to the temperature rise due to the adsorption process, q refers to the solid phase loading, $(q/Y)_F$ refers to feed conditions, ΔH refers to the heat of adsorption, C_{pb} refers to the heat capacity of the carrier fluid, and C_{ps} refers to the heat capacity of solid.

Using Equation 30, the maximum temperature rise for the adsorption process of all three solvents (MEK, Toluene, and Xylene) is presented in Table 27.

Table 27: Maximum expected temperature rise for pure component adsorption based of major solvents in the VOC emission.

Parameter	Toluene	Xylene	MEK
q	0.161	0.334	0.225
ΔH	344 kJ/kg	235 kJ/kg	277 kJ/kg
C_{pb}	1.012 kJ/(kg*K)	1.012 kJ/(kg*K)	1.012 kJ/(kg*K)
C_{ps}	33.18 – 55.8 kJ/(kg*K)	33.18 – 55.8 kJ/(kg*K)	33.18 – 55.8 kJ/(kg*K)
$(q/Y)_F$	869	1,225	1,054
ΔT (calculated from Equation 30)	0.065 K	0.065 K	0.060 K

According to the calculations developed above, the maximum temperature rise expected during the adsorption process is minimal, and thus the process can be considered isothermal.

As discussed earlier, the use of operational diagrams can predict realistic operation if a physical understanding of the process is developed. In this particular case, all three compounds, Toluene,

Xylene, and MEK exhibit what is known as a Type I isotherm (shape is concave down). During adsorption, solutes that exhibit Type I isotherm character will take the form of a rectangular discontinuity (at equilibrium, neglecting mass transfer effects); meaning that a sudden mass of solute will move through the bed [57]. Using this relationship, Basmadjian was able to develop a simple design equation that relates adsorption time, with bed thickness, fluid and bed densities [57]. This was done by equating the cumulative amount of solute adsorbed at a given time, with the cumulative amount of solute adsorbed over a given distance in the bed. The result is the following Equation:

$$V = \frac{z}{t} = \frac{\rho_f v}{\rho_b \Delta q / \Delta Y} \qquad \textbf{Equation 31}$$

In Equation 31, V refers to the propagation velocity of sorption front, z is the distance into the adsorber bed, t is time, ρ_f is the fluid density (air), v is the superficial velocity through the bed, ρ_b is the bed density, Δq is the mass loading of solvent in the solid phase, and ΔY is the concentration of the pollutant in emission stream. Interestingly enough, a similar expression will be obtained from use of the local equilibrium model. In this model, the material balance for the adsorbate is solved assuming that there is no concentration gradient within the particle or the film surrounding the particle [59].

By rearranging Equation 31 to isolate t, and replacing z with L – length of the adsorber bed, the adsorption time can be determined for adsorption of a Type I system. For the components in this study, this method has been utilized to obtain an approximation of adsorption times assuming the process goes to completion. These values have been compiled in Table 12 below.

Table 28: Adsorption times for VOC compounds in the emission stream.

Compound	Conc. P_i	Conc. ΔY	Δq	T_{ads} (hrs)
Toluene	5.82×10^{-5}	1.86×10^{-4}	0.161	78
Xylene	8.57×10^{-5}	3.14×10^{-4}	0.334	95
MEK	6.70×10^{-5}	1.67×10^{-4}	0.225	121

If transport resistance is not considered, the adsorption phase of the entire process will appear to be instantaneous [58]. As previously stated, this means that the entire feed concentration will suddenly appear out of the adsorber bed outlet once the working capacity of the adsorber bed has been reached. In actuality, this does not happen, and transport resistance works to elongate the contaminant front that is moving through the bed. The result is that the leading edge of the contaminant front is composed of a concentration gradient. This area is termed the Mass Transfer Zone (MTZ). The length of the MTZ is dependent upon transport resistance, and as would be expected determines the minimum depth the bed can be. If the MTZ is larger than the bed depth, premature breakthrough would result, resulting in non-compliant operation.

In typical adsorption system design, a breakthrough concentration is decided upon that can be used as a marker to indicate a safe time in which the beds can be switch over to the regeneration phase of the process. In this particular case, the breakthrough concentration will be considered to be 0.01 (or 1%) of the feed concentration.

To account for transport resistance, design charts developed by Hiester and Vermeulen, and modified by Basmadjian were used [57]. These design charts allow for the system behaviour to be expressed as dimensionless parameters related to fractional saturation (breakthrough concentration of 1% in our case) and depletion of medium, its dimensions and transport resistance, time scale and fluid throughput, and the equilibrium isotherm itself .

To utilize these design charts, there are three parameters that must be identified. The first is the separation factor (r), the second is a dimensionless time variable (T) which refers to the breakthrough time, and third is the dimensionless distance (N) which is a parameter that incorporates transport resistance effects into the mass transfer zone. Each of these is explained in detail below.

The separation factor is simply a measure of how favourable the equilibrium isotherm performs. In the case at hand, three isotherms are considered, and all are Type I. Separation factors between 0 and 1 represent effective Type I isotherms, and typical values for low boiling

impurities range between values of 0.3 – 0.7. The formal definition of the separation factor is presented below.

$$\boldsymbol{r = \frac{(\Delta Y/\Delta Y_0)(1-\Delta q/\Delta q_0)}{(\Delta q/\Delta q_0)(1-\Delta Y/\Delta Y_0)}} \qquad \textbf{Equation 32}$$

In Equation 32, ΔY and Δq denote the equilibrium curve to a particular point on it, while ΔY_0 and Δq_0 refer to the entire range of the curve.

In order to quantify the dimensionless time and distance variables, mass transfer coefficients must be developed to represent the transport resistant phenomena. For conventional purification processes, Basmadjian was able to develop guidance regarding what diffusivities and mass transfer coefficients could be expected [57]. These are presented in Table 13.

Table 29: Range of Transport Coefficients with a particle radius set at 1 mm. [57]

	Fluid Phase	**Solid Phase**
Diffusivity (cm^2/s)	$D_f = 10^{-2}$ to 10^{-3}	$D_s = 10^{-5}$ to 10^{-6}
Mass Transfer Coefficient (s^{-1})	$k_fa = 10$ to 10^{-1}	$k_sa = 10^{-2}$ to 10^{-3}

It is important to note that the values presented in Table 13, represent those for a particle diameter of 1 mm, and can be adjusted using the Glueckauff relationships to transform diffusivities into mass transfer coefficients [57].

$$\boldsymbol{k_f a = 15 D_f / R^2} \qquad \textbf{Equation 33}$$

$$\boldsymbol{k_s a = 15 D_s / R^2} \qquad \textbf{Equation 34}$$

In this case, D refers to diffusivity, the subscripts f and s refer to the fluid and solid phases, k_fa and k_sa refer to the respective fluid and solid mass transfer coefficients.

The last parameters required to utilize the design charts are the dimensionless time and distance variables. These are presented in the equations below.

$$N = k_f a \left(\frac{z}{v}\right) f(r) = k_s a \left(\frac{z}{v}\right) \left(\frac{\rho_b}{\rho_f}\right) \left(\frac{\Delta q}{\Delta Y}\right) f(r) \qquad \textbf{Equation 35}$$

$$\mathrm{T} = k_s a * t * f(r) = k_f a * t \left(\frac{\rho_f}{\rho_b}\right) \left(\frac{\Delta Y}{\Delta q}\right) f(r) \qquad \textbf{Equation 36}$$

$$f(r) = \frac{2}{1+r} \qquad \textbf{Equation 37}$$

In Equations 35 and 36, f(r) is a function that uses r (separation factor) to correct for the non-linearity of the equilibrium isotherms. The f(r) expression shown in Equation 37 is valid for Type 1 isotherms. The expression changes for Type III isotherms ($f(r) = r^{-1/2}$, with linear isotherms being defined when r = 1, meaning f(r) = 1.

Five design charts corresponding to various fractional fluid and fractional solid concentrations will allow determination of the effect of transport resistance on the adsorption process. For the conditions outlined in this particular system, the dimensional N can be used to determine the limiting values of z and v. These can be used as design specifications to begin the adsorption process design.

For instance, in this particular case, the adsorption system was seen to require a diameter of 6 m with a depth of only 0.5 m, with a superficial velocity set at 1 m/s. In actuality the minimum bed depth or velocity can be calculated for various values of z and v, mass transfer coefficients are known. An example of how to calculate the minimum bed thickness required to ensure instantaneous breakthrough is not observed is provided below

Givens:	$v = 1$ m/s, $k_f a = 10$, $N \leq 4.5$, $r = 0.5$
Rearrange Equation 35 solving for z:	$z \geq N/[f(r)* k_f a/v]$
Minimum thickness (z)	$\geq 4.5/[(2/1.5)*10/1] \geq 0.3375$ m

Therefore, the minimum bed thickness required to ensure that instantaneous breakthrough does not occur is 0.3375 m. Table 30 provides calculated values for various bed depths and superficial velocities to ensure instantaneous breakthrough does not occur.

Table 30: Calculated values for minimum bed depths and associated maximum superficial velocities to maintain conditions that do not favour instantaneous breakthrough.

Set v	Calculated Minimum z		Set z	Calculated Maximum v
0.25	0.0844		0.25	0.741
0.5	0.1687		0.5	1.481
1	0.3375		1	2.963
1.5	0.5062		1.5	4.444
2	0.6750		2	5.926
2.5	0.8437		2.5	7.407
3	1.012		3	8.889

The original dimensions considered were 0.49 m in thickness, with a velocity of 1 m/s, which in comparison to the values in Table 30, are clearly acceptable.

The next calculations involve determining the adsorption time, and the length of the mass transfer zone. To calculate the adsorption time, first the dimensionless distance is computed using Equation 35. This calculation is provided below:

Givens: $v = 1$ m/s, $z = 0.5$ m, $k_f a = 10$, $r = 0.5$

Equation 35 $N = k_f a*(z/v)* f(r)$

Therefore N $= 10*(0.5/1)*(2/1.5) = 6.667$

The next step is to read the dimensionless time off of the appropriate design chart (the one with the fractional concentration considered). Therefore, from the 1% design chart (Figure 22) the T value = 1.2. This is read by drawing a vertical line from the appropriate r value (r = 0.5), then following the contour line from the N value to the vertical line drawn. The last step is to move horizontally from this point to the T axis and read off the T value.

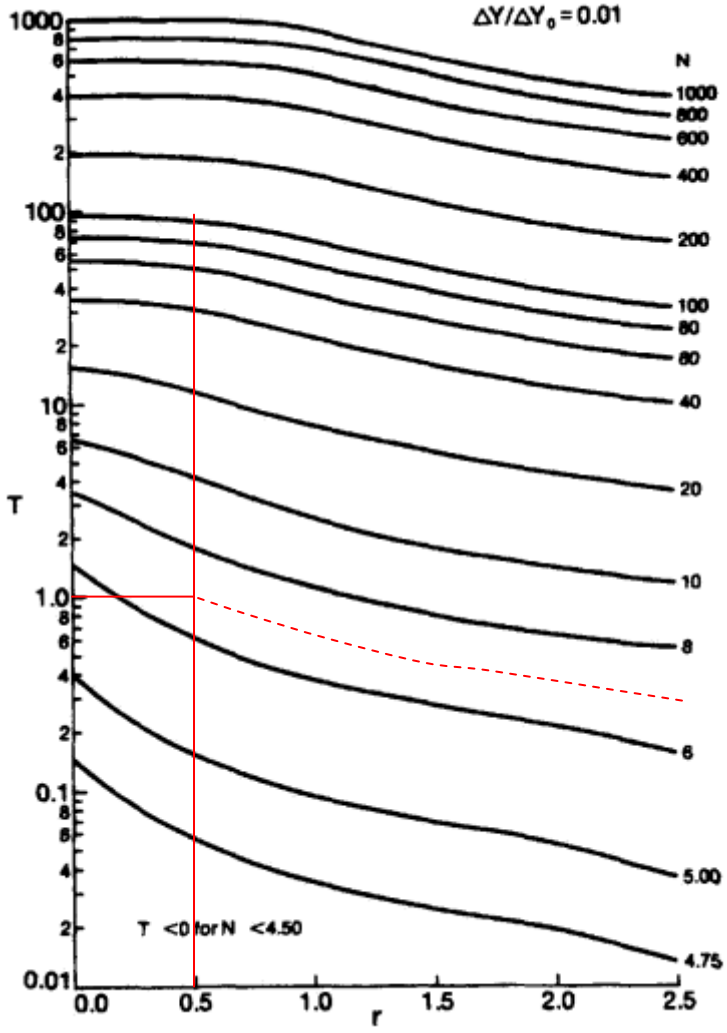

Figure 22: Modified Hiester-Vermeulen plots for fractional gas compositions of 0.01. [57].

The value T/N is a correction factor that can be used to determine the adsorption time associated with a fractional concentration (in this case 1%) of the feed breaking through the outlet of the adsorber. Furthermore, the correction factor also incorporates mass transfer considerations upon the equilibrium isotherm. The overall result is a breakthrough time that is specific to the system considered. Equation 38 below illustrates how the correction factor is utilized onto the equilibrium adsorption times, and Table 15 summarizes the anticipated breakthrough times.

$$t_a = t_e(T/N) \qquad \textbf{Equation 38}$$

Table 31: Fractional breakthrough times calculated through the incorporation of mass transfer through dimensionless time and distance parameters.

Fractional Composition	t_e (hours)	T/N	t_a (hours)
1%	Toluene = 78 Xylene = 95 MEK = 121	0.18	Toluene = 12 Xylene = 14 MEK = 18

In order to ensure pre-mature breakthrough will not occur as a result of our preliminary dimension calculations, the length of the mass transfer zone (LMTZ) must be determined and compared to the bed thickness being used. The LMTZ is determined by calculating the dimensionless N value from the dimensionless T values established for an adsorption cycle time. Two values of N will be determined, one from the solid phase design chart representing a solid phase concentration of 0.01 saturation, and one representing a solid phase concentration of 0.99 saturation. The distance between these two values is the length of the mass transfer zone. A sample calculation for Toluene is presented below. Note: here an 8 hour step time is used. This ensures pre-mature breakthrough will not occur. Furthermore, because the daily production time is 16 hours, it allows for two full adsorption-desorption cycles to be completed in the day.

Considerations	8 hour step time
Equation 36	$T = k_f a * t * (\rho_f/\rho_b)(\Delta Y/\Delta q) f(r)$
Equation 36 with values	$T = 10 * 28{,}800 * (1.2/400) * (1.81 \times 10^{-4}/0.161) * (2/1.5)$
Therefore	$T = 1.29$
N will be read from the design charts	$N_{0.01} =$, $N_{0.99} = 0$
z is calculated by rearranging Equation 35	$z = (N/k_f a) * (v/f(r))$
$z_{0.01}$	$z_{0.01} = (6.5/10) * (1/(2/1.5)) = 0.487$
$z_{0.99}$	$z_{0.99} = (0/10) * (1/(2/1.5)) = 0$
LMTZ	$LMTZ = z_{0.01} - z_{0.99} = 0.487$ m

From the calculation above, operating the adsorption cycle for 8 hours assuming the entire composition of the solvent is Toluene would yield a mass transfer zone of 0.487 m. The calculated preliminary adsorbent bed depth was 0.49 m, very close to that of the calculated mass transfer zone. Standard practice is to design bed depths to be multiples of the mass transfer zone,

thus, in this case, it would not harm the system to increase the bed depth to 1.0 m provided the pressure drop through the system was reasonable.

Desorption Times

To regenerate the adsorbent a process cycle must be developed to remove the adsorbate. This involves sending inert gas through the adsorbing bed while altering the physical parameters (pressure or temperature) of the system. The inert material acts to drive the adsorbate from the adsorbent pores, and the altered physical parameters act to reduce the affinity of the adsorbate to the adsorbent – making the process more efficient.

Under the conditions of a Type I isotherm, the sorption propagation velocity is inversely proportional to the equilibrium isotherm at each point [57]. Therefore each point of the isotherm will exert an effect on the velocity of the solute front resulting in decreasing desorption rates as the desorption process continues. This greatly contrasts the adsorption cycle, in which the adsorption cycle time will depend upon the feed and final concentrations, and not each individual point of the isotherm. The design equation developed for desorption therefore differs with respect to adsorption because the term $\Delta q/\Delta Y$ is replaced with dq/dY [57].

$$\boldsymbol{V = \frac{z}{t} = \frac{\rho_f v}{\rho_b dq/dY}} \qquad \textbf{Equation 39}$$

To evaluate the desorption time at any point along the isotherm, the derivative dq/dY must be evaluated. Over time, the process results in an ever expanding desorption front. The result is an in-efficient desorption process. To compensate for this a Temperature Swing desorption cycle will be used.

Temperature Swing desorption involves passing hot purge gas through the adsorption bed to remove the adsorbate. The physical consequence of using hot purge is the enrichment of the adsorbate as it is eliminated from the adsorbent. The overall effect is a decrease in desorption time, increase in concentration of the adsorbate being evolved, and thus an increase in the

efficiency of the desorption cycle. The effect of this has been quantified by Basmadjian for both hot inert purge gas, and is presented below as Equation 40 [57].

$$(Y_P)_{Max} = \frac{C_{pb}}{2\Delta H}(T_R - T_F) + \frac{Y_F}{2} \qquad \textbf{Equation 40}$$

In Equation 40, Y_P refers to the maximum enriched concentration of the solute in the gas phase, C_{pb} refers to the heat capacity of the carrier gas, ΔH refers to the enthalpy of adsorption, T_R refers to the regenerant temperature, T_F refers to the adsorption temperature, and Y_F refers to the feed gas concentration. If steam is used for the purge gas, the driving force for enrichment is the latent heat of vaporization of water, and the heat of adsorption. The result is that the enrichment factor (Yp) is driven towards unity because both the ΔH_{H2O} and ΔH are approximately equal to 2500 kJ/mol, which is seen in Equation 41 [57].

$$(Y_P)_{Max} \cong \frac{\Delta H_{H2O}}{\Delta H} = 1 \qquad \textbf{Equation 41}$$

If desorption is attempted at ambient conditions, enrichment will not occur. In fact, if T_R in Equation 40 is set equal to T_F, the maximum attainable concentration of the solute will be ½ that of the original feed concentration. This is because the part of the energy of the stream is being used to feed the endothermic process of desorption, thus lowering the temperature of the adsorption bed, and increasing the affinity of the adsorbate for the adsorbent. If high temperature purge is used, an intermediate temperature level is reached, at which desorption will occur easier, concentrating the adsorbate as it is removed [57]. Pictorially, this is described in the figure below.

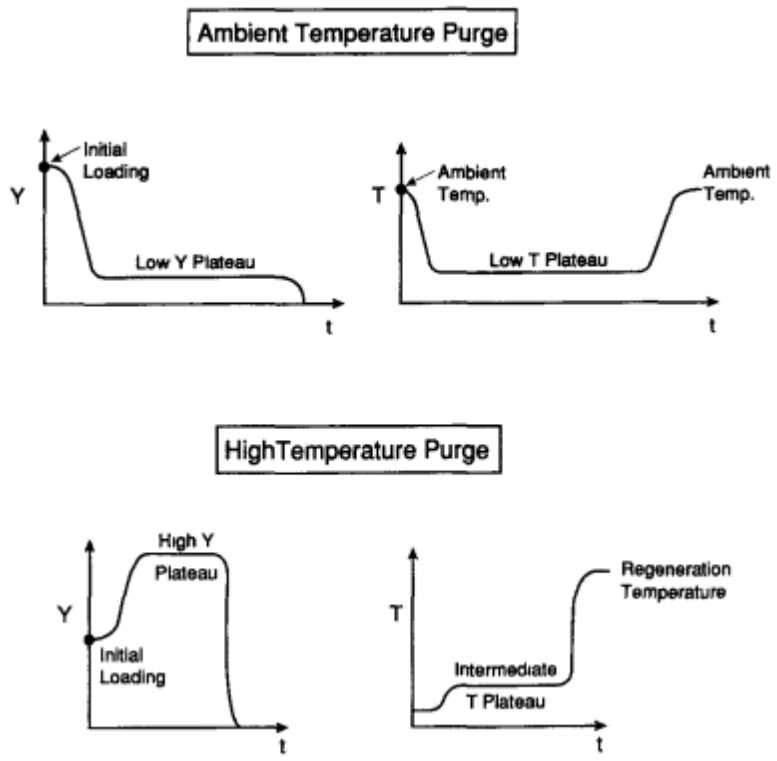

Figure 23: A comparison of desorption breakthrough curves at low and high temperatures. High temperature purge conditions leads to solute enrichment, while ambient purge leads to solute levels below initial loading values [57].

In adsorption-desorption systems, it is desirable to always have one fresh bed ready for adsorption. To ensure this, desorption cycles are designed to be faster than adsorption cycles. In this system, to adsorb the entire mass of contaminant, the minimum time required would be approximately 12 to 18 hours for a 1% breakthrough (Table 31). In practical applications adsorption cycles are kept closer to 8 hours, therefore, we will begin purging after 8 hours of the adsorption cycle. This means desorption (which includes purge, cooling, and drying of the bed), should occur faster than 8 hours.

To calculate the desorption time, 1 hour will be allotted towards drying and cooling of the bed (EPA estimates that this can occur in approximately 15 minutes), the rest of the time will be used for purge. This means, at a maximum, the purge step (desorption) should take no more than 6 hours – so that the total desorption step will take 7 hours leaving a safety factor of 1 hour. To calculate the actual desorption time, the purge requirements will be determined by matching them to the expected ratio of purge to solvent required. As seen in the previous discussion, if

steam is used as the purge gas, the maximum enrichment ratio expected will be on the order of unity. Typical systems utilize 0.3 to 1 kg of steam per kg of carbon [1]. For our system this translates into 2 to 6 moles of steam per mole of solvent recovered. Steam flow rates for various purge times and steam to VOC ratios are calculated in the table below.

Table 32: Calculated molar flow (kgmole/hr) of purge (steam) for various desorption times.

Steam Ratio	Mass of Steam (kg)	Molar flow of steam (kgmole/hr)			
		2 hr	3 hr	4 hr	5 hr
2	834	23.17	15.44	11.58	9.27
3	1251	34.75	23.17	17.38	13.90
4	1668	46.33	30.89	23.17	18.53
5	2085	57.92	38.61	28.96	23.17

Overall Adsorption Subsystem Description in HYSYS

With the overall design parameters calculated for the adsorption system, knowledge of the desorbed VOC-steam stream will be required. This is because the desorbed stream will be the feed for the Reformer and SOFC units. Using the steam ratios in Table 32, mole fractions for the desorbed VOC components can be calculated. These are summarized in the table below.

Table 33: Calculated mole fractions of VOC within the desorbed stream. Based on anticipated daily cycles (two 8 hr. adsorption cycles - 2 desorption cycles).

Steam Ratio	Total Mass of Steam (kg)	Mole Fraction of VOCs			
		Tol	Xyl	MEK	nBA
2	832	0.015	0.034	0.031	0.011
3	1251	0.011	0.023	0.021	0.007
4	1668	0.008	0.018	0.016	0.005
5	2085	0.006	0.014	0.013	0.004

As is evident from the Table 33, the mole fractions of the VOC substances are extremely low, meaning the composition of fuel being sent to the Reformer and SOFC is not adequate for power production. To alleviate this concern, excess water can be removed from the stream by partial condensation. This is done by cooling the desorbed stream enough to condense out water without letting the VOC compounds leave the gas phase. In this particular system, the Adsorber Subsystem contained a *Cooler* and *Separator* function that acted as a condensing unit. In fact, the actual results of the system indicate that the condensed phase contains less than 1% by mole of VOC in it.

All the VOCs in this system with the exception of MEK have boiling points that range between 110^0C to 136^0C. Furthermore, the starting concentration of the VOCs within the desorbed stream is low to begin with. For these reasons, it is expected the system will behave non-ideally, and thus outlet concentrations may not be as expected (which is the case here). Therefore, this portion of the model should be explored experimentally in the future.

4.2.3 Modeling the Heat Exchanger Subsystem

In practical application, SOFC operational temperatures range between 750^0C – 1000^0C [41]. In particular, the SOFC hybrid model has been set so that the SOFC operates at 900^0C. Upon exit, the SOFC exhaust materials will also be at 900^0C, meaning the SOFC exhaust will contain significant amounts of thermal energy. In order to recapture some of this energy, the SOFC hybrid model includes a Heat Exchanger Subsystem. This Subsystem is used to transfer exhaust thermal energy to the incoming air and water streams, thus increasing overall system efficiency.

The heat exchanger subsystem in the SOFC model is seen below:

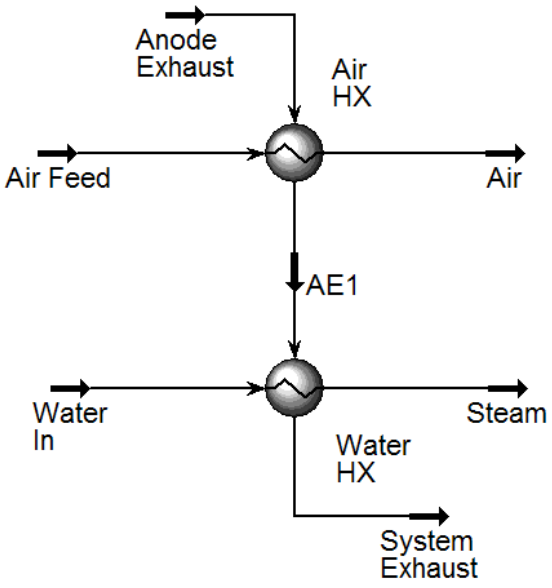

Figure 24: *HYSYS* Heat Exchange Subsystem.

HYSYS provides three basic heat exchanger models designed for steady-state applications utilizing the shell and tube configuration. In the *Heat Exchange Subsystem*, we will be using two of these three.

The first model is termed the *Endpoint* model. This model treats the heat curves for both *Heat Exchanger* sides as linear [60]. For simple problems where there is no phase change and Cp is relatively constant, this model can provide relatively accurate results with very low computational requirements [60]. This model is utilized for the heat exchanger named *Air HX* [60].

The second model, termed the *Weighted Model*, is an excellent model to deal with non-linear heat curve problems such as the phase change of pure components in one or both *Heat Exchanger sides* [60]. With the *Weighted model*, the heating curves are broken into intervals, and an energy balance is performed along each interval [60]. A log-mean-temperature-difference (LMTD) and UA are calculated for each interval in the heat curve, and summed to calculate the overall exchanger UA [60]. The *Weighted model* is available only for counter-current exchangers, and is essentially an energy and material balance model [60]. This model is used for the *Water HX* because there is a phase change involved [60].

Stream conditions will change depending on the run, but for the basic system, running at atmospheric pressure and no fuel recycle, the molar flow rates, and temperatures of the streams are provided in Table 34.

Table 34: Stream conditions for the basic Heat Exchanger Subsystem model. In this run, there is no Fuel Recycle, the excess air ratio is set at 1.2, and other conditions are as below.

Stream	Molar Flowrate (kgmole/hr)	Temperature (K)
Anode Exhaust	6.869	1173
AE1	6.869	1142
System Exhaust	6.869	1013
Air Feed	2.837	298.1
Air Out	2.837	400
Water In	0.68	288.1
Steam In	0.68	500

4.2.4 Modeling the Reformer Subsystem

During the development of the SOFC hybrid model, it was determined that an Autothermal Reforming system would be used. The flowsheet for the Reformer Subsystem is presented below.

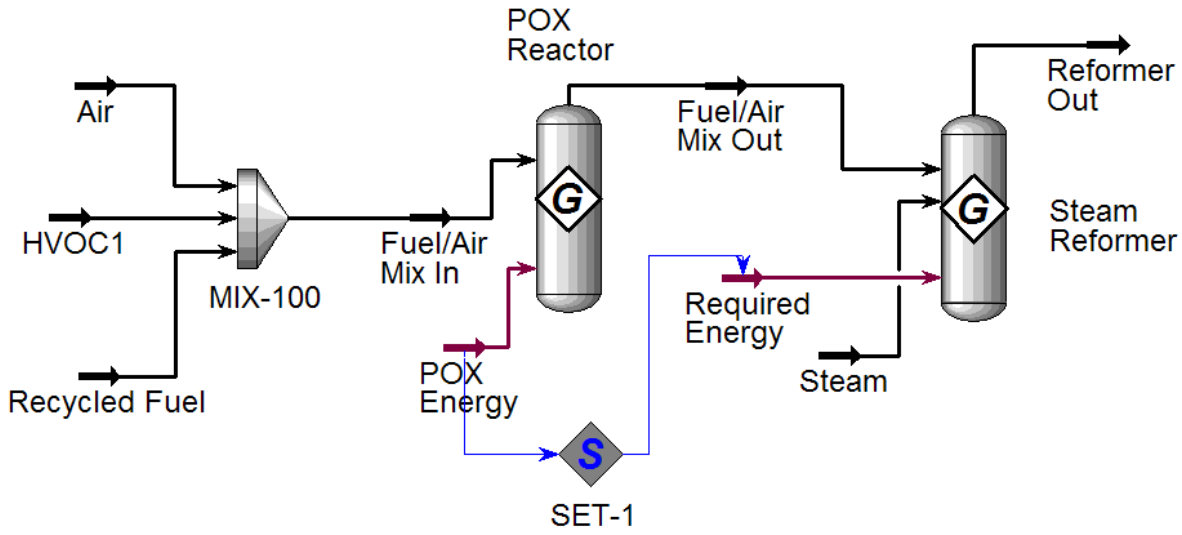

Figure 25: Reformer Subsystem Model for the SOFC Hybrid abatement system model.

Air coming from the *Heat Exchange Subsystem*, and Humidified VOC (*HVOC1)* coming from the Adsorber Subsystem, are mixed together in a *HYSYS Mixer* operation and sent to the POX Reactor. The POX reactor is modeled as a *Gibbs* reactor which calculates energy and material balances by minimizing the change in the Gibbs energy function. To utilize this function, it is assumed that the reaction will go to equilibrium, and therefore this should be checked experimentally in future research.

The influence of various streams and reactor parameters upon the overall reforming process is studied in model validation section of this thesis, however, the ratio of oxygen sent to the POX reactor greatly influences the conversion of VOC's to smaller hydrocarbon components (C1 components). Too high a ratio will result in a full combustion reaction occurring while too low a ratio will result in poor conversion rates. Optimizing the molar flow of air into the POX reactor will result in a product mixture consisting primarily of nitrogen, carbon dioxide, and hydrogen.

The outlet of the POX reactor is combined with excess steam to form the inlet reaction mixture for the Steam Reactor. The main reactions taking place include the steam reforming reaction and the water-gas shift reaction. The presence of excess steam will function to drive the water gas shift reaction in the forward direction, thus creating more hydrogen from the reaction mixture.

In this case, the Steam Reforming Reactor is also modelled as a *HYSYS Gibbs* reactor. In order to ensure the endothermic steam reforming reactions are sustained, the energy from the POX reactor is sent into the Steam Reforming reactor. This is accomplished using the *HYSYS Set* function.

4.2.5 Modeling the SOFC Subsystem

As with the other Subsystems, the model of the SOFC consists only of *HYSYS* models and functions. The reformer outlet stream (consisting primarily of nitrogen, hydrogen, carbon monoxide, and steam) was sent to the Anode side of the SOFC.

This mixture is sent to a *Component Splitter* that is used to set the Fuel Utilization factor. The fuel being utilized is sent to a *HYSYS Gibbs* reactor with the appropriate stoichiometric ratio of oxygen from the incoming air stream. The appropriate molar flow of air required is calculated

via the *Spreadsheet* function in *HYSYS*. This is done by first setting a desired air utilization factor, and using it to determine the required oxygen content to ensure complete conversion. The airflow is calculated based on the assumption that 20.5% of the air used is composed of oxygen.

This airflow is preheated by exchanging heat with the *Cathode Exhaust stream*. Preheated, the air stream is sent through a *Component Splitter* which is used to simulate the movement of the oxygen anion across the electrolyte. Once through the *Component Splitter*, the air stream is separated into two streams, one consisting only of oxygen (called *Cathode O2 In*), and another consisting of nitrogen, unused oxygen, and argon (*Excess Air*). The *Cathode O2 In* stream is then sent to the *Gibbs Reactor* representing the Anode.

The Excess Air stream is heated using the *Heater* function to simulate it obtaining heat from the SOFC cell prior to its exit. Once through the *Heater*, the *Excess Air* stream is termed the *Cathode Exhaust* stream

The exhaust of the SOFC is then mixed with the unused fuel which has been heated through a *HYSYS Heater* model that is used to simulate the unused fuel going through the SOFC and exiting at the cell temperature. This combined mixture is termed the *Anode Exhaust*, and is split via a *HYSYS Tee* model to allow for the recycling of a percentage of the unused fuel. The *Anode Exhaust* is then sent to the *Heat Exchange Subsystem* to preheat the air and water streams being used in the *Reformer Subsystem*.

The fuel to be recycled is sent through a *HYSYS Recycle* function. The *Recycle* installs a theoretical block in the process stream [60]. The feed into the block is termed the calculated recycle stream, and the product is the assumed recycle stream. The following steps take place during the convergence process:

1. *HYSYS* uses the conditions of the assumed stream and solves the Flowsheet up to the calculated stream [60];
2. *HYSYS* then compares the values of the calculated stream to those in the assumed stream [60];

3. Based on the difference between the values, *HYSYS* modifies the values in the calculated stream and passes the modified values to the assumed stream [60];
4. The calculation process repeats until the values in the calculated stream match those in the assumed stream within specified tolerances [60].

As previously described, the *Recycled Fuel* is then sent to the *Reformer Subsystem* to recycle the steam contained within the *Anode Exhaust* stream. The *SOFC Subsystem* is shown below.

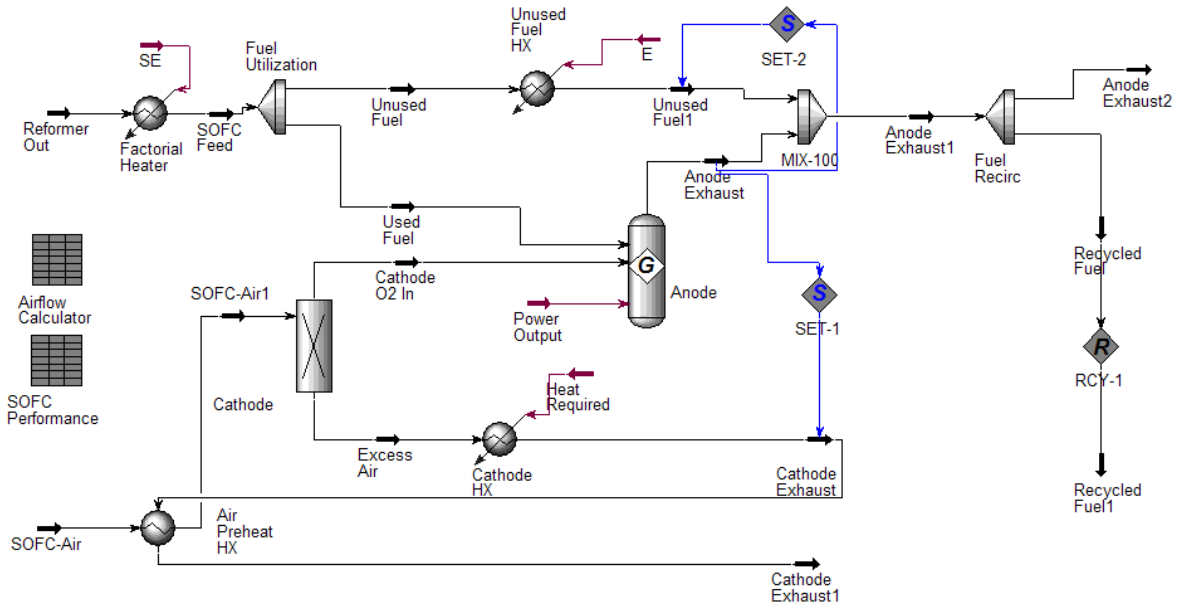

Figure 26: HYSYS SOFC Subsystem Model.

Chapter 5: Model Validation and Optimization

Model validation will occur via two avenues. The first is through examination of the factorial analyses presented in Sections 3.2.3.1 and 3.2.3.2 for both the SOFC and Reformer subsystems. A comparison of factor effects on the model to those anticipated in actual operation will be examined to outline if the model is behaving appropriately. The second validation is by comparison to a published model of an SOFC/Reformer operational system. Again, these results will be examined to outline if the model is predicting performance accurately.

5.1 Factorial Analysis of the Reformer Subsystem

The Reformer Subsystem model is presented the figure below.

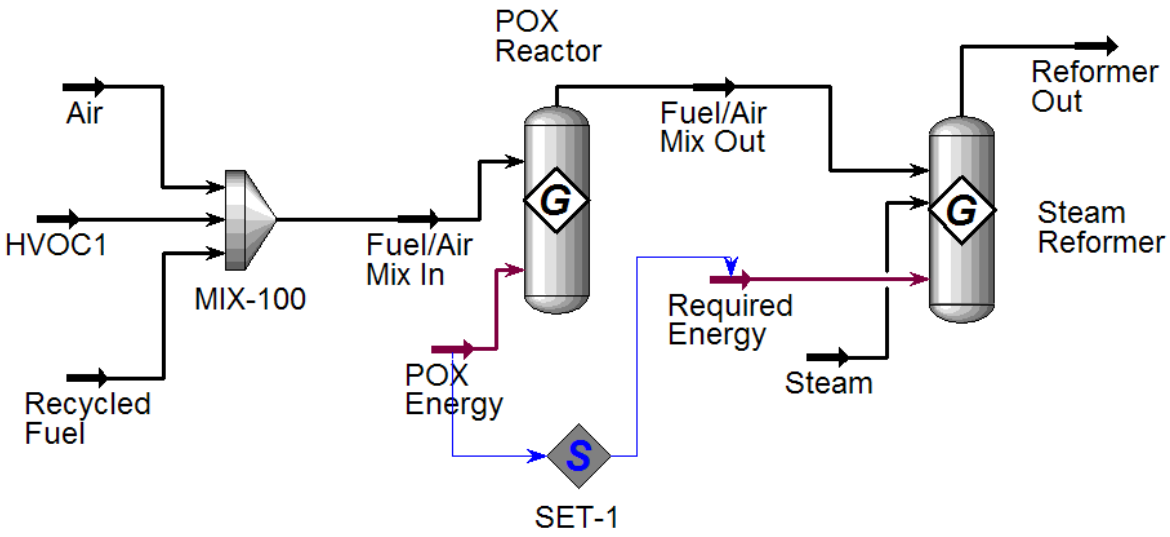

Figure 27: Auto-Thermal Reformer Subsystem flowsheet.

The basic reformer system configuration is that of an Autothermal Reformer consisting of two separate operational units – one POX reactor, and one Steam Reactor. Air and the VOC vapour is premixed, and sent into the POX reactor.

The goal of the Auto-Thermal Reformer is to convert all of the VOC components into a mixture of hydrogen and carbon monoxide. To optimize the process, and help validate the results of the model, a full Design of Experiments 2^5 factorial analysis was performed on the Reformer Subsystem. The conditions of the humidified VOC stream being sent into the Reformer are presented in Table 35, while the factors considered in the factorial experiment are presented in Table 36.

Table 35: Reformer inlet conditions.

Variable	Value
Molar Flow rate	0.337 kgmole/hr
Composition	0.134 Toluene, 0.150 MEK, 0.064 Xylene, 0.043 nBA, 0.608 H_2O

Table 36: Experimental set-up of a 2^5 Factorial Analysis for the Reformer Subsystem.

Factor	Description	Lower Level (-)	Higher Level (-)
a	VOC Temp	400 K	800 K
b	Air Temp	400 K	800 K
c	Air Molar Flow	0.25 kgmole/hr	0.75 kgmole/hr
d	Steam Molar Flow	0.422 kgmole/hr	0.844 kgmole/hr
e	POX Reactor Temp.	800 K	1200 K

A detailed explanation of factorial analyses is presented in Appendix E, while the results of this particular analysis are developed here. The effect of each factor, and all interactions of factors were analyzed on the following three output variables:

1. Mole fraction of CO in the Reformate;
2. Mole fraction of H_2 in the Reformate; and,
3. Mole fraction of CO_2 in the Reformate.

In this particular analysis, the effect of each factor was identified through the use of normal probability plots. Outliers in the plots were identified as significant factors, and those were then examined by inspection to determine appropriate operational conditions. ANOVA analyses could not used because an appropriate method to quantify experimental error was not present.

Factor Effects on the Mole Fraction of Carbon Monoxide

The normal probability plot of the effects on the Mole Fraction of carbon monoxide in the reformate is provide in the figure below.

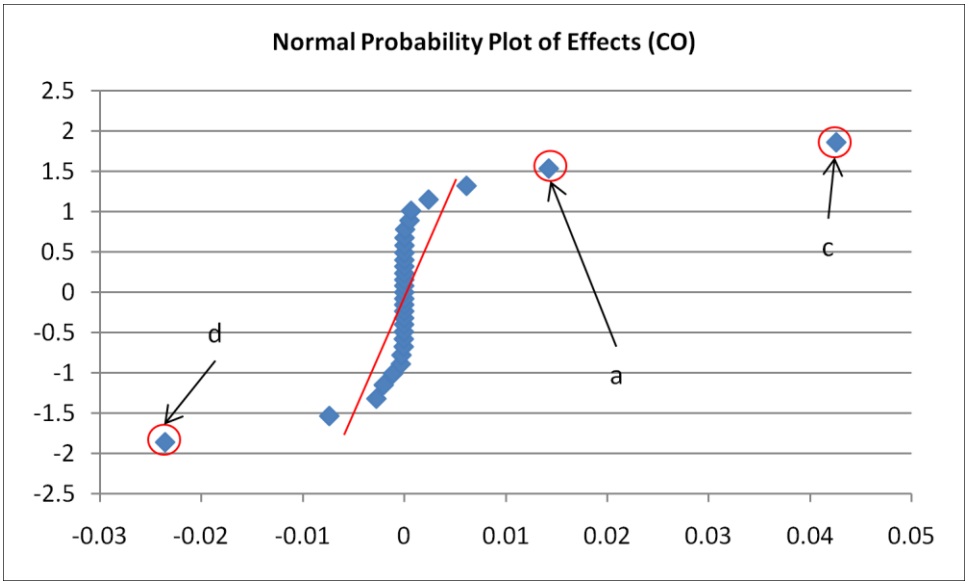

Figure 28: Normal probability plot for the mole fraction of CO in the reformate.

The outliers in the figure above have been identified and labelled. The labels are referred to in the table below.

Table 37: Significant factors as identified by the normal probability plot of effects on CO mole fraction in the reformate. The factors are ordered from the most negative effect to the most positive effect.

Factor	Description	Effect
d	Molar steam flow	-0.024
a	VOC Pre-heat Temperature	0.014
c	Molar air flow	0.043

Molar Flow of Steam: This factor was identified as a negative main effect. Increasing the molar flow of steam above what is required by the steam reaction will cause the water-gas shift reaction to occur. This will convert CO and the excess water to hydrogen and CO_2.

VOC Pre-heat Temperature: VOC Pre-heat temperature was found to be a positive main effect. This is an expected result.

Molar Air Flow: Molar air flow was identified as a positive main effect. Increasing the oxygen content in the reaction vessel will drive the POX reaction in the forward direction.

Factor Effects on the Mole Fraction of Hydrogen

The Normal Probability Plot for the effect of the factors on the mole fraction of H_2 in the reformate is presented in the figure below.

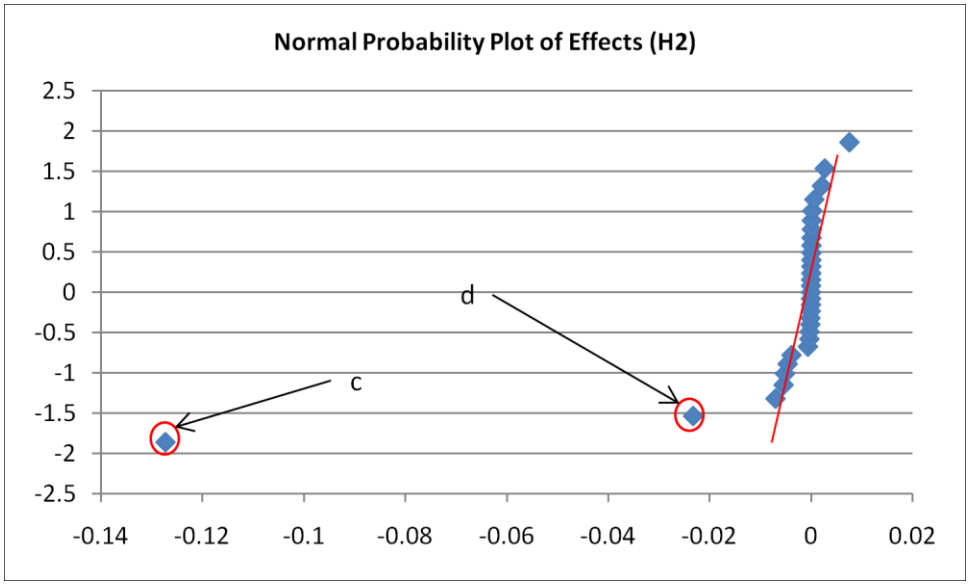

Figure 29: Normal probability plot for the mole fraction of H_2 in the reformate.

The table below identifies the factors that exerted a significant effect on the mole fraction of hydrogen in the reformate.

Table 38: Significant factors as identified by the normal probability plot of effects on H_2 mole fraction in the reformate. The factors are ordered from the most negative effect to the most positive effect.

Factor	Description	Effect
c	Molar air flow	-0.127
d	Molar steam flow	-0.023

Molar Air Flow: This factor was identified as exerting a negative main effect. This means an increase in the air flow would effectively decrease the mole fraction of hydrogen in the reformate. This is examined further in the Factorial Analysis Summary discussion.

Molar Steam Flow: This factor was identified as exerting a negative main effect. This means an increase in the steam flow would effectively decrease the mole fraction of hydrogen in the reformate. This is occurring because there is already sufficient steam being supplied in the HVOC stream, as well as in the Recycled Fuel Stream to drive the water-gas shift reactions and the steam reforming reactions in the forward reaction.

Factor Effects on the Mole Fraction of Carbon Dioxide

The normal probability plot of the factor effects on the mole fraction of CO_2 in the reformate is outlined in the figure below.

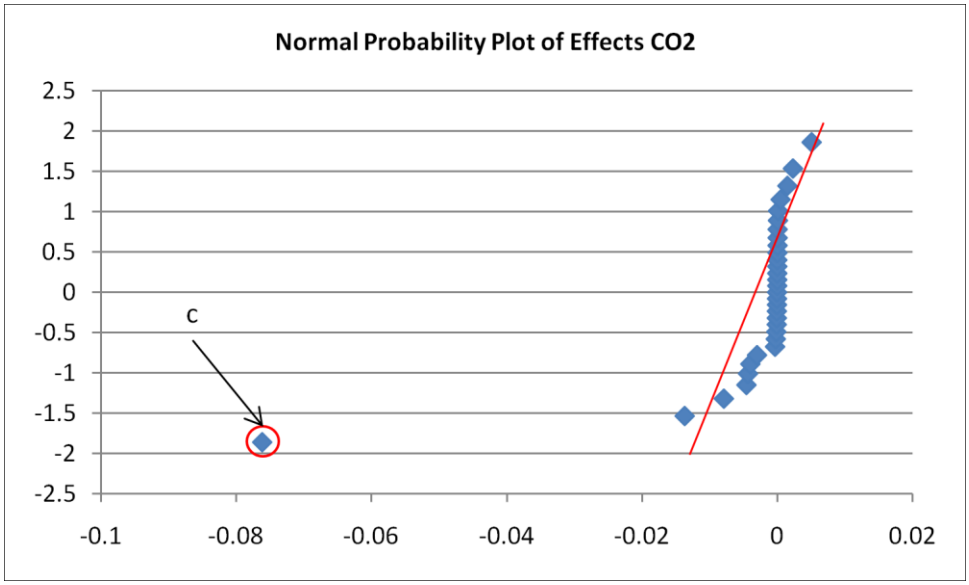

Figure 30: Normal probability plot for the mole fraction of CO_2 in the reformate.

The significant factors identified are summarized in the table below.

Table 39: Summary of the significant factors using xCO_2 in the reformate gas as the output variable, and the factors outlined in Table 18.

Factor	Description	Effect
c	Molar air flow	-0.0761

Molar Air Flow: Molar air flow was identified as a negative main effect. Air flow rate does not directly impact CO_2 concentration in the reformate. A discussion on this effect is presented below in the Factorial Analysis Summary.

Factorial Analysis Summary

To fully appreciate the results of this factorial analysis, it is important to understand how varying each factor would affect the output variables simultaneously (mole fractions of CO, H_2, and CO_2). It is expected that the pre-heat temperature of the humidified VOC or air streams would not significantly affect the Reformer Subsystems Model performance. This is because the first section of the reactor is a POX reactor, which is set at fixed temperatures in this model. The reason the temperature is set, is to understand the effect temperature plays upon the system. In most cases, the temperature would actually be set by reaction conditions. The effect of this is that regardless of what temperature the inlet is (within reason), the overall reaction temperature will remain at the fixed POX reactor temperature.

The real effect of increasing the Humidified VOC or Air stream temperatures would be to increase the kinetics of the reactions (because reaction temperature is reached faster). This, coupled with the fact that the composition of CO in the POX reactor is small (being consumed by WGS reaction), means any small change in its formation or reduction will be noticeable. Lastly, as the reactor temperature increases above 450^0C the equilibrium of the WGS reaction begins to move towards the production of H_2O and CO [49]. Therefore it is expected that these factors will either not be significant, or show a minor positive effect on the concentration of CO in the reformate gas. As predicted, the pre-heat temperature of VOC affected the molar concentration of CO, and nothing else.

The feed entering the reformer consists of recycled fuel from the fuel cell and humidified VOC coming from the adsorption system. As indicated previously, the reformer here is modelled as two separate reactors in series, a partial oxidation (POX) reactor and a steam reformer (SR). To initiate the reaction in the first reactor (POX reactor), oxygen will be required. The first part of the reaction zone in the reactor is for full combustion, which forms CO_2 and generates heat to feed the rest of the reactions. After this initial zone, the partial oxidation reactions occur (generating CO and H_2).

The reaction mixture, now primarily consisting of H_2, CO, N_2, and to a lesser degree water and CO_2 is sent to the SR reactor. In this reactor, the heat generated in the POX reactor is utilized in the endothermic water gas shift (WGS) reaction. The excess steam aids in preventing coking and driving the steam reaction in the forward direction. The result is to have an end product consisting primarily of H_2 and CO.

In this particular experiment the initial molar flow of air (0.25 kgmole/hr) will supply the oxygen to begin the reactions in the POX reactor. It can be hypothesized that the minimum air flow supplied enough oxygen to virtually convert all the hydrocarbons (VOCs) into a mixture of H_2 and CO, and to a lesser degree CO_2. This is confirmed by viewing the composition of the mixture after the POX reactor. At this point the only remaining hydrocarbon is toluene. Any increase in the molar air flow should generate even more hydrogen, CO, and dilute the amount of CO_2 present until all of the hydrocarbons have been converted.
Experimentally, increasing the molar flow of air served to increase the concentration of CO and decrease the concentrations of CO_2 and H_2. This is actually expected under these reaction conditions because once the hydrocarbons have been converted, and with temperatures above 450^0C, the reverse water gas shift reaction can take place. This would essentially increase the CO concentration, while decreasing both the H_2 and CO concentrations. This type of behaviour was noted by Ming et al [49].

In the steam reforming reactor, steam is used to transform any CO present to hydrogen and CO_2 through the WGS reaction, and also to prevent coking of the hydrocarbon compounds. In this

experiment, increasing the molar flow of steam from the initial value served to decrease the mole fractions of CO, H_2, and CO_2. The hypothesis for this is that the humidified VOC stream already contained sufficient steam to allow for the SR reactions to proceed. Any increase in steam only served to dilute the product, causing a decrease in H_2, CO, and CO_2.

Overall, the reformer subsystem model is operating predictably, and thus can be utilized for the overall abatement system model.

The factorial experiment also served to outline ideal operational parameters for the Auto-thermal reformer. These were identified as run 17 in the experiment, and are presented in Table 40 below. In this run, all factors were set at the lowest level. The results of this run are presented in Table 41. These results are set with a Fuel Recycle Ratio (FRR) of 0.5, and a Fuel Utilization of 0.85.

Table 40: Factorial settings for ideal reformer performance.

Factor	Description	Value
a	VOC preheat temperature	800 K
b	Air Flow preheat temperature	400 K
c	Air Molar Flowrate	0.25 kgmole/hr
d	Steam Molar Flowrate	0.422 kgmole/hr
e	POX Reactor Temperature	800 K

Table 41: Optimized reformer results. Factors set to levels for run 17.

Substance	Value
CO	0.051
H_2	0.409
CO_2	0.294
H_2O	0.151
N_2	0.095
Total	1

5.2 Model Validation: Factorial Analysis of the SOFC Subsystem

As with the Reformer Subsystem, a 'Design of Experiment' full 2^5 factorial analysis could be run on the process parameters to optimize the process and help verify model performance. The reformer system was set at the parameters outlined in Table 41, and the factors used are summarized in Table 42.

Table 42: 2^5 Factorial design for the SOFC Subsystem model.

Factor	Description	Lower Level (-)	Higher Level (-)
a	FRR	0.25	0.5
b	Air Temperature	400 K	700 K
c	Fuel Utilization (U_f)	0.7	0.9
d	Excess Air (λ)	1.2	1.8
e	Current Density	150 mA/cm^2	300 mA/cm^2

The theory behind factorial experiments is presented in Appendix E; however, the results of the analysis are developed here. There were four output variables for the system, and the effect of each factor, and all interactions of factors was analyzed on these three output variables. The output variables are listed below:

1. SOFC Stack Voltage;
2. Total Power;
3. Stack DC Power Produced; and,
4. Stack Heat produced.

In this particular analysis, the effect of each factor was identified through the use of normal probability plots. Outliers in the plots were identified as significant factors, and these were then further examined through optimization techniques to determine appropriate operational conditions. ANOVA analysis was not used as experimental error for this system could not be appropriately quantified.

Factor Effects on SOFC Stack Voltage:

The normal probability plot of the effects on the SOFC stack voltage is presented in the figure below.

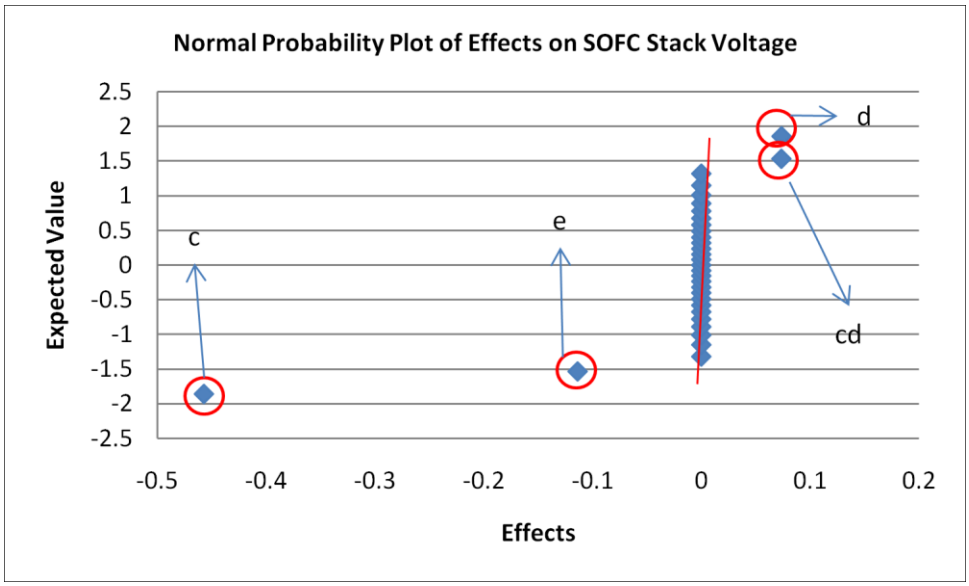

Figure 31: Normal probability plot for SOFC Single cell voltage using the factors.

The outliers in the figure above have been identified and labelled. The labels are referred to in the table below.

Table 43: Significant factors as identified by the normal probability plot of effects on SOFC single cell voltage. The factors are ordered from the most negative effect to the most positive effect.

Factor	Description	Effect
c	Fuel Utilization	-0.457
e	Current Density	-0.114
d	Air Utilization	0.074
cd	Interaction of Air and Fuel Utilization	0.074

Fuel Utilization: Fuel utilization is shown to exert a strong negative effect on the SOFC stack voltage. This is an expected result, because current is seen proportional to fuel utilization. Therefore as fuel utilization increases, so will the current, decreasing the Nernst potential.

Current Density: Current density is shown to exert a strong negative effect on the SOFC stack voltage. This is an expected result because an increase in current will also increase polarization effects, decreasing cell voltage.

Excess Air: Excess air is shown to exert a mild positive effect on the SOFC stack voltage. This is an expected result.

Interaction of Air and Fuel Utilization Factors: The interaction effect of these two factors is shown to exert a negative effect on the SOFC stack voltage.

Factor Effects on Total Power (Heat and SOFC DC Power)

The normal probability plot of the effects on the total power in terms of heat and DC electricity is presented below in the figure below.

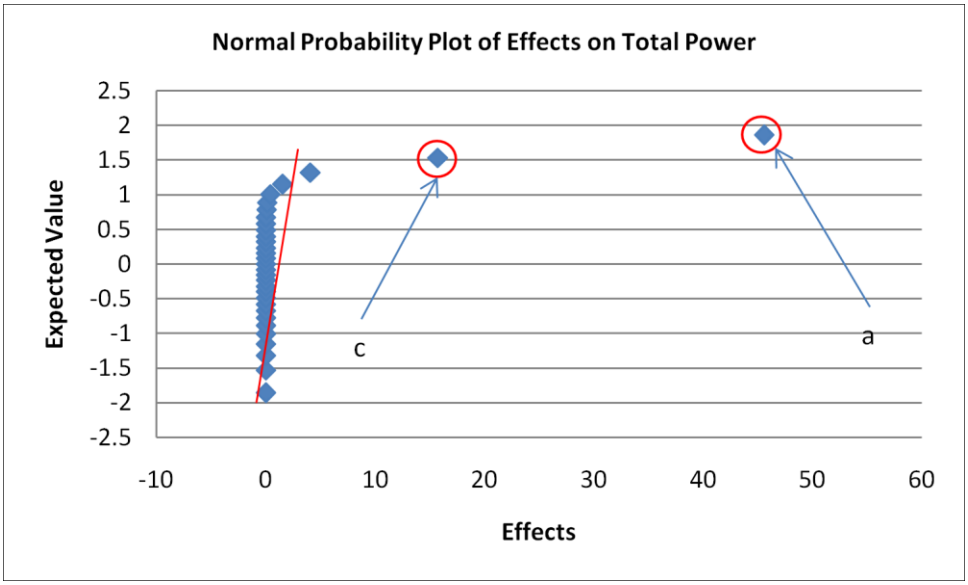

Figure 32: Normal probability plot of effects on Total Power.

The outliers in the figure above have been identified and labelled. The labels are referred to in the table below.

Table 44: Significant factors as identified by the normal probability plot of effects on total power. The factors are ordered from the most negative effect to the most positive effect.

Factor	Description	Effect
c	Fuel Utilization	15.8
a	FRR	45.6

Fuel Utilization: This factor exerts a positive effect on the total power produced from the SOFC stack. This is an expected result, as an increase in the amount of fuel utilized, means an increase in reaction. Regardless of whether this improves cell performance or not, the total power produced in terms of heat and electricity will increase.

FRR: This factor exerts a large positive effect on the overall power produced from the Fuel Cell. This is expected in that increasing the FRR will increase the total flow of material moving through the cell. Regardless of whether this improves cell performance or not, the total power produced in terms of heat and electricity will increase.

Factor Effects on the SOFC DC Power Produced

The normal probability plot of the effects on the SOFC stack DC power produced is presented in the figure below.

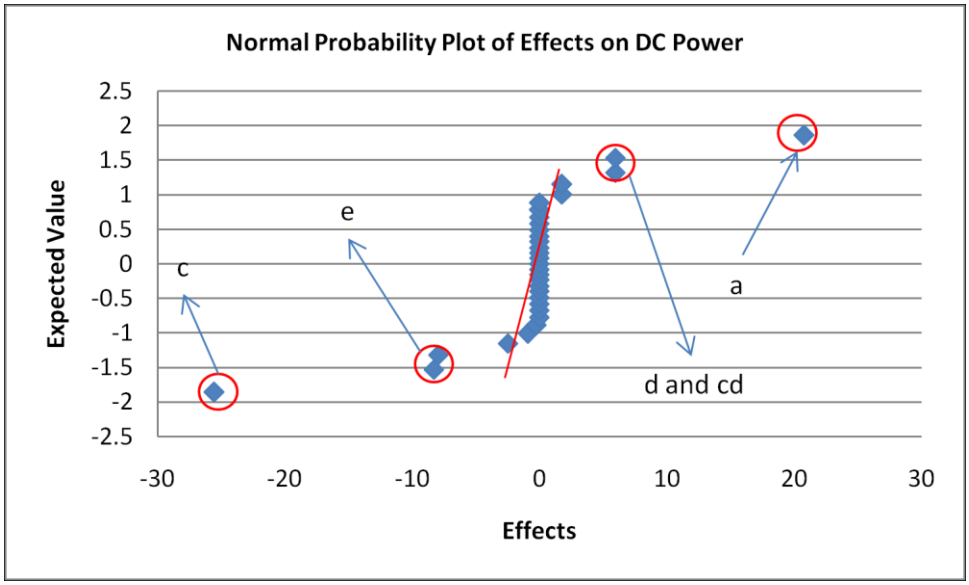

Figure 33: Normal probability plot of effects on DC Power produced.

The outliers in the figure above have been identified and labelled. The labels are referred to in the table below.

Table 45: Significant factors as identified by the normal probability plot of effects on DC power produced. The factors are ordered from the most negative effect to the most positive effect.

Factor	Description	Effect
c	Fuel Utilization	-25.5
e	Current Density	-8.31
ac	Interaction: FRR x Fuel Utilization	-7.98
d	Excess air	5.97
cd	Interaction: Fuel Utilization x Excess Air	5.98
a	FRR	20.8

Fuel Utilization: Fuel utilization is shown to exert a strong negative effect on SOFC stack DC Power production. This is an expected result, as an increase in current increases polarization effects; and current is proportional to fuel utilization.

Current Density: Current density is shown to exert a strong negative effect on SOFC stack DC Power production. This is an expected result, as an increase in current increases polarization effects, thus reducing cell voltage.

Interaction – Fuel Utilization x Excess Air: This factor exerts a negative effect on SOFC stack DC Power production.

Excess Air: Excess air is shown to exert a positive effect on SOFC stack DC Power production. This is an expected result, as an increase in excess air allows for better system cooling, and thus better system performance.

Interaction – Fuel Utilization x Excess Air: This factor exerts a positive effect on SOFC stack DC Power production.

FRR: This factor exerts a strong positive effect on SOFC stack DC Power production. This is an expected result, as an increase the FRR would increase the equivalent amount of hydrogen and carbon monoxide to the fuel cell.

Factor Effects on the SOFC Heat Production

The normal probability plot of the effects on the SOFC heat production is presented in the figure below.

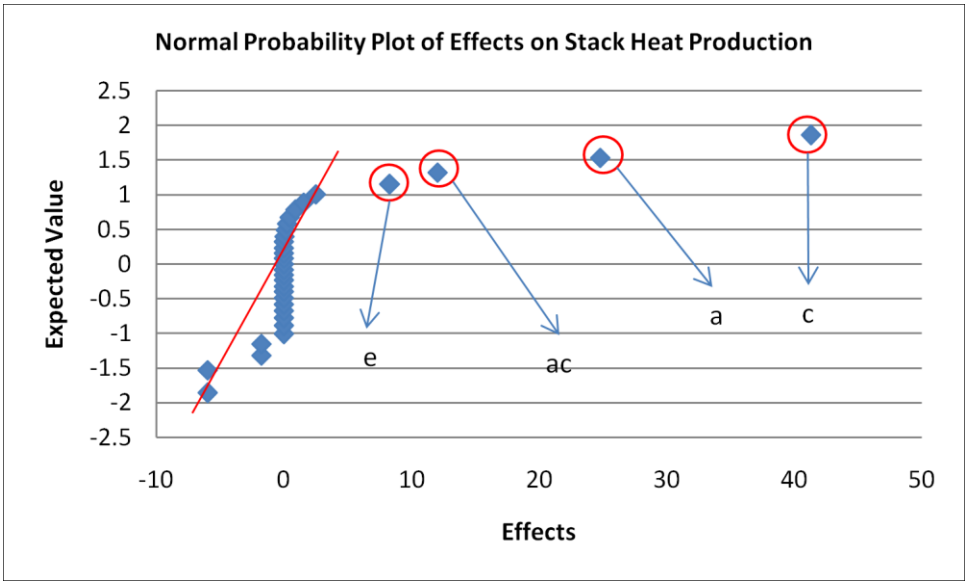

Figure 34: Normal probability plot of effects on heat produced.

The outliers in the figure above have been identified and labelled. The labels are referred to in the table below.

Table 46: Significant factors as identified by the normal probability plot of effects on heat produced by the SOFC. The factors are ordered from the most negative effect to the most positive effect.

Factor	Description	Effect
e	Current Density	8.31
ac	Interaction: Fuel Recycle x Fuel Utilization	12.1
a	FRR	24.8
c	Fuel Utilization	41.3

Current Density: Current density is shown to exert a positive effect on SOFC stack heat production. This is an expected result, as an increase in current works against the potential difference. This causes increases in ohmic polarization effects, decreasing fuel cell efficiency.

Interaction FRR x Fuel Utilization: This factor has been shown to exert a positive effect on SOFC stack heat production.

FRR: This factor exerts a strong positive effect on SOFC stack heat production. This is an expected result, as an increase the FRR would increase the overall flow of material to the system, and as the actual fuel gets diluted, the actual ratio of heat produced to DC power produced should increase.

Fuel Utilization: Fuel utilization is shown to exert a positive effect on SOFC stack heat production. Fuel utilization is proportional to current, and so an increase in fuel utilization would have the same effect as an increase in current density (*i.e.* increase polarization – decreasing cell efficiency and increasing the generation of heat within the cell).

Summary of SOFC Factorial Analysis

For the SOFC Subsystem, the factorial analysis included three output variables and five factors. As with the Reformer Subsystem Factorial Analysis, the effect of each variable will be discussed and compared in terms of expected and predicted results.

To begin, an increase in the FRR will increase the total flow of material to the fuel cell. Therefore regardless of fuel cell performance, the overall energy being sent to the cell will increase. When examining the effect of the FRR on DC power produced, the factor exerts a positive effect. This is because in the range between 0.25 and 0.5 (recycle ratio) the equivalent amount of hydrogen being sent to the fuel cell increases. Since this evaluation identifies that increasing the FRR will increase both output variables (DC power produced and heat produced), it is important to quantify how much of each. One way to do this is to examine the change in

hydrogen concentration (mole fraction) and total molar flow as the FRR is increased. The figure below displays this effect.

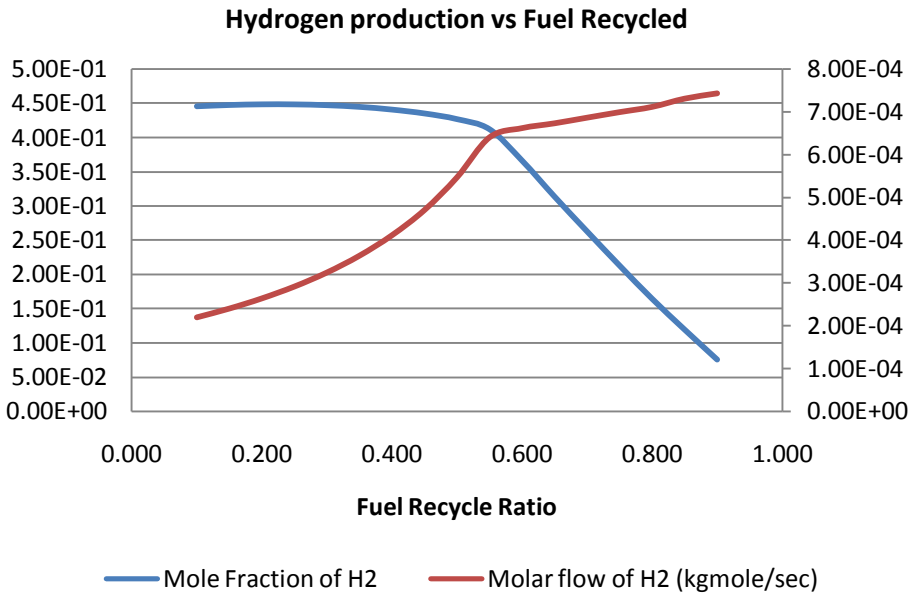

Figure 35: Hydrogen composition and flow as a function of the FRR. Fuel Utilization is set at 0.7, and Excess air ratio is set at 1.8.

As seen in the above figure, although the amount of hydrogen increases as the fuel recycle ratio (FRR) increases, the mole fraction of hydrogen in the reformate peaks at a FRR of 0.25. Once 0.25 is reached, the mole fraction of hydrogen in the reformate gradually declines until the approximate value of 0.55. At this point, the mole fraction of hydrogen becomes severely diluted, and drops off substantially with increasing FRR. Ideally, the most efficient power production will come when the hydrogen concentration is the highest in the SOFC feedstream. This confirms why the FRR should remain at 0.25.

The air temperature in the range of concern (600 K to 1000 K) does not seem to significantly impact SOFC performance. Lower temperatures will emphasize polarization effects, but because the fuel cell has been set to run at a fixed temperature of 1173 K, this effect will not be seen. Therefore, the effect of this factor is as expected.

Fuel utilization and current density are closely related and therefore will be discussed together. The maximum current is a function of the number of electrons moving through the potential difference. This, in itself is determined through the number of electrons available for transport assuming all of the fuel is used. U_f is the ratio of fuel used with respect to the amount of fuel being sent to the SOFC. Equations 42, 43, and 44, outline this effect, with I_{max} representing the maximum current, n_{e^-} representing the moles of electrons transferred per mole of fuel, $n_{fuel(inlet)}$ refers to the molar flow of fuel sent to the SOFC, $n_{fuel(used)}$ is the amount of fuel used in the SOFC, and I is the operational current.

$$I_{max} = n_{(e^-)} F n_{fuel_{(inlet)}} \quad \textbf{Equation 42}$$

$$U_f = \frac{n_{fuel_{(used)}}}{n_{fuel_{(inlet)}}} \quad \textbf{Equation 43}$$

$$I = U_f I_{max} \quad \textbf{Equation 44}$$

In the fuel cell, current is the attempt by the fuel cell to reduce the potential difference between the electrodes. Increasing current will decrease voltage because it will reduce the charge difference between the electrodes, and as seen in Chapter 2, it will increase both concentration and ohmic polarization effects. This means an increase in current will decrease cell voltage, decrease DC power produced, and increase the amount of heat produced in the cell. As seen by the expressions 42, 43, and 44 above, U_f is directly proportional to the operational current which is directly proportional to current density. U_f is also directly proportional to Nernst potential through Equation 45 (previously seen as Equation 21).

$$E = E^0 + \frac{RT}{nF} \ln \left[\frac{X_{H_2OAnO}}{X_{H_2AnO} X_{O_2CaO}{}^{1/2} P_T{}^{1/2}} \right] \quad \textbf{Equation 45}$$

As U_f increases, the mole fraction of water at the anode increases (numerator), and the mole fractions of hydrogen at the anode, and oxygen at the cathode decrease. This corresponds to a reduction in the Nernst potential.

Therefore, the anticipated effect of increasing U_f and/or the current density will be a reduction in cell voltage, a reduction in DC power produced, and an increase in heat produced. The factorial analysis on the SOFC Subsystem model regarding the effect of U_f and current density predict these trends. This means that running the system at lower current densities and lower Uf will amount to better fuel performance. Although this is correct, the amount of power produced will be minimal, and the amount of fuel wasted would be significant. Therefore although the fuel cell may run efficiently, much of the fuel heating value would be wasted as it passes through the cell unused. In most literature systems reviewed here, U_f was found to be set between 0.8 – 0.85 [54, 61-64].

In this analysis, excess air has been shown to exert a positive effect on the stack DC power produced. Air serves two main functions in the fuel cell. First it acts as an oxidising agent, and second it provides a method of cooling the fuel cell [43]. Operating at excess air ratios of between 1 and 2 ensures there is enough flow through the cell to assist with heat removal. The effect is a moderate increase in stack voltage [43]. This trend was initially presented in the *"Modeling Solid Oxide Fuel Cells",* and is reproduced here in the figure below [43].

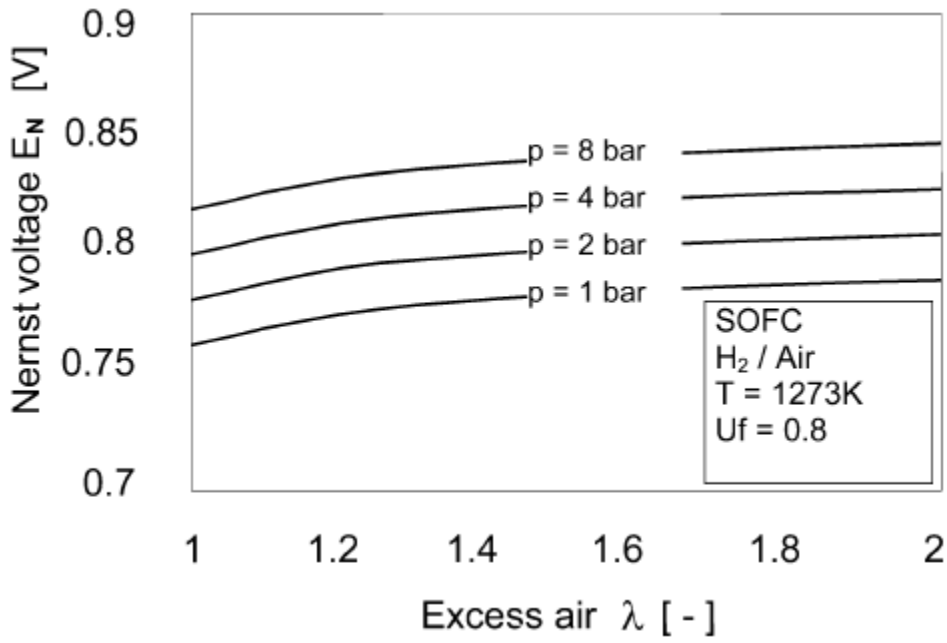

Figure 36: Reproduction of the effect of excess air ratios on the ideal potential of an SOFC at various pressures. [43]

Overall, this discussion provides evidence that the SOFC and the Reformer Subsystem models are behaving predictably, and can give reliable performance during various modelling scenarios.

The ideal system parameters have been determined by using the results of the factorial analysis. These are presented in the tables below, the first one representing the factor settings, and the second one outlining the SOFC performance.

Table 47: Factorial settings for ideal reformer performance.

Factor	Description	Value
a	FRR	0.25
b	Air Flow preheat temperature	400 K
c	Fuel Utilization Factor	0.80
d	Excess Air Factor	1.8
e	Current Density	150

Table 48: SOFC parameters with a first optimization of the Reformer and SOFC Subsystems.

Parameter	Value
Stack Voltage (V)	0.685
Total Power Produced (kW)	51.81
DC Power Produced (kW)	35.15
Stack Heat Loss (kW)	16.03

5.3 Model Validation: Comparison to Published Results

No system was found in literature that utilized volatile organic compounds as a fuel source. Therefore, in order to validate the performance of the SOFC hybrid model, it had to be converted to run on compounds similar to those systems found in literature. The most common fuels used in systems published in literature were methane or natural gas.

The published model being examined is entitled: *"Feasibility Analysis of Methanol Fuelled SOFC Systems for Remote Distributed Power Applications*" [65]. The purpose of this study was to determine through both experimental and model means the feasibility of converting a 5 kW natural gas SOFC power generator system to run on methanol. For the purposes of the model validation, only the modelling portion of this publication will be examined.

The model developed by Staite et al, was completed in Aspentech *HYSYS*, and made to run on natural gas and methanol. A summary of the results they had achieved from their model (for natural gas only) is compared to the values obtained from the SOFC hybrid abatement model (altered to run on natural gas) in the table below.

Table 49: Comparison between Staite et al Power Generating SOFC model vs. the SOFC Hybrid Model (retrofitted to run on natural gas).

System Model Parameter	Staite et al[65]	SOFC Hybrid Model @ 67% recycle fuel	SOFC Hybrid Model @ 40% recycled fuel
Reformer Heat Duty (kW)	3.9	N/A	N/A
Actual Fuel Flowrate	18.7 slpm	18.7 slpm	18.7 slpm
Gross DC Power Output (kW)	5.95	6.30	5.91
Recirculation Fuel (%)	67%	67%	40%
Exhaust-Fuel Heat Exchanger Duty (kW)	0.18	0.19	0.19
Exhaust-Air Heat Exchanger Duty (kW)	6.6	6.27	5.88
Stack Radiation Heat Available to Air (kW)	2.26	3.24	2.81
Recovery Water Heat Exchange Available for Cogen.	5.3	N/A	N/A
Fuel Utilization (%)	83	80	80
Air Utilization (%)	40	40	40
Reformate Composition after Pre-reformer	CO – 23.6%, H_2 – 39.1%, Steam – 27%, CO_2 – 10.3%	CO – 5.13%, H_2 – 15.1%, Steam – 34.0%, CO_2 – 12.4%, N_2 – 33.1%,	CO – 7.5%, H_2 – 26.9%, Steam – 22.1 %, CO_2 – 10.0%, N_2 – 33.1%,

The comparison outlined in the table above indicates that the SOFC Hybrid Model can provide realistic comparisons to a published model. The main difference between the two models lies in the reformate composition, reformer duty values, and to a lesser degree percentage of fuel recycled. The first two factors can be attributed to differences in the reforming system used between Staite et al's model and the SOFC hybrid model. The difference in the percentage of fuel recycled would be dependent upon the physical characteristics of the fuel cell.

At first glance, it was difficult to ascertain what type of reformer was used in Staite et al's model. This was because no steam or oxygen stream was sent into the reformer. In fact, only two streams were sent to the Reformer Subsystem. These were the fresh fuel, and the recycled fuel

streams. The recycled fuel came off the anode side of the SOFC, meaning it would be composed of unused fuel, carbon dioxide, and steam. With the inputs composed of only these materials, the reformer subsystem could only be acting as a steam reformer.

In the case of the SOFC hybrid model, the reformer was developed to resemble an auto-thermal reformer, in which two separate reactions are working simultaneously in two separate reactors. The POX reaction requires oxygen, and in the model, oxygen is supplied as air. This is significant because it means that a substantial portion of the reformate would not only consist of reformed fuel, but also nitrogen. Furthermore, the Auto-thermal Reformer developed in the SOFC model was designed so that the exothermic reactions taking place in the POX reactor could generate the heat required by the endothermic reactions of the steam reformer. This means that in an idealized case, the net heat duty would be zero, and therefore be substantially different then the 3.9 kW identified for the Steam Reformer designed in Staite et al's model.

Calculation of Gross DC power accurately requires physical cell parameters such as active cell area. Without the active cell area, current density could not be calculated, and therefore, the voltage drop as a result of polarization effects would not be available. Therefore, increasing the percentage of fuel recycled decreased the molar composition of hydrogen and carbon monoxide in the reformate, while increasing the total molar flow of reformate. The overall effect was a slight increase in the equivalent molar flow of hydrogen to the fuel cell.

As has been shown previously (Equation 42), an increase in molar flow of fuel will increase the current produced. This alone will increase power. However, increasing current also increases current density, which decreases voltage. Without knowledge of the active cell area, current density is unavailable, therefore, to compare the two models appropriately, two conditions were considered:

1.) Compare the models if both are run at the same recycle rate; and,
2.) Compare the models if both are run such that reformate compositions are similar.

Therefore, although the current density was unknown, comparable performance was achieved by the SOFC hybrid model to the Staite et al's model. Differences between the models can be

attributed to the difference in reformer designs as well as unknown SOFC active cell area. For the purposes of this SOFC model, a current density of 250 mA/cm^2 was assumed.

5.4 Optimization of the SOFC Abatement System Model

With the model validated, model performance can be assessed and compared to current VOC abatement technologies; specifically those outlined in Chapter 3 of this work. To assess this system's performance, quantification of the thermal and electrical efficiencies, as well as operational costs must be determined. To do this, the design criteria must be explored in order to develop ideal operational parameters.

In Section 3.2, a case study regarding the treatment of VOC emissions from a moderate sized automotive parts coating facility was outlined. The main design goal from this problem was the treatment of 417 kg of VOC per day. In order to ensure long term operation of this SOFC hybrid abatement system the main operational criterion is to ensure the SOFC portion of the abatement system is run continuously. This is to prevent thermal cycling, which would cause damage to the electrolyte and electrodes [41]. In order to do this, a stream of VOC components (or fuel) must be supplied to the SOFC on a continuous basis. The case study in question indicated that the daily process time for this industrial coating operation was 16 hours per day for 240 days annually. The automotive industry in North America normally undergoes two-two week shutdown periods annually for maintenance. This means, to run continuously, the system must actually be running for 337 days annually at 24 hours per day.

There are two ways in which this can be done. The first method is split the VOC emission stream after the adsorption-desorption cycle such that a portion is being sent to a storage tank for off production use, while the rest is being treated. The second method is to size the system for the 417 kg of VOCs/16 hours, and then run natural gas through the system during shutdown periods. In this work, only the first method will be investigated.

5.4.1 Optimized Operation of the Adsorber

As outlined in Section 4.2.2, the adsorption system was designed such that excess air from the process stream would be eliminated, leaving only concentrated the VOCs. The VOCs are desorbed using steam as a purge gas. However, the concentration of this is still low because 2 kg of steam are required per kg of VOC desorbed (Refer to Section 4.2.2). To further concentrate the system, a condenser unit was placed after the desorbing bed to eliminate a substantial amount of moisture from the emission stream. The condensed water contains < 1% VOC by mole. This results in 99% recovery of the VOC for treatment. To ensure that the SOFC can operate continuously during non-process hours, approximately 53% of the stream must be sent for storage, while 47% is treated.

Table 50: Breakdown of concentrated VOC compounds.

Substance	Annual mass (kg)	Molecular weight (g/mole)	Annual Moles (kmoles)	Current flow (kmoles/hr)	Adjusted flow For continuous operation (kmoles/hr)
Xylene	20,000	106.18	188	0.0495	0.0232
MEK	30,260	72.12	419	0.109	0.0518
Toluene	35,094	92.15	380	0.099	0.0471
nBA	14,463	116.18	126	0.032	0.0155
Total	**100,000**			**0.290**	**0.137**

This translates in system requirement to handle 0.337 kgmole/hr of a mixture of 60% steam and 40% VOC in the Reformer and SOFC subsystems.

For optimized operation, the adsorption system stream characteristics, as well has heat exchanger duties are presented in the tables below.

Table 51: Adsorption System Stream Characteristic Summary.

Stream ID.	Temp. (K)	Press. (bar)	Molar Flow (mole/hr)	Gas Composition (mole %)						
				O_2	N_2	Tol	MEK	Xyl	nBA	H_2O
Process Emission	298	1.013	4,224	0.209	0.781	2.3e-5	2.6e-5	1.2e-5	8e-6	0
VOC Vapour	385.5	1.013	0.2874	0	0	0.342	0.376	0.169	0.113	0
*Air (N/A)	-	-	-	-	-	-	-	-	-	-
HVOC	378.7	0.993	1.787	0	0	0.055	0.061	0.027	0.018	0.839
HVOC1	*359.0*	0.983	1.787	0	0	0.055	0.060	0.027	0.018	0.839
HVOC2	359.0	0.983	0.7109	0	0	0.134	0.015	0.64	0.043	0.608
WW	359.0	0.983	1.706	0	0	0.003	0.001	0.003	0.001	0.992
HVOC Stored	359.0	0.983	0.3739	0	0	0.134	0.015	0.64	0.043	0.608
HVOC3	359.0	0.983	0.3370	0	0	0.134	0.015	0.64	0.043	0.608
Cathode Exhaust	1071	0.980	3.219	0.102	0.892	0	0	0	0	0
Water	*288*	*1.013*	*1.500*	0	0	0	0	0	0	1
Exhaust	364.7	0.970	3.219	0.102	0.892	0	0	0	0	0
Heated Water	*385*	1.003	1.500	0	0	0	0	0	0	1

**Note: This stream would simply be air at atmospheric temperature and pressure. The system does not accurately represent the actual adsorption-desorption process, just outcome.*

Table 52: Heating system duties.

Unit Operation	Heat Duty (kW)
Cathode HX	19.82
Condenser HX	-13.12

5.4.2 Optimization of the Reformer and SOFC Subsystems

For this system to effectively treat the emission stream presented in Section 3.2 the Reformer and SOFC components must also be optimized. In fact, these two components are the key to developing an abatement system that can operate with reduced operational costs. The incoming

stream characteristics are those coming from the Adsorber Subsystem. More specifically, the characteristics are those outlined in Table 50 labelled *HVOC3*.

As seen in the Factorial Analysis of the Reformer Subsystem (Section 5.1), the initial parameters that should optimize Reformer performance would be those with the settings depicted in the Table 53 below. The results of the optimized Reformer performance are presented in Table 53.

Table 53: Factorial settings for ideal reformer performance.

Factor	Description	Value
a	VOC preheat temperature	800 K
b	Air Flow preheat temperature	400 K
c	Air Molar Flowrate	0.25 kgmole/hr
d	Steam Molar Flowrate	0.422 kgmole/hr
e	POX Reactor Temperature	800 K

Table 54: Optimized reformer results. Factors set to levels for run 17.

Substance	Value
CO	0.051
H_2	0.409
CO_2	0.294
H_2O	0.151
N_2	0.095
Total	1.00

At this point, it should be noted that the FRR was set at 0.5 for the Reformer Factorial Analysis.

The SOFC factorial analysis indicated that SOFC performance peaks at a FRR of 0.25. When this value is substituted into the model, reformate compositions will change. Most notably, a small percentage of Toluene (2.9%), and Xylene (0.4%) will not be completely reformed. Molar composition of the reformate is presented in the table below.

Table 55: Reformate composition at 0.36 FRR.

Substance	Value
CO	0.042
H_2	0.429
CO_2	0.251
H_2O	0.152
N_2	0.108
Toluene	0.017
Xylene	0.002
Total	1

If the Toluene and Xylene left in the reformate were to breakdown in the SOFC, this would not be a problem, however, this is not the case. These trace amounts remain in the SOFC even after operation. This means a portion of these contaminants will be released into the atmosphere, which is specifically against the an important criteria (removal of all contaminants). Therefore, the Reformer conditions must be altered to eliminate both toluene and xylene from the reformate.

The easiest way this can be done without altering design constraints is to incrementally increase the steam or air flow rates being sent to the Reformer Subsystem. From the factorial analysis (Section 5.1), it has already been determined that an increase in the molar flow rate of steam will actually decrease the amount of hydrogen the in system because there is already enough steam in the reaction mixture to sustain the steam reforming and WGS reactions. Furthermore, because air is a much more economical material to use then steam, it makes more sense to adjust this factor first. In this instance, the molar flow rate of air will be increased incrementally until all of the toluene and xylene have been removed from the reformate. The reason this is being done slowly, is to find the maximum hydrogen concentration. Figure 37 illustrates the effect increasing the molar flow rate of air will have on the composition of toluene and xylene in the reformate. Figure 38 illustrates the effect increasing the molar flow rate of air will have on H_2, CO, and CO_2 in the reformate.

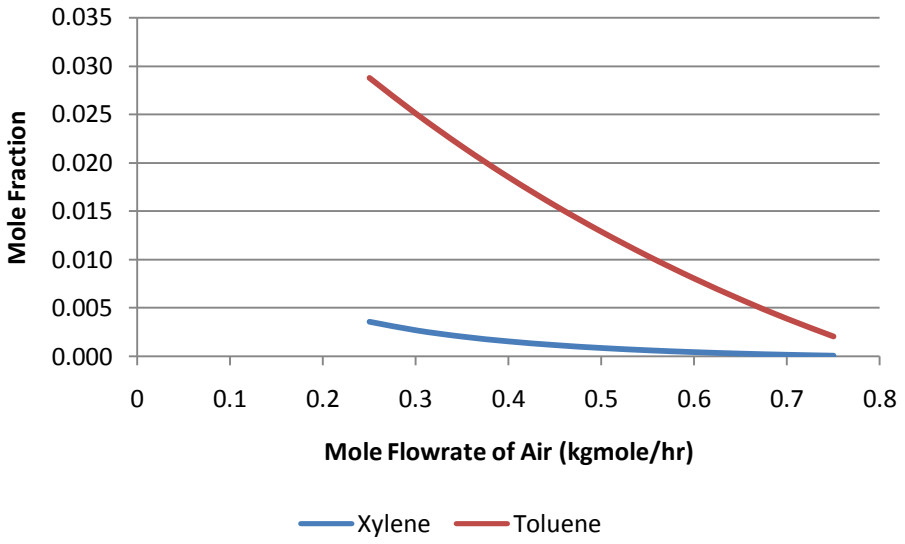

Figure 37: The effect of increasing the molar flow rate of air on the molar composition of Toluene and Xylene in the reformate.

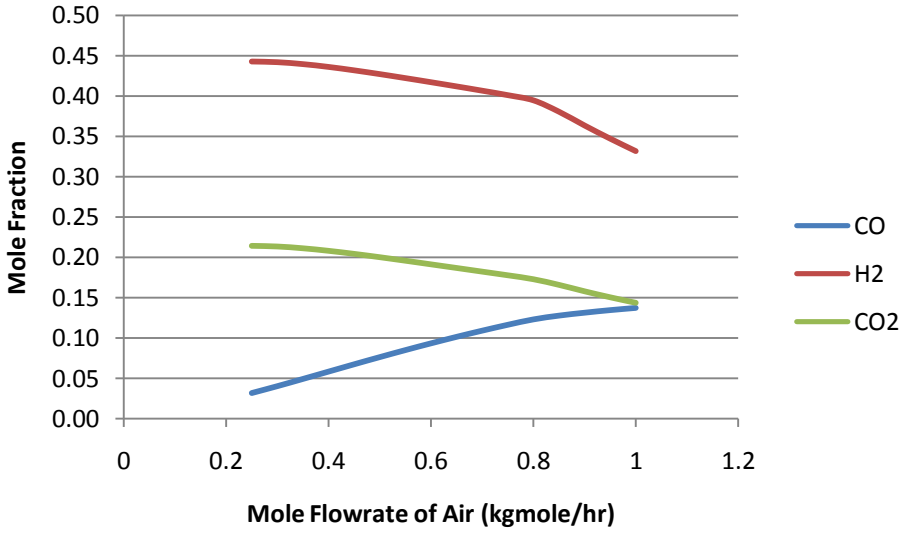

Figure 38 The effect of increasing the molar flow rate of air on the molar composition of H_2, CO, and CO_2 in the reformate.

Figure 37 indicates that the xylene and toluene are not completely removed from the reformate until the molar air flow rate reaches 0.75 kgmole/hr. Increasing the molar air flow this high only moderately reduces the mole fraction of H_2 and CO_2 in the reformate, while increasing the

amount of CO. Interestingly enough, these trends are also supported by the Reformer Factorial Analysis previously performed. Since the SOFC can utilize CO as well as H_2, the effect of this reduction in hydrogen in the reformate will not substantially impact SOFC performance.

Before making this change to the system parameters, a check can be performed to see how increasing the molar air flow to the reformer will affect SOFC performance. This is presented in the table below.

Table 56: SOFC performance assessment with increasing molar air flow being sent to the Reformer.

Molar flow of air (kgmole/hr)	Total Power (kW)	DC Power (kW)	Heat Loss (kW)	% Heat Loss
0.25	50.1	35.0	16.0	31.3%
0.30	55.0	37.5	17.4	31.7%
0.35	59.0	40.0	18.9	32.1%
0.40	62.9	42.5	20.4	32.4%
0.45	66.8	44.9	21.8	32.7%
0.50	70.7	47.3	23.3	33.0%
0.55	74.4	49.7	24.8	33.2%
0.60	78.3	52.0	26.2	33.5%
0.65	82.0	54.3	27.7	33.7%
0.70	85.7	56.6	29.1	33.9%
0.75	89.3	58.8	30.5	34.1%
0.80	92.4	60.6	31.7	34.3%
0.85	92.7	60.8	31.9	34.4%
0.90	91.7	60.1	31.6	34.4%
0.95	90.6	59.4	31.2	34.5%
1.00	89.5	58.6	30.9	34.5%

Table 56 indicates that the overall power generated from the cell increases without an appreciable change in energy lost to heat. This is important, because in this range of change, DC peak power output occurs at a molar air flow of 0.80, which for practical purposes, is the level at which all VOCs have been reformed completely. For this reason, optimal performance can be achieved by raising the molar flow rate of air to the reformer from 0.25 kgmole/hr to 0.80 kgmole/hr.

The last thing that needs be done on this system is a thermal analysis. To calculate the SOFC power production, the *HYSYS Gibbs* function was used to model the anode. The *Gibbs* reactor representing the anode was able to calculate the power produced from the reaction, and with use of the relationships presented in Appendix F the anticipated DC power could be calculated. The remaining energy would represent the heat lost. The primary mode in which heat would be removed from the cell would be the exhaust streams (*Anode Exhaust* and *Cathode Exhaust*). To model the appropriate fuel utilization and oxygen transfer processes across the electrolyte, the streams were split prior to entering the fuel cell, then mixed back together subsequent to the reaction. This means that the streams that have been split off prior to entering the cathode or anode must be heated to the exhaust temperature of the fuel cell. To do this two *HYSYS Heater* functions were used on both the *Unused Fuel*, stream, and the *Excess Air* Stream. Under these conditions there is a problem. The system calculates that only 31.6 kW of energy is lost as heat, while the *Excess Air* stream requires 38.0 kW and the *Unused Fuel* stream requires 1.22 kW. In total the system is short 7.62 kW.

The problem is that there is too much flow moving through the system. Therefore, the SOFC operational temperature of 1173 K is too high, and must be reduced. This would lower the heat demand of both the *Excess Air* and *Unused Fuel* streams. By lowering the SOFC operating temperature to 1073 K, the heat duty of both the *Excess Air* and *Unused Fuel* Streams decrease to 31.93 kW and 0.512 kW, where as the excess energy available for heat is calculated to be 32.4 kW. Furthermore, as a result of this temperature change, the voltage of the SOFC also increased, altering all power calculations. This is due to the effect that a reduction in temperature would have on the Nernst potential.

Therefore, the optimal conditions for this system running on 0.337 kgmole/hr of humidified mixed VOC is presented in Table 57, with the SOFC energy output displayed in Table 58. Stream characteristics for each subsystem at theses conditions are presented in Appendix G.

Table 57: SOFC hybrid model optimal parameters.

Description	Value
VOC preheat temperature	800 K
Air Flow preheat temperature	400 K
Air Molar Flowrate (to reformer)	0.80 kgmole/hr
Steam Molar Flowrate (to reformer)	0.422 kgmole/hr
POX Reactor Temperature	800 K
Fuel Recycle Ratio	0.25
Contaminant Stream after adsorption	0.337 kgmole/hr
System Pressure	1 bar
Air temperature	298 K
Water temperature	288 K
Fuel Cell Operational Temperature	1,073 K

Table 58: SOFC parameters with a first optimization of the Reformer and SOFC Subsystems.

Parameter	Value
Stack Voltage (V)	0.703
Total Power Produced (kW)	93.0
DC Power Produced (kW)	60.6
Stack Heat Loss (kW)	32.4

5.4.3 SOFC System Efficiency

With the model optimized, the electrical and total efficiencies can be determined. The electrical efficiency is the amount of power produced from the fuel cell vs. the lower or higher heating value of the feedstock. The total efficiency examines the total amount of energy usable energy extracted from the system in comparison to the lower or higher heating value of the feedstock.

The table below summarizes the Higher Heating Values (HHV) of the contaminants in the emission stream.

Table 59: Electrical efficiency calculation. HHV for the individual VOC compounds have been obtained from the indicated resources.

Component	Mass flow rate (kg/sec)	Daily Mass (lbs/hr)	HHV (Btu/lbs)	Reference
Toluene	$1.15x10^{-3}$	9.19	17,620	Lewandowski, 2000[21]
Xylene	$6.33x10^{-4}$	8.00	17,760	Lewandowski, 2000[21]
MEK	$1.01x10^{-3}$	5.01	13,480	Cheremisinoff, 1999[67]
nBA	$4.72x10^{-4}$	3.74	13,130	Cheremisinoff, 1999[66]

To calculate the total efficiency of the system, the thermal energy extracted from the processes must be included in the total analysis. This means determining the amount of heat extracted from the exhaust streams. The cathode exhaust stream was used to preheat the fresh air being sent to the cathode as well as generate steam for the adsorption process. The anode exhaust stream was used to preheat the incoming air and water feeds supplying the reforming processes. Lastly, heat was also removed from the desorbed steam/VOC stream in the *Condenser* unit. All of these contributions are listed in the table below.

Table 60: Total Heat Duty of Heat Recovery Systems.

Heat Exchanger ID	Incoming Streams	Outgoing Streams	Subsystem Location	Heat Duty (kW)
Air HX	Anode Exhaust, Air Feed	AE1, Air	Heat Exchanger	0.666
Water HX	AE1, Water in	Water HX, System Exhaust	Heat Exchanger	6.025
Steam Boiler	Cathode Exhaust, Water	Exhaust, Steam	Adsorber	19.82
Condenser	HVOC1	HVOC2	Adsorber	13.12
Air Preheat HX	Cathode Exhaust, SOFC-Air	Cathode Exhaust1, SOFC-Air1	SOFC	5.12
Total (kW)				**44.78**

The efficiency calculations are provided in the table below.

Table 61: Electrical and Total Efficiency calculations based upon the HHV of the feedstock.

Energy Term	Source	Value
Total Energy In	Table 58	420,670 Btu/hr
Total Power Produced	Table 57	60.6 kW = 206,571 Btu/hr
Total Heat Energy Extracted	Table 59	44.78 kW = 152,900 Btu/hr
Electrical Efficiency	**N/A**	**49.2%**
Total Efficiency	**N/A**	**85.5%**

At this point, the model has been validated and optimized to treat the VOC emission stream coming from the Automotive Coating facility described in Section 3.2. The system is now ready to be evaluated using the Technology Comparison Tool outlined in Section 3.1, and compared to the results of the other technologies developed in Section 3.3.

5.5 Technological Evaluation of the SOFC Hybrid Abatement System

5.5.1 Regulatory Requirements

To estimate the removal efficiency, the anode exhaust stream of the SOFC model can be analyzed. The anode gas composition using the optimized system conditions are as presented below:

Table 62: Anode gas composition using the optimized SOFC Abatement System at a molar flow rate of 4.101 kgmole/hr.

Substance	Value
Oxygen	0.000
Nitrogen	0.245
Argon	0.001
Toluene	0.001
MEK	0.000
Xylene	0.000
nBA	0.000
CO	0.023
CO2	0.269
Water	0.381
NO2	0.000
Hydrogen	0.079

This indicates that all but one of the contaminants has been destroyed. For this system, 25% of the exhaust will be re-circulated back into the actual reformer, and thus, only 75% of the toluene will be emitted. In total, the actual percentage of toluene that has escaped capture is 5.2%. Of the other species, everything has been destroyed, therefore all intensive purposes, the destruction efficiency of this system can be termed > 95%.

5.5.2 Lifecycle Costs

Capital costs will be a combination of costs for each subsystem. This means individually determining costs for the Adsorber, Reformer, and SOFC systems. The costs for the adsorber have already been established, however, they must be altered because they were established for a standalone adsorber. This means the cost analysis includes hazardous waste disposal and energy costs associated with steam generation, both of which would not be relevant when using the adsorber as a pre-concentrating system for the SOFC system. The new cost analysis is presented in the table below.

Table 63: Adsorber Subsystem Capital and Operational Costs.

Purchased and installed equipment costs:					
			Factor	Cost	Subtotals
Vessel Cost				$99,500	
Carbon Cost				$22,700	
Equipment Cost (1994 Costs)				$166,948	
Equipment Cost (2006 Costs) - factor:			1.621	$270,623	
Taxes			0.15	$40,593	
Freight			0.03	$8,119	
Foundations and Support			0.08	$21,650	
Handling and Erection			0.14	$37,887	
Electrical			0.04	$10,825	
Piping, Painting and Installation			0.04	$10,825	
Subtotal Direct Installation Costs					$400,522
Indirect Costs					
Engineering			0.1	$27,062	
Construction and Field expense			0.15	$40,593	
Start-up and Performance testing			0.03	$8,119	
Contingencies			0.03	$8,119	
Subtotal Indirect Installation Costs					$83,893
Total Installation Costs					$484,415
Direct Annual Costs					
Utilities					
	Steam (Gas Cost)			$0	
	Water Cost			$7,001	
	Electricity (system fan + cooling fan)			$40,851	
Labour		hours work	rate of pay		
	Supervisor	8/week	$20/hr	$5,486	
	Labour	15% of labour		$823	
Maintenance					
	Labour	8/week	$25/hr	$6,857	
	Material	same as labour		$823	
Solvent Disposal		$300/drum		$0	
Subtotal Direct Costs					$61,841
Indirect Annual Costs					
Overhead	0.6 of		0.6	$162,374	
Administration					
	Property Taxes		0.01	$2,706	
	Insurance		0.01	$2,706	
	Capital Recovery		0.1628	$44,057	
Subtotal Indirect Costs					$211,843
Total Annual Costs					$273,700

Costs for the SOFC vary. Horne reported that most SOFC developers are targeting installation costs between $800 - $1,000 /kW (Horne, 2002). Other references indicate current costs to be closer to $2,000 / kW. The basic SOFC costs in this work will be based upon the $2,000 /kW rate, with our system being sized to generate 75 kW. For the method of capital investment, Peters and Timmerhaus' method will be used [67]. The cost factors used for this analysis are presented below.

Table 64: Capital Cost Development for a 75 kW SOFC based upon cost factors developed by Peters and Timmerhaus [67].

Purchased and installed equipment costs:	**Factor**	**Cost**	**Subtotals**
SOFC purchased equipment	0.32	$150,000	
installation	0.08	$37,500	
instrumentation	0.06	$28,125	
piping	0.08	$37,500	
electrical	0.04	$18,750	
building	0.04	$18,750	
land (and yard)	0.04	$18,750	
service facilities (installed)	0.13	$60,938	
Subtotal Direct Installation Costs			**$370,313**
Indirect Costs			
Engineering	0.05	$23,438	
Construction and Field expense	0.09	$42,188	
Start-up and Performance testing	0.02	$9,375	
Contingencies	0.05	$23,438	
Subtotal Indirect Installation Costs			$98,438
Total Installation Costs			**$468,750**

Chen and Elnashaie developed costs for pilot sized autothermal reforming systems (100 kg/H_2 day) as well as for industrial sized systems [68]. The production value of 100 kg/H_2 day is similar to that in this study, and therefore, their reported capital cost estimates will be used here. For the equipment alone, they estimate amounted to $73,250 (USD). It included several items which are not needed for this system (e.g. desulphurization tank, liquid hydrocarbon pump, etc...). This cost was assumed to be approximately 32% of the total capital investment for the reformer, and thus the total system cost was found to be approximately $269,300 (USD). Here, it is important to note that Chen and Elnashaie developed these costs based upon finding a suitable catalyst. If this was not the case, costs would likely be higher. The breakdown of these factors and overall Reformer capital cost is presented in the table below.

Table 65: Reformer Capital Costs based upon cost factors developed by Chen and Elnashaie [68].

Purchased and installed equipment costs:	Factor	Cost	Subtotals
Reformer purchased equipment	0.32	$73,248	
installation	0.08	$18,312	
instrumentation	0.06	$13,734	
piping	0.08	$18,312	
electrical	0.04	$9,156	
building	0.04	$9,156	
land (and yard)	0.04	$9,156	
service facilities (installed)	0.13	$29,757	
Subtotal Direct Installation Costs			**$180,831**
Indirect Costs			
Engineering	0.05	$11,445	
Construction and Field expense	0.09	$20,601	
Start-up and Performance testing	0.02	$4,578	
Contingencies	0.05	$11,445	
Subtotal Indirect Installation Costs			$48,069
Total Installation Costs			**$228,900**

With the capital cost of both the Reformer and SOFC Subsystems developed, all that is left is the determination of the operational costs. As outlined in Section 5.4.3, the system has been designed to re-coup much of the heat that is generated. In typical SOFC and Reforming systems, costs can be as high as 44% of the total investiture [64]. This is because the prime objective of SOFC technology is to generate power from a fuel source. For most practical applications this means the use of large quantities of natural gas.

In this application, the feedstock is the waste stream of another process. This means the feedstock has no value associated with it. Therefore the primary operational costs are removed, only those associated with maintenance, and pumping air through the system are remaining. For the Reformer, Chen and Elnashaie, developed cost factors for a pilot plant creating 100 kg of hydrogen per day [68]. The costs were based upon the amount of hydrogen produced and could be transferable to the Reformer case presented here. Therefore operational based upon Chen and Elnashaie's cost factors costs for electricity only are presented in the table below. The cost for process water is based upon the flow rate of water being sent to the Reformer costing an average

of $0.6/m^3$. Here it also should be noted that the reformer system cited here are for a fluidized bed, meaning there will be some flow limitations [68].

The operational costs are summarized in the table below.

Table 66: Total Operational Costs for the Reformer Subsystem.

Reformer System Operational Costs		
Process Water		
Molar flow Required	0.422	kgmole/hr
Mass flow per day	182.304	kg/day
Volume per day	182.304	L/day
Volume per day	0.182304	m3/day
Cost	$0.11	$/day
Total Annual Water Cost	**$37**	**$/year**
Electrical Costs		
Mole flow of H_2	1.35	kgmole/hr
Mole flow of CO	0.39	kgmole/hr
Equivalent mass flow of H_2	1.74	kgmole/hr
Mass flow of H_2	3.49	kg/hr
Annual H_2 flow	28,210.94	kg/annually
Cost factor electricity	$0.69	$/kgH2
Total Annual Electrical Cost	**$19,324**	**$/year**
Labour Costs		
*Supervisor	0	
*Maintenance	0	
Total Operational Costs		**$19,361**

**Note: "It is assumed that for small plants, the reformers could operate unattended accept for maintenance and emergency repairs"[69] .*

For the SOFC, the situation is similar, and the operational costs will be limited to the electrical consumption required to send air through the SOFC at a rate of 6.127 kgmole/hr. Therefore electrical costs can actually be developed by using rule of thumb measurements. The Handbook of Mechanical Engineering Calculations outlines that 22 horsepower (16.4 kW) is required to push every 100 cfm of air. This rule of thumb can be used to determine the amount of electrical

power required to supply the 6.127 kgmole/hr of air needed to the SOFC system. The calculation is presented below.

Flowrate of drying-cooling air (cfm)	= 6.187 kgmole/hr = 87 cfm
Size of motor required (hp)	= 22 hp (oversize as a safety)
Power rating (kW)	= 16.4 kW
Annual operation (hrs)	= 337 days x 24 hrs/day = 8,088
Cost per kWh	= $0.08
Annual Cost	= 16.4 kW x 8,088 x 0.08 = $10,611

Therefore, SOFC annual operational costs are $10,611, assuming maintenance and labour costs are lumped in the adsorber costs. To determine the total system cost for the SOFC Abatement system, the capital and operational costs are for each subsystem are summed together. This is summarized in the table below.

Table 67: SOFC first year investment requirements.

Description		**Totals**
Adsorber Capital Cost	$485,415	
Reformer Capital Cost	$468,750	
SOFC Capital Cost	$228,900	
Subtotal		**$1,183,065**
Adsorber Operational Cost	$61,841	
Reformer Operational Cost	$19,361	
SOFC Operational Cost	$10,611	
Subtotal		**$91,813**
Total First Year Investment		**$1,274,878**

Lifecycle costs are then established using a discount rate of 3% which is outlined in the NIST Handbook 135 Life-cycle costing Manual for the Federal Energy Management Program[53]. Cost factors for energy requirements were determined from within the NIST Handbook [53]. Table 66 above describes the calculated capital and operational costs, whereas Table 67 outlines the

lifecycle costs associated with treating the Case study facility presented in Section 3.2 of this work.

Abatement System	Case Study Costs
SOFC Hybrid	$3,268,107

It is important to note that this cost is only based upon the operational and capital costs, and does not taken into account the value of the electricity that will be produced. The anticipated annual amount of electricity generated from this system is calculated below:

DC Power Produced	= 60.5 kW
Hours operating	= 8,088 hours
Annual kW hours generated	= 489,324 kWh
Annual Value of Electricity (assume $0.08/kWh)	= $39,145

Over a 10 year period, the value of this electricity can be determined and subtracted from the Lifecycle costs displayed in Table 67 above. The cost reduces by $266,186, altering the actual 10 year Lifecycle cost of the SOFC system to a value of $3,001,921.

5.5.3 Operational Flexibility

There are no technologies in published literature that have been developed for this purpose. For this reason, operational issues are not known. However, there are several operational characteristics of each subsystem that make the overall technology more robust.

First off, the reformer can reform most hydrocarbons to usable fuels [70]. This means that even if the composition of the emission were to change, the abatement system as a whole could still operate. Realistically, the only adjustments that would require being made would be molar air and steam flow rates. Secondly, unlike heat engine styled power generation devices, SOFC's run very well on partial load [43]. This means that the overall system could be sized slightly larger than is required to anticipate future increases in production without detrimentally affecting

performance, and if emissions and/or operations were to decrease the fuel cell could be operated at part load.

The adsorber system also adds another piece of flexibility in the system, because it can act as a as a standalone pollution treatment device if problems arise with the Reformer and/or SOFC.

Realistically, the main flexibility issues would be those associated with the adsorber. As described in Section 3.5, the design of adsorption systems tends to be quite precise. The carbon requirement dictates the overall load that can be treated, and once the system is sized it is very difficult to make alterations for different loading levels or different flow rates. Therefore if the load is increased substantially, the system will not be able to handle the increase in load unless the overall configuration of the system is changed. More carbon would have to be added (new bed added), cycling and regeneration times would have to be re-calculated, and in extreme cases these changes may not be feasible.

Moreover, changes in load composition pose other unique problems. The original design of these systems relies on the adsorption characteristics between the most difficult species to adsorb. If a new compound was included into the emission mixture, and this new compound was more difficult to adsorb than the assumptions used in the original design, a breakthrough situation may occur during operation. This simply means the system would have to be redesigned according to the new compound's adsorption characteristics. Likely this would result in a change in volume or type of adsorbent needed for the emission change.

Conversely, this system can operate both continuously and intermittently. This offers the advantage of not using extra energy to operate the system when production is down, or to start-up the systems when production times fluctuate substantially.

Overall, SOFC hybrid abatement system will be moderately tolerant to flow rate variations, fairly intolerant to changes in emission composition, and very tolerant to intermittent vs. continuous operational strategies. The table below outlines the operational flexibility scores for adsorption based VOC abatement technologies.

Table 68: Overall operational flexibility scores for thermal oxidation abatement technologies.

Abatement System	Start-up times	Continuous vs. intermittent operation	Flexibility: Flow tolerance	Flexibility: Conc. tolerance
SOFC hybrid	3	3	2	1

5.6 Final Technology Comparison

Now the technologies can be compared. Overall, in terms of the ability of each technology to meet current and future regulatory requirements, the Thermal Oxidation systems all appear to have the highest destruction efficiencies. The only foreseeable problem with Thermal Oxidation systems is the fact that they emit substantial amounts of NO_x and CO.

Adsorption systems also have relatively high removal efficiencies, but they can be limited if concentrations change or if compositions change. This means limitations for future facility change.

Biological systems have the lowest destruction efficiency, and although they can meet current limits, these systems can be problematic if changes in composition or flowrate occur.

The SOFC hybrid system is limited by those same ones imposed by the adsorption system. The adsorption system will dictate what contaminants get capture and concentrated and thus which contaminants will get treated. Overall, the system's destruction efficiency was seen to be above 95%.

The regulatory scores for these systems are presented in the table below.

Table 69: Criteria rating for all technologies in the Regulatory Performance category.

Abatement System	Regulatory Compliance
*Regenerative Thermal Oxidation	3
Biofilter	2
Adsorption	3
SOFC Hybrid Abatement	3

**Note: The scores are the same for all three variations of the Regenerative Thermal Oxidation technology.*

The SOFC system has the lowest 10 year Lifecycle cost out of any of the technologies studied here. This is because approximately 85% of the energy of the emission is being recaptured to do useful work somewhere else in the system. The RTO systems all have substantial operational costs, and the biofilter requires a tremendous amount of area to ensure the appropriate residence time can be met. The stand-alone adsorption system is really the only technology that can competitively compete with the SOFC hybrid abatement system. The 10 lifecycle costs for all four of these technologies are presented below.

Table 70: Ten year lifecycle cost analysis on all technologies that could treat the emissions from the facility outlined in Section 3.2.

Abatement System	Regulatory Compliance
Thermal Oxidation (RTO) – Recuperative	$14,319,941
Thermal Oxidation (RTO) - Regenerative	$8,794,107
Thermal Oxidation (RCO)	$6,192,087
Biofilter	$11,644,813
Adsorption	$3,060,874
SOFC Hybrid Abatement	$3,001,921

Lastly, the technology with the most operational flexibility is Thermal Oxidation. These systems can all handle almost any contaminant, and have a large range in which concentrations can change within the emission [21]. Safety limitations prevent treatment of too high a concentration, while economic issues would prevent the treatment of too low a concentration [21].

Performance of biofilters is very difficult to predict. Start-up times can range between several days to a month, and if the microbial populations are killed, the work required to restore the system is immense [24]. For these reasons, this system is the least operationally flexible.

The advantage of using an adsorption system is that start-up times are fast, and the system can be run intermittently, without performance issues [1]. Issues only arise if future change is expected in the facility. If contaminants that are not compatible with the size of adsorption beds are suddenly run through the system, breakthrough could occur, making the system less flexible.

Lastly, the SOFC hybrid system has operational characteristics from two systems that make it more robust then either sub-system by itself. For instance even if breakthrough were to occur on an adsorption bed, the contaminant would be directed to the Reformer, in which it would be destroyed anyway. The adsorption bed allows for a secondary stand-alone system to be integrated into the overall system. This ensure that if the Reformer or SOFC breakdown, processes could still go on because the adsorber could still capture the emissions.

Overall, although the SOFC system may suffer from similar issues as the adsorber system, it would be more operationally flexible. A summary of the operational flexibility scores is presented in the table below.

Table 71: Operational Flexibility Scores for all systems treating the facility profile described in Section 3.2.

Abatement System	Start-up	Continuous vs. Intermittent	Flexibility: Flow	Flexibility: Conc.	Total
Thermal Oxidation (RTO) – Recuperative	2	2	1	3	12
Thermal Oxidation (RTO) - Regenerative	2	2	1	3	12
Thermal Oxidation (RCO)	2	2	1	3	12
Biofilter	1	3	1	1	3
Adsorption	3	3	2	1	18
SOFC Hybrid Abatement	3	3	2	1	18

From this analysis, the SOFC abatement system is a technology that can compete with the currently used VOC abatement technologies. The system has a lower 10 Lifecycle cost than any other system, and it is the most operationally flexible. Its destruction efficiency is high (> 95%), and its exhaust components are environmentally benign. Overall the system shows promise.

However, there are two main issues with this system. The first is that in order to have a reasonably sized SOFC and Reformer unit, the desorbed stream coming off the Adsorption system had to be partially condensed. This removed substantial amounts moisture from the system and simultaneously extracted 13.12 kW of energy which could be used elsewhere in the plant. The problem is that a small fraction (< 1% by mole) of solvent liquid was trapped in this aqueous phase. Although these compounds compose a very small mole fraction of the total stream, they are still significant. For instance, in the York Region (north of Toronto), the sewer use By-Law S-0064-2005-009 sets limits on three of the four VOC contaminants in this emission stream. The table below compares the concentration of VOC in the condense water to the York Sewer Use By-Law limits. As is evident, this contaminated water cannot be disposed of in the sanitary sewer.

Table 72: Comparison of the concentration of VOC contaminants in the condensed phase of the WW stream of the Adsorber HYSYS subsystem model to the York Region Sewer Use By-Law S-0064-2005-009 Limits.

Component	Concentration (mole fraction)	Molecular Weight (g/mol)	Concentration (mg/L)	York Sewer Use Limits (mg/L)
Toluene	0.00264	92.15	13,628	0.27
MEK	0.00114	72.12	4,605	8.00
Xylene	0.00303	106.18	18,023	14.00
nBA	0.00151	116.18	9,828	N/A

This presents a potentially challenging problem. First of all, it means that in order to treat or dispose of the water, extra costs will be incurred. This could push the overall cost of this system fairly high, especially when considering what costs could be to dispose of solvent contaminated materials.

The second main issue is in regards to technology maturity. The cost of SOFC technology is extremely high because commercial use and production has not begun. Literature references indicate that in order for SOFC technology to become more accessible, costs will have to drop to \$400/kW [71]. If this were to occur, the cost of this abatement system would substantially decrease. Along with this is the fact that there are very few SOFC units in operation, and of those, only one has been designed to run on VOC compounds.

Chapter 6: CONCLUSIONS AND RECOMMENDATIONS

6.1 Conclusions

Volatile organic compounds are dangerous to handle, and are designated smog precursors. Regulatory bodies around the world are implementing tighter and tighter limitations on the emission of these compounds from industrial sources. As a result, many industrial facilities are searching for economical and efficient treatment options.

Unfortunately, although many current technologies are efficient, they tend to be costly to operate, and in some cases, inflexible. For this reason, technologies must be developed that can be effective, economic, and operationally flexible.

The technology proposed in this work consists of an adsorption system coupled with a Solid Oxide Fuel Cell (SOFC), which allows for energy recovery from the VOC stream. This thesis examined the use of model-based design to develop and optimize a hybrid VOC abatement technology that uses a SOFC for energy recovery. The model was built using existing *HYSYS* unit operation models, and was able to provide a detailed thermodynamic and parametric analysis of the hybrid SOFC-VOC abatement system. The model was validated by comparison to published literature results and through the use of several Design of Experiment factorial analyses.

As the developed model indicates, the system is not only cost effective, it is also very efficient. In comparison to three other VOC abatement technologies, the SOFC hybrid system was seen to have the lowest operational cost over a 10 year lifecycle, and the highest operational flexibility rating in a decision analysis. More specifically, the model illustrated that this type of system could achieve a 95% destruction efficiency with a lower ten year lifecycle cost then Thermal Oxidation, Biological Oxidation, or Adsorption VOC abatement systems. The 10 year life cycle cost for the Hybrid SOFC system was $3M. For this reason, this system has promise in becoming a very useful mainstream VOC abatement tool.

The cost of SOFC technology is high, and will remain so for several years until the technology matures. This means that although the system shows promise, pilot testing should be done to verify model results and prove the robustness of the system. Secondly, studies should be conducted on improvement of the adsorption system and possible removal techniques of the VOC from the condensed stream.

6.2 Recommendations

Although the system shows promise, there are several avenues in which this research should move to ensure appropriate technological maturation. The first and most important recommendation is to further develop the adsorption subsystem model through experimental trials and dynamic model development. For this abatement system, the adsorber removal efficiency will likely be the greatest single factor contributing to the overall destruction efficiency. This is for several reasons:

1. The reaction conditions of the reforming system can easily be altered to accommodate different concentrations and compositions of compounds; and,
2. The SOFC efficiency will be dependent upon the concentration and composition of material coming out of the reformer, and since the reformer can theoretically reform any hydrocarbon, the SOFC should never have a problem with regards to the fuel stream.

Study of the Adsorption subsystem would include development of a dynamic adsorption model to study the adsorption-desorption cycles, and steam ratios required for desorption. Once developed, adsorption experiments should be carried out to optimize the model for VOC systems.

A second recommendation would be to begin experimental trials on the Reformer and SOFC units. The goal would be to confirm some of the issues identified during the Factorial experiments.

For the reformer this would include experimentally determining if utilizing the Gibbs function is appropriate by confirming that equilibrium would be obtained. Another avenue of research would be to determine if enough steam was already present to drive the steam reforming reactions to completion and minimize coke formation. Lastly, it would be advisable to experiment with the partial oxidation reactions to determine under what conditions the reverse water-gas shift reactions would occur, and how to prevent them.

For the SOFC, the primary concerns would focus on the predictable performance of the model vs. actual operation, and how well the system would operate on an unreformed mixture of VOCs. Both these issues could be checked with the same apparatus, and with only a small number of actual cells – perhaps 3 or 4. In this way experimental costs are kept low, and if the presence of hydrocarbons on the electrodes do cause issues (such as degradation or performance problems), only minimal costs are expended.

The final recommendation is to perform experimental trials that would mimic an industrial process emitting exhaust for only a portion of the day. Suggested trials for this investigation would involve the following scenarios:

1. Storing VOCs in an adsorber bed;
2. Always desorbing the system, and storing the concentrated VOCs in a holding vessel; or,
3. Running the entire flow of VOCs through the system as they are desorbed, then switching the system over to natural gas for off-line operation.

APPENDICES

Appendix A: Thermal Oxidation Calculations

Recuperative Type

RTO Calculations: These calculations are based upon those completed in EPA's Handbook of Air Pollution Control Technologies. The process of calculating operational and cost criteria is displayed below:

Step 1: Determine the Oxygen Content

This is done to determine if excess air must be supplied to promote combustion. In most cases, the VOC compounds are so diluted in air, no excess is needed.

$$\textbf{Volume \% of Air} = 100 - \frac{\mathbf{V_{VOC}}}{\mathbf{V_{Air}}} \textbf{ x } 100\%$$

$$\%O_2 = 0.205x\ Volume\%\ of\ air$$

Step 2: Determine the LEL of the VOC Mixture

This is done to ensure the VOC mixture is not too concentrated. Most North American jurisdictions place restrictions on the LEL concentration to be below 25% of the concentration of the LEL.

$$LEL_{mix} = \left[\sum_{j=1}^{n} \frac{x_j}{(\sum_{i=l}^{n} x_i)LEL_j}\right]^{-1}$$

Here:

Xi Volume fraction of combustible component i

LELj Lower explosive limit of component j (ppmv)

n Number of combustible components in the mixture

Step 3: Establish Temperature of Operation

The residence time and combustion temperature denote the percentage destruction. For VOC compounds, typically a temperature of 1,600 F with a residence time of 0.75 seconds will provide an overall destruction rate of 98%.

Step 4: Calculate waste gas temperature at the end of the pre-heater

This balances the costs between needing a large heat exchanger vs. using more natural gas. The larger (or better) the heat exchanger, the less natural gas is required.

$$F_{ER} = \frac{T_{wo} - T_{wi}}{T_{fi} - T_{wi}}$$

Where:

T_{wo}	= Temperature of waste gas out	Solving for this gives: 1,283 F
T_{wi}	= Temperature of waste gas in	= 77 F
T_{Fi}	= Temperature of exhaust gas in	= 1,800 F
F_{ER}	= Fractional Heat Recovery	= 70%

By setting the fractional heat recovery to a desired level, one can re-arrange the equation and solve for T_{wo}. Here the fractional heat recovery was set at 70%. It is important to note that the T_{wo} should be lower than that required to initiate combustion. A sufficiently high Two could initiate reaction (with heat release) in the pre heater. This is only the case for recuperative type systems, not regenerative type systems in which heat recovery percentages are set around 95%.

Step 5: Calculated Auxiliary Fuel Requirements

$$Q_{fg} = \frac{D_e \, x \, Q_e \, x \, [C_{p_{air}}(1.1 \, x \, T_c - T_{he} - 0.1T_r) - h_e]}{D_f \, x \, [h_f - (1.1 \, x \, C_{p_{air}}(T_c - T_r)]}$$

Where:

D_e	Energy Density of VOC (Btu/scf)	= 0.0739
Q_e	Max emission flowrate (cfm)	= 60,000
$C_{p(air)}$	Heat capacity of air (Btu/lbF)	= 0.253
T_c	Combustion Temperature (F)	= 1,800
T_{he}	Temperature Entering Incinerator (F)	= 1,283

T_r	Temperature entering incinerator w/o heat exchange (F)	= 77
D_f	Energy Density of natural gas (Btu/scf)	= 0.0408
h_f	Fuel heating value (Btu/lb)	= 21,600
h_e	VOC heating value (Btu/lb)	= 0
Q_{fg}	Fuel Gas Flow (cfm)	= 897 (Calculated)

Step 6: Calculate electrical requirements to push air through system

Equations here are used in terms of acfm. Therefore the first step is to transform the scfm of the flow of contaminant gas into acfm.

$$Q_{com,a} = Q_{com}\left[\frac{T_{co} + 460}{537}\right]$$

Q_{com}	Flow rate of emission stream (scfm) ($Q_{fg} + Q_e$)	= 897 + 60,000 = 60,897
T_c	Combustion Temperature (F)	= 1,800
$Q_{com,a}$	Flow rate of emission stream (acfm)	= 256,289 (calculated)

$$Fp = 1.81\ x\ 10^{-4}\ x\ Q_{com,a}\ x\ \Delta P\ x\ HRS$$

$Q_{com,a}$	Flow rate of emission stream (acfm)	= 256,289
ΔP	Pressure Drop (inches of water)	= 15 (from table in EPA manual)
HRS	Annual hours operating (240x16 = 3,840)	= 3,840
F_p	Annual Power Requirement (kW)	= 2,671,970(calculated)

Regenerative Type

RTO Calculations: These calculations are based upon those completed in EPA's Handbook of Air Pollution Control Technologies. The process of calculating operational and cost criteria is displayed below:

Steps 1 and 2 are identical to that found in the calculation for the Recuperative type RTO

Step 3: Establish Temperature of Operation

The residence time and combustion temperature denote the percentage destruction. For VOC compounds, typically a temperature of 1,600 F with a residence time of 0.75 seconds will provide an overall destruction rate of 98%.

Step 4: Calculate waste gas temperature at the end of the pre-heater

This balances the costs between needing a large heat exchanger vs. using more natural gas. The larger (or better) the heat exchanger, the less natural gas is required.

$$F_{ER} = \frac{T_{wo} - T_{wi}}{T_{fi} - T_{wi}}$$

Where:

T_{wo}	= Temperature of waste gas out	Solving for this gives: 1,714 F
T_{wi}	= Temperature of waste gas in	= 77 F
T_{Fi}	= Temperature of exhaust gas in	= 1,800 F
F_{ER}	= Fractional Heat Recovery	= 95%

By setting the fractional heat recovery to a desired level, one can re-arrange the equation and solve for T_{wo}. Here the fractional heat recovery was set at 95%.

Step 5: Calculated Auxiliary Fuel Requirements

$$Q_{fg} = \frac{D_e \; x \; Q_e \; x \; [C_{p_{air}}(1.1 \; x \; T_c - \; T_{he} - 0.1T_r)]}{D_f \; x \; [h_f - (1.1 \; x \; C_{p_{air}}(\; T_c - T_r)]}$$

Where:

D_e	Energy Density of VOC (Btu/scf)	= 0.0739
Q_e	Max emission flowrate (cfm)	= 60,000
$C_{p(air)}$	Heat capacity of air (Btu/lbF)	= 0.253
T_c	Combustion Temperature (F)	= 1,800
T_{he}	Temperature Entering Incinerator (F)	= 1,714
T_r	Temperature entering incinerator w/o heat exchange (F)	= 77
D_f	Energy Density of natural gas (Btu/scf)	= 0.0408
h_f	Fuel heating value (Btu/lb)	= 21,600
h_e	VOC heating value (Btu/scf)	= 0.0314

Q_{fg}	Fuel Gas Flow (cfm)	= 337 (Calculated)

Step 6: Calculate electrical requirements to push air through system

Equations here are used in terms of acfm. Therefore the first step is to transform the scfm of the flow of contaminant gas into acfm.

$$Q_{com,a} = Q_{com}\left[\frac{T_{co} + 460}{537}\right]$$

Q_{com}	Flow rate of emission stream (scfm) ($Q_{fg} + Q_e$)	=337 + 60,000 = 60,337
T_{co}	Temperature of catalyst bed (F)	=1,714
$Q_{com,a}$	Flow rate of emission stream (acfm)	= 253,930 (calculated)

$$Fp = 1.81\ x\ 10^{-4}\ x\ Q_{com,a}\ x\ \Delta P\ x\ HRS$$

$Q_{com,a}$	Flow rate of emission stream (acfm)	= 253,930
ΔP	Pressure Drop (inches of water)	= 15 (from table in EPA manual)
HRS	Annual hours operating (240x16 = 3,840)	= 3,840
F_p	Annual Power Requirement (kW)	= 2,647,372 (calculated)

Recuperative Catalytic Type

RTO Calculations: These calculations are based upon those completed in EPA's Handbook of Air Pollution Control Technologies. The process of calculating operational and cost criteria is displayed below:

Steps 1 and 2 are identical to that found in the calculation for the Recuperative type RTO

Step 3: Establish Temperature of Operation

For a system to obtain 98 – 99% destruction efficiency, Catalyst bed temperature at the inlet should be around 600 F and the catalyst bed at the outlet should be between 1,000 and 1,200 F. The minimum temperature ensures an adequate initial reaction rate, while the 1,000 F outlet

temperature ensures an overall adequate reaction rate. It should be noted that a lower temperature may be feasible in some situations.

Step 4: Calculate waste gas temperature at the end of the pre-heater

The temperature of the temperature out of the catalyst bed must be determined to see if it falls in the 1,000 F to 1,200 F range. If note, adjustments must be made to the initial temperature.

$$T_{CO} = T_{Ci} + 50\, h_e$$

Where:

T_{CI} = Temperature of catalyst bed at inlet = 600 F (first guess)

h_e = VOC Fuel Value (Btu/lb) = 0.0314 Btu/scf

T_{CO} = Temperature of catalyst bed at outlet = 601

The temperature of the catalyst bed at the outlet is not in the range of 1,000 F to 1,200 F, and therefore, the temperature of at the inlet of the catalyst bed must be adjusted.

$$T_{Ci} = 1000 - 50\, h_e$$

Where:

T_{Ci} = Temperature of catalyst bed at outlet = 998 F (Calculated)

h_e = VOC Fuel Value (Btu/lb) = 0.0314 Btu/scf

Step 5: Calculated Auxiliary Fuel Requirements

$$Q_{fg} = \frac{D_e\, x\, Q_e\, x\, [C_{p_{air}}(1.1\, x\, T_c - T_{he} - 0.1T_r) - h_e]}{D_f\, x\, [h_f - (1.1\, x\, C_{p_{air}}(T_c - T_r)]}$$

Where:

D_e	Energy Density of VOC (Btu/scf)	= 0.0739
Q_e	Max emission flowrate (cfm)	= 60,000
$C_{p(air)}$	Heat capacity of air (Btu/lbF)	= 0.253
T_c	Combustion Temperature (F)	= 998
T_{he}	Temperature Entering Incinerator (F)	= 952
T_r	Temperature entering incinerator w/o heat exchange (F)	= 77
D_f	Energy Density of natural gas (Btu/scf)	= 0.0408

h_f	Fuel heating value (Btu/lb)	= 21,600
Q_{fg}	Fuel Gas Flow (cfm)	= 178 (Calculated)

Step 6: Calculate electrical requirements to push air through system

Equations here are used in terms of acfm. Therefore the first step is to transform the scfm of the flow of contaminant gas into acfm.

$$Q_{com,a} = Q_{com}\left[\frac{T_{co} + 460}{537}\right]$$

Q_{com}	Flow rate of emission stream (scfm) ($Q_{fg} + Q_e$)	=178 + 60,000 = 60,178
T_{co}	Temperature of catalyst bed (F)	=1000
$Q_{com,a}$	Flow rate of emission stream (acfm)	= 163,387 (calculated)

$$Fp = 1.81\ x\ 10^{-4}\ x\ Q_{com,a}\ x\ \Delta P\ x\ HRS$$

$Q_{com,a}$	Flow rate of emission stream (acfm)	= 163,387
ΔP	Pressure Drop (inches of water)	= 21 (from table in EPA manual)
HRS	Annual hours operating (240x16 = 3,840)	= 3,840
F_p	Annual Power Requirement (kW)	= 2,384,782 (calculated)

Appendix B: Adsorption System Criteria

The pure component isotherms shown in section 3.2.1 are all based upon the Langmuir parameters obtained from literature. The formulae used to develop the isotherms are below:

$$q = \frac{ap}{1 + bp}$$

Where:

q Mass loading of adsorbent (mol/g)

a Empirical Langmuir parameter

b Empirical Langmuir parameter

p Partial pressure of pure component

To convert to mass ratios:

$$\frac{p}{P_{tot} - p} = \frac{M_2}{M_1} Y$$

Where:

p Partial pressure of pure component

P_{tot} Total pressure

M_1 Molecular weight of solute gas (g/mol)

M_2 Molecular weight of carrier gas (g/mol)

Y Mass loading of contaminant in the carrier gas (kg/kg)

Using the second expression, and rearranging for p, and substituting into the first expression, the mass loading of the adsorbent can be made into a kg/kg basis.

$$q = \frac{P_{tot} M_2 a Y}{1 + \left(\frac{M_2}{M_1} + b P_{tot} \frac{M_2}{M_1}\right) Y}$$

Where:

q Mass loading of contaminant on the adsorbent (kg/kg)

p Partial pressure of pure component

P_{tot} Total pressure

M_1 Molecular weight of solute (g/mol)

M_2 Molecular weight of carrier gas (g/mol)

Y Mass loading of contaminant in the carrier gas (kg/kg)

This last expression is used to obtain the isotherms in terms of mass loading q (kg/kg) vs. Y (kg/kg).

Lifecycle Cost Analysis of the Adsorption System

The lifecycle cost of the system depends on direct and indirect installation costs, as well as direct and indirect operational costs. The costs tabulated for the adsorption system in the main body of this work include cost factors to estimate most of the indirect and direct costs. These cost factors are dependent upon the actual size and operational criteria of the system.

The only costs that are not transparent are the ones associated with the vessel, the carbon, and power requirements. These will be presented here.

To determine vessel costs, an empirical equation is presented in EPA's Handbook for Control Technologies of Hazardous Air Pollutants that relies on the estimated surface area of the vessel. The equation below determines provides a relationship to estimate the surface area of the vessel based upon measurements of the vessel already established in the main body of the thesis.

$$S = \pi D_v (L_v + \frac{D_v}{2})$$

Where:

D_v	Diameter of the vessel (m)	= 6
L_v	Length (or thickness) of vessel (m)	= 1
S	Surface Area (m^2)	= 75.49 (calculated)

The cost of each vessel can then be computed using the following empirical relationship

$$C_v = 271\, S^{0.778}$$

Where:

S	Surface Area (ft^2) (must S into ft^2)	= 75.49 m^2 x 10.7639 ft^2/m^2 = 812.57 ft^2

C_v	Cost of the vessel (USD)	= $49,759

The next step is to calculate the cost of carbon required. This is again a very simple empirical relationship. The EPA suggests a value of $2.00/lb of carbon, whereas more recent data indicates that carbon costs can range between $1.05 to $1.15 /lb of carbon. Historically, the price between 1997 and 2002 was seen to decline by 0.9%, whereas after that period, it was anticipated to rise by 3%. For this reason, the standard cost of $2.00/lb was used for this calculation.

The total capital cost of the system then becomes a combination of costs between the vessel, carbon, and any auxiliary system costs. These auxiliary system costs can be estimated using a cost factor based upon the flow rate of material running through the adsorber. This is presented below:

$$R_c = 5.82 Q_a{}^{-0.133}$$

Where:

Q_a	Contaminant flow rate (acfm)	= 60,000 acfm
R_c	Auxiliary equipment factor	= 1.347

Now the auxiliary cost factor can be utilized to determine overall equipment costs (meaning carbon vessel, carbon, ductwork, fans, pumps, condensers, internal piping, etc...)

$$EC = R_c[C_c + C_v(N_A + N_D)]$$

Where:

EC	Equipment Cost (USD)	= $164,702
R_c	Auxiliary equipment factor	= 1.347
C_c	Carbon Cost ($2.00 per pound) (USD)	= 5,167 kg x 2.2 lbs/kg x 2 vessels = $22,737
C_v	Vessel Cost (USD)	= $49,759
N_A	Number of adsorbing vessels	= 1
N_D	Number of desorbing vessels	= 1

Steam Costs were based upon the knowledge that 2 kg of steam were required for every kg of solvent liberated from the adsorption bed. Therefore, on a daily basis 834 kg of steam were required. This translates into 200,160 kg of steam annually.

The energy requirement to produce 1 lb of steam was found to be 1,028 Btu (Ref). The cost required for 1 MBtu is $9.64 USD. The total cost of steam therefore is simple multiplication.

$$C_s = M_s \, x \frac{E_s}{(1 \, x \, 10^6)} \, C_{SE}$$

Where:

M_s	Annual steam requirement (kg)	= 200,160 kg = 440,352 lbs
C_{SE}	Energy cost (USD)	= $9.64 / MBtu
E_S	Energy Requirement (USD)	= 1,028 Btu/lbs of steam
C_S	Annual Cost of Steam (USD)	= $4,365

To determine the electrical power required for the system, the pressure drop must be determined in order to calculate the required horsepower to push air through the bed.

The Ergun equation was used to determine the pressure drop through the bed.

$$R_e = \frac{D_p V_s \rho}{(1-\varepsilon)\mu} \qquad f_p = \frac{150}{R_e} + 1.75$$

Where:

D_p	Particle diameter (m)	= 0.001
V_s	Superficial velocity (m/s)	= 1
ρ	Carrier density - air (kg/m^3)	= 1.2
ϵ	Bed Porosity	= 0.44
μ	Kinematic Viscosity (m^2/s)	= 1.26x10^{-5}
fp	Friction factor	= 1.96
R_e	Reynold's number	= 707 (Calculated)

$$\Delta p = \frac{f_p L \rho {V_s}^2}{D_p} \left(\frac{1-\varepsilon}{\varepsilon^3} \right)$$

Where:

L	Bed thickness or Length (m)	= 1
D_p	Particle diameter (m)	= 0.001
V_s	Superficial velocity (m/s)	= 1
ρ	Carrier density - air (kg/m^3)	= 1.2
ϵ	Bed Porosity	= 0.44
fp	Friction factor	= 1.96
Δp	Pressure drop (Pa)	= 71.6 (Calculated)

With the pressure drop determined, the system fan horsepower can be determined:

$$hp_{sys} = 2.5\ x\ 10^{-4}(Q_a)(\Delta p + 1)$$

Where:

Δp	Pressure drop (inches of water)	= 2.06
Q_a	Particle diameter (acfm)	= 60,000
hp_{sys}	Horsepower (hp)	= 53

The system fan cost can then be calculated by knowing the kW price, and the hours in operation

$$C_E = 0.746\ x\ hp_{sys}\ x\ HRS$$

Where:

hp_{sys}	Horsepower (hp)	= 53
HRS	Annual hours operating (240 days x 16 hours/day)	= 3,840
C_E	Electrical Cost (USD)	= $12,233

The bed cooling and drying fan horsepower can be determined in a similar way, however the overall operational time is different, as well as the flow rate. The operational time is equivalent to the number of hours the cooling and drying fan would operate (1 hour per cycle, which is 2 hours per day, which is a total of 480 hours). The flow rate is different, because it is expected that about 100 ft3 air / lbs carbon is required to cool and dry the bed:

$$FR_{dcf} = 100(M_e)/\theta_{dry-cool}$$

Where:

M_e	Mass of adsorbent per vessel (lbs)	= 11,367
$\Theta_{dry\text{-}cool}$	Dry-cool cycle time (hr)	= 1
FR_{sys}	Flowrate of drying-cooling air (ft^3/hr)	= 1,136,894

The total annual cost of drying-cooling fan can now be calculated:

$$C_{dcf} = [1.86\ x\ 10^{-4}\ x\ FR_{dcf}\ x\ (\Delta P + 1)\theta_{dcf}]E_{rate}$$

Where:

FR_{sys}	Flowrate of drying-cooling air (ft^3/hr)	= 1,136,894
Δp	Pressure drop (inches of water)	= 2.06
Θ_{dcf}	Annual operational time (hr)	= 480
E_{rate}	Electrical rate (USD/kWh)	= 0.08
C_{dcf}	Cost of the dry-cool fan (USD)	= $28,619

Appendix C: Biofilter Cost Model

The main parameter in developing a Biofilter model is realizing the importance of residence time. For most applications, residence time within the biofilter is of paramount importance, thus most systems are sized according to appropriate residence times. The biofilter system modeled here is simple outdoor bed. Meaning the site is excavated and lined, with the appropriate media is placed within it.

This system will be based upon a 50 second residence time. Typical times range between 25 seconds to 60 seconds depending on VOC concentrations.

$$V = Q\ x\ EBRT$$

Where:

EBRT	Empty Bed Residence Time (hours)	= 50 x 1 hour /3600 seconds = 0.0139
Q	Flow rate of contaminant (m^3/hour)	= 101,940
V	Volume of media required (m^3)	= 1416 (Calculated)

Using a 20% safety factor will increase the Volume of media required to 1699 m^3. In most cases, bed depths must remain between 1 m to 1.5 m or less to ensure that the media does not undergo significant bed compaction, or that the pressure drop is not too significant. With these restrictions, the bed depth dimensions can be calculated, assuming our bed will be square in shape.

$$L\ (or\ width) = (V/D)^{\frac{1}{2}}$$

Where:

V	Volume of media required (m^3)	= 1699
D	Bed depth (m)	= 1.06 m
L	Volume of media required (m^3)	= 40

The system will also include a section of gravel, about 1/3 the depth of the overall media. This means, an extra 0.3 m of gravel would be required for this system, which equates to a volume of gravel to be 480 m^3. Therefore, the total volume required would be 2,179 m^3. Site preparation costs will be based upon this volume. Site excavation costs are estimated to be \$7.1/m^3. Total cost for site preparation are = \$15,470.

All other capital costs are transparent on the original table presented in the main body of the document.

Operating Costs

As with any system, operational costs will depend upon the resources and labour required to keep the system operating. Electricity and costs will be based upon how much power is required to force air through the bed, while water costs will be based upon the volume required to maintain bed moisture. Labour costs are transparent in the main body of this document and will not be presented here.

In this case, empirical parameters were taken to determine pressure drop through the system. Philips et al developed a pressure drop equation for varying media materials. For our cases, we used the parameters for a material consisting of 40% heather and 60% peat.

$$\Delta P = au^b$$

Where:

a	Empirical parameter	= 5940
U	Superficial velocity (m/s)	= 1.06
b	Empirical parameter	= 1.35
ΔP	Pressure drop (Pa/m)	= 7,597 (Calculated)

With the pressure drop determined, the system fan horsepower can be determined:

$$hp_{sys} = 2.5\ x\ 10^{-4}(Q_a)(\Delta p + 1)$$

Where:

Δp	Pressure drop (inches of water)	= 22.4
Q_a	Particle diameter (acfm)	= 60,000
hp_{sys}	Horsepower (hp)	= 351 (Calculated)

The system fan cost can then be calculated by knowing the kW price, and the hours in operation

$$C_E = 0.746\ x\ hp_{sys}\ x\ HRS$$

Where:

hp_{sys}	Horsepower (hp)	= 336
HRS	Annual hours operating (240 days x 16 hours/day)	= 3,840
C_E	Electrical Cost (USD)	= $81,734

Appendix D: NIST Cost Factor Lifecycle Analysis

Note: To ensure the method outlined here is clear, the example of the Recuperative type RTO will be used.

Dollars generally lose value over time. For this reason, the cost of operating a piece of machinery, or even purchasing machinery (using a fixed payment schedule) over time will change (most likely getting smaller).

To obtain the future compounded amount for operational and capital investitures, it is then important to develop relationships to yield this amount.

$$P_t = P_0(1 + i)^t$$

Where:

P_0	Present value (USD)	$273,991 (w/o taxes instrumentation or freight)
i	Interest rate	4.75
t	Time period in years	10
P_t	Future value after time period t	$435,789 (Calculated)

The above example illustrates a simple way in which to determine the cost of a piece of equipment if amortized over a 10 year period.

To obtain the future value of energy costs (natural gas, electricity, and water), there is normally one method. It is termed the FEMP UPV* factor, which is used to calculate the annually reoccurring energy costs over n years at a non-constant escalation rate based on the US Department of Energy predictions.

FEMP UPV* factors are calculated for the current discount rate 3% and have been published in The Annual Supplement to Handbook 135. The most recent one found for this application was from 2006. Note, the values used were from Table Ba-1, and represent values for the most geographically closest area to Toronto. The time period considered here is 10 years.

$$PV = A_0 \; x \; UPV^*$$

Where:

PV_{elec}	Present Value of Electricity (USD)	= $1,816,933
UPV^*_{gas}	DOE Gas Factor	= 6.65

UPV^*_{elec}	DOE Electricity Factor	= 6.8
$A_{0(gas)}$	Initial Annual Value of Gas (USD)	= $1,755,772
$A_{0(elec)}$	Initial Annual Value of Electricity (USD)	= $267,196
PV_{gas}	Present Value of gas (USD)	=$11,675,884 (Calculated)

Appendix E: Factorial Analysis (Reformer Example)

To analyze the effect of various factors affecting the Reformer and SOFC models, a full 2^5 factorial analysis was performed. This involved developing an experimental design to test the effect to all factors on the output variables. Here, the Reforming Subsystem model was used as an example.

The five factors chosen were as follows:

Variables	Low level	High Level
VOC temp = Factor a	400 K	800 K
Air temp = Factor b	400 K	800 K
Molar Air flow = Factor c (kgmole/hr)	0.25	0.75
Molar Steam flow = Factor d (kgmole/hr)	0.422	0.845
Fuel Recycle Ratio = Factor e	0.25	0.5

The four output variables for this system were: Molar flow of CO, Molar flow of H_2, and the molar flow of H_2O. The treatment combinations and results were as follows:

Run	A	B	C	D	E	Combination		VOC Temp	Air Temp	Air Flow	Steam Flow	Fuel Recycle	CO	H2	CO2	H2O
1	1	1	1	1	1	1		400	400	0.25	0.422	0.25	0.0118	0.3955	0.1964	0.2196
2	1	1	1	1	e	e		400	400	0.25	0.422	0.5	0.0415	0.4155	0.2669	0.1559
3	1	1	1	d	1	d		400	400	0.25	0.845	0.25	0.0048	0.3691	0.1840	0.3161
4	1	1	1	d	e	de		400	400	0.25	0.845	0.5	0.0252	0.4116	0.2676	0.2155
5	1	1	c	1	1	c		400	400	0.75	0.422	0.25	0.0934	0.3958	0.1813	0.0728
6	1	1	c	1	e	ce		400	400	0.75	0.422	0.5	0.0952	0.3103	0.2078	0.1541
7	1	1	c	d	1	cd		400	400	0.75	0.845	0.25	0.0484	0.4147	0.2060	0.1272
8	1	1	c	d	e	cde		400	400	0.75	0.845	0.5	0.0621	0.2860	0.1987	0.2540
9	1	b	1	1	1	b		400	800	0.25	0.422	0.25	0.0161	0.4118	0.2015	0.1992
10	1	b	1	1	e	be		400	800	0.25	0.422	0.5	0.0469	0.4199	0.2678	0.1488
11	1	b	1	d	1	bd		400	800	0.25	0.845	0.25	0.0063	0.3854	0.1906	0.2953
12	1	b	1	d	e	bde		400	800	0.25	0.845	0.5	0.0283	0.4146	0.2686	0.2102
13	1	b	c	1	1	bc		400	800	0.75	0.422	0.25	0.1165	0.4024	0.1711	0.0643
14	1	b	c	1	e	bce		400	800	0.75	0.422	0.5	0.1064	0.3002	0.1972	0.1638
15	1	b	c	d	1	bcd		400	800	0.75	0.845	0.25	0.0638	0.4130	0.1968	0.1269
16	1	b	c	d	e	bcde		400	800	0.75	0.845	0.5	0.0698	0.2781	0.1907	0.2619
17	a	1	1	1	1	a		800	400	0.25	0.422	0.25	0.0360	0.4508	0.2083	0.1486
18	a	1	1	1	e	ae		800	400	0.25	0.422	0.5	0.0652	0.4301	0.2677	0.1305
19	a	1	1	d	1	ad		800	400	0.25	0.845	0.25	0.0138	0.4299	0.2072	0.2373
20	a	1	1	d	e	ade		800	400	0.25	0.845	0.5	0.0392	0.4096	0.2604	0.2142
21	a	1	c	1	1	ac		800	400	0.75	0.422	0.25	0.1258	0.4044	0.1667	0.0615
22	a	1	c	1	e	ace		800	400	0.75	0.422	0.5	0.1107	0.2957	0.1929	0.1683
23	a	1	c	d	1	acd		800	400	0.75	0.845	0.25	0.0701	0.4069	0.1905	0.1331
24	a	1	c	d	e	acde		800	400	0.75	0.845	0.5	0.0729	0.2750	0.1876	0.2650
25	a	b	1	1	1	ab		800	800	0.25	0.422	0.25	0.0439	0.4593	0.2082	0.1367
26	a	b	1	1	e	abe		800	800	0.25	0.422	0.5	0.0711	0.4323	0.2671	0.1261
27	a	b	1	d	1	abd		800	800	0.25	0.845	0.25	0.0170	0.4412	0.2106	0.2223
28	a	b	1	d	e	abde		800	800	0.25	0.845	0.5	0.0431	0.4055	0.2575	0.2172
29	a	b	c	1	1	abc		800	800	0.75	0.422	0.25	0.1477	0.4059	0.1549	0.0583
30	a	b	c	1	e	abce		800	800	0.75	0.422	0.5	0.1204	0.2850	0.1828	0.1793
31	a	b	c	d	1	abcd		800	800	0.75	0.845	0.25	0.0850	0.3919	0.1754	0.1482
32	a	b	c	d	e	abcde		800	800	0.75	0.845	0.5	0.0804	0.2676	0.1801	0.2724

The effects of each treatment were then determined, and plotted against the residuals in a Normal Probability Plot to determine significant effects.

APPENDIX F: SOFC CALCULATIONS

The SOFC Subsystem Model developed in HYSYS is seen below.

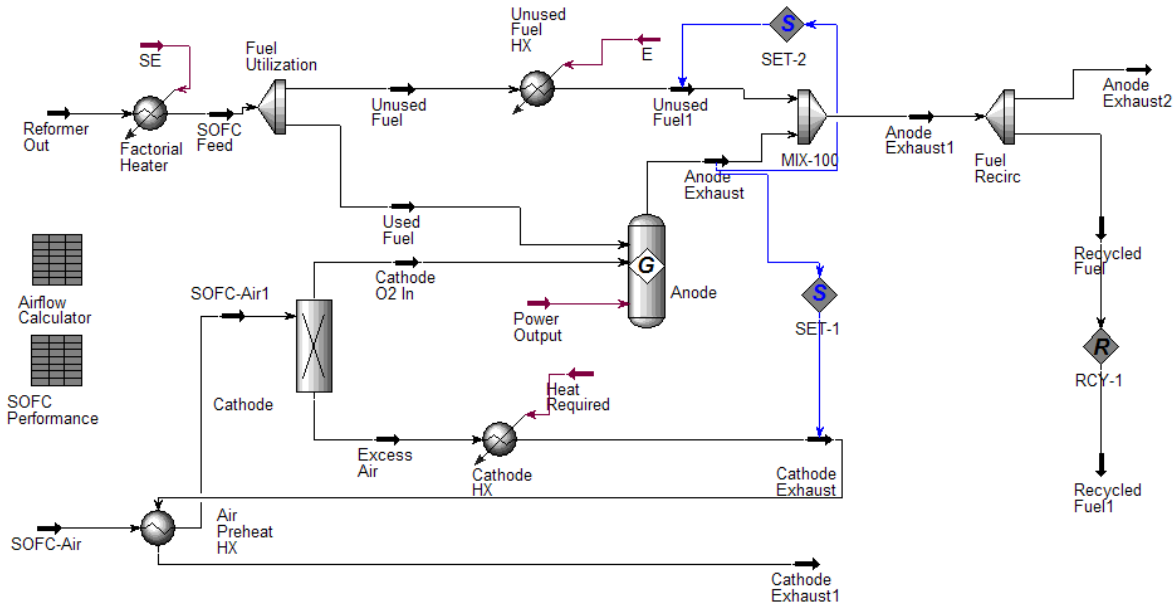

The details of this flowsheet are explained in Section 4.2.5, and so here, the focus will be on the calculations used to determine DC power created from the SOFC.

As explained in Section 2.4.4, the fuel cell voltage can be calculated either by knowing the gas compositions at the anode or cathode, or by using the fuel utilization factor and excess air. To calculate the voltage from the fuel utilization and excess air factors, Equation 26 is used

$$E_{ideal} = E^0 + \frac{RT}{nF} \ln \left[\frac{U_{fH_2}\left(\frac{\lambda}{0.21} - U_{fH_2}\right)^{\frac{1}{2}}}{\left(1 - U_{fH_2}\right)\left[\left(\lambda - U_{fH_2}\right)P_T\right]^{\frac{1}{2}}} \right] \qquad \textbf{Equation 26}$$

In this particular case, the fuel utilization factor and excess factors were set according the results of the optimization of the model. For the optimized model these factors were set at $U_f = 0.8$, and $\lambda = 1.8$. Using these factors, the ideal potential equated to -0.7718 V.

-0.7718 reflects the ideal potential, and thus does not include loss as a result of concentration, activation or ohmic polarization effects. To account for these effects, the relationships outlined in Section 2.4.4 will be used. Equation 16 refers to the Tafel equation, and describes the effects of the activation polarization.

$$\eta_{Act} = \frac{RT}{\alpha nF} \ln\left(\frac{i}{i_0}\right) \quad \textbf{Equation 16}$$

To determine the effect that kinetic polarization exerts on this system, Equation 17 (Explained in Section 2.4.4) will be used

$$\eta_{Conc} = \frac{RT}{nF} \ln\left(1 - \frac{i}{i_L}\right) \quad \textbf{Equation 17}$$

Lastly, to determine the effect that resistance within the cell will exert on the actual voltage, Equation 18 must be used.

$$\eta_{Ohm} = iR \quad \textbf{Equation 18}$$

In Equations 16 through 18, cell parameters such as the exchange current density (i_0), the limiting current density (i_L) and the charge transfer co-efficient (α) are established from literature.

$$E_{actual} = E_{ideal} - (\eta_{Act} + \eta_{Conc} + \eta_{Ohm}) \quad \textbf{Equation 19}$$

REFERENCES

(1) Vatavuk, W. M.; Klotz, W. L.; Stallings, R. L.; van der Vaart, Donald R.; Spivey, J. J. In *Handbook of Control Technologies for Hazardous Air Pollutants*; US EPA, Office of Research and Development **2002**, 195-388.

(2) Chen, E. In *Thermodynamics and Electrochemical Kinetics;* Hoogers, G., Ed.; Fuel Cell Technology Handbook; CRC Press Boca Raton: 2003;

(3) Harrison, R. M.; Hester, R. E. In *Volatile organic compounds in the atmosphere;* Issues in environmental science and technology, 1350-7583; Royal Society of Chemistry: Cambridge, U.K., 1995;

(4) Farley, J. M. *Annu. Rev. Pharmacol. Toxicol.* **1992**, *32*, 67-88.

(5) Cape, J. N. *Environmental Pollution* **2008**, *155*, 391-397.

(6) AnonymousEnvironment Canada, Volatile Organic Compounds in Consumer and Commercial Products Home Page. www.ec.gc.ca/nopp/voc/EN/bkg.cfm (accessed Februrary 20th, 2009). .

(7) AnonymousNational Emission Standards for Hazardous Air Pollutants (NESHAP) Home Page. http://www.epa.gov/ttn/atw/mactfnlalph.html (accessed February 20th, 2009).

(8) AnonymousUS Environmental Protection Agency. New Source Review Home Page. http://www.epa.gov/nsr/ (Accessed February 20th, 2009). .

(9) AnonymousSouth Coast Air Quality Management District Home Page. http://www.aqmd.gov/rules/index.html (Accessed February 20th, 2009).

(10) AnonymousBay Area Air Quality Management District Home Page. http://www.baaqmd.gov/dst/regulations/index.htm (Accessed February 20th, 2009). .

(11) AnonymousIllinois Pollution Control Board Home Page. www.ipcb.state.il.us/SLR/IPCBandIEPAEnvironmentalRegulations-Title35.asp (Accessed February 20th, 2009). .

(12) AnonymousDepartment of Air Quality Home Page. http://www.deq.state.mi.us/apcrats/toc_collapsible_2.shtml (Accessed February 20th, 2009). .

(13) AnonymousThe Pennylvania Code Chapter 129 Standards for Sources Home Page. http://www.pacode.com/secure/data/025/chapter129/chap129toc.html (Accessed Februrary 20th, 2009). .

(14) AnonymousMinnesota Pollution Control Agency Home Page. http://www.pca.state.mn.us/air/air_mnrules.html (Accessed Februrary 20th, 2009).

(15) AnonymousNew York State Department of Environmental Conservation Home Page. http://www.dec.ny.gov/regs/4214.html (Accessed February 20th, 2009). .

(16) AnonymousOhio State EPA Home Page. http://www.epa.state.oh.us/dapc/regs/3745-21/21_09.pdf (Accessed February 20th, 2009). .

(17) AnonymousThe Wisconsin Department of Natural Resources. Current Air Pollution Control Rules. http://dnr.wi.gov/air/rules/NR400toc.htm (Accessed Februrary 20th, 2009). .

(18) Doble, M.; Kumar, A. In *Biotreatment of Industrial Effluents;* Butterworth-Heinemann: 2005; , pp 1-337.

(19) Baukal, C. E. In *Industrial combustion pollution and control;* Environmental science and pollution control series ; 27; Marcel Dekker: New York, 2004; , pp 904.

(20) Moretti, E. C. *Chem. Eng. Prog.* **2002***, 98*, 30-40.

(21) Lewandowski, D. A. In *Design of thermal oxidation systems for volatile organic compounds;* Lewis Publishers: Boca Raton, Fla. ; London, 2000; , pp 348 p.

(22) Gibson, D., A. **1999***, 106*, 45.

(23) Delhoménie, M.; Heitz, M. *Critical Reviews in Biotechnology* **2005***, 25*, 53.

(24) Devinny, J. S.; Deshusses, M. A.; Webster, T. S. In *Biofiltration for air pollution control;* Lewis Publishers: Boca Raton, Fla., 1999; , pp 299 p.

(25) Malhautier, L.; Khammar, N.; Bayle, S.; Fanlo, J. *Appl. Microbiol. Biotechnol.* **2005***, 68*, 16-22.

(26) Tien, C. In *Adsorption calculations and modeling;* Butterworth-Heinemann series in chemical engineering; Butterworth-Heinemann: Boston, 1994;

(27) Ruthven, D. M. (. M. In *Adsorption Fundamentals;* Kirk-Othmer Encyclopedia of Chemical Technology; John Wiley and Sons Inc.: 2001; Vol. 1, pp 582-617.

(28) Department of the Army, U.S. Army Corps. Engineers **2001**.

(29) Knaebel, K., S. 'Adsorbent Selection', internal company report, Adsorption Research Inc., Dublin, Ohio, 43016 **(2000)**
http://www.adsorption.com/publications/AdsorberDes1.pdf (Accessed August 8th 2009)

(30) Ruthven, D. M. (. M. In *Principles of adsorption and adsorption processes;* Wiley: New York, 1984;

(31) Yang, R. T. In *Gas separation by adsorption processes;* Series on chemical engineering ; v; Imperial College Press: London, 1997; , pp x, 352 p.

(32) Cooper, C. D. In *Air pollution control : a design approach;* Waveland Press: Prospect Heights, Ill., 2002; , pp 738.

(33) Khan, F. I.; Ghoshal, A. K. *J. of Loss Prevention in the Process Industries* **2000**, *13*, 527-545.

(34) Kohl, A. L.; Nielsen, R. In *Gas Purification;* Elsevier Gulf: 1997; , pp 1-900.

(35) Yamamoto, O. *Electrochimica Acta* **2000**, *45*, 2423-2435.

(36) Song, X. P.; Guo, Z. C. *Energy Conv. Manag.* **2006**, *47*, 560-569.

(37) Energy Technology Training Center, College of the Desert **2001**, *0*, 4-1-4-54.

(38) Song, C. *Catalysis Today , 77*, 17-49.

(39) Ormerod, R. M. *Chem. Soc. Rev. , 32*, 17-28.

(40) McIntosh, S.; Gorte, R., J. *Chem. Rev.* **2004**, *104*, 4845-4866.

(41) EG&G Technical Services Inc. and Science Application International Corporation. In *Fuel Cell Handbook;* US Department of Energy, Ed.; 2002; , pp 451.

(42) Van Ness, H. C. (. C.). In *Understanding thermodynamics [by] H. C. Van Ness.* McGraw-Hill [1969]: New York, 19uu; .

(43) Winkler, W.; Nehter, P. In *Thermodynamics of Fuel Cells;* Bove, R., Ubertini, S., Eds.; Modeling Solid Oxide Fuel Cells, Methods, Procedures and Techniques; Springer Science + Business Media: 2008; Vol. 1, pp 13-50.

(44) Kee, R. J.; Zhu, H.; Sukeshini, A. M.; Jackson, G. S. *Combustion Sci. Technol.* **2008**, *180*, 1207-1244.

(45) The Solid Oxide Fuel Cell Diagram Home Page. http://science.nasa.gov/headlines/y2003/images/fuelcell/sofc-brochure-new.gif (accessed April 12th, 2009). .

(46) Joensen, F.; Rostrup-Nielsen, J. R. In *In Conversion of hydrocarbons and alcohols for fuel cells;* Journal of Power Sources; ELSEVIER SCIENCE BV: AMSTERDAM; PO BOX 211, 1000 AE AMSTERDAM, NETHERLANDS, 2002; Vol. 105, pp 195-201.

(47) Balat, M. *Energy Sources, Part A: Recovery, Utilization, and Environmental Effects* **2009**, *31*, 39-50.

(48) Ahmed, S.; Krumpelt, M. *Int J Hydrogen Energy* **2001**, *26*, 291-301.

(49) Ming, Q. M.; Healey, T.; Allen, L.; Irving, P. In *In Steam reforming of hydrocarbon fuels;* Catalysis Today; ELSEVIER SCIENCE BV: AMSTERDAM; PO BOX 211, 1000 AE AMSTERDAM, NETHERLANDS, 2002; Vol. 77, pp 51-64.

(50) Cheekatamarla, P. K.; Finnerty, C. M. *Int J Hydrogen Energy* **2008**, *33*, 5012-5019.

(51) AnonymousInvestment Ontario Home Page. http://www.2ontario.com/facts/fact10.asp. (Accessed November 17th, 2008).

(52) Vatavuk, W. M. *Chemical Engineering* **2006**, *113*, 68-68.

(53) Fuller, S. K.; Petersen, S. R. *NIST Handbook 135: Life-Cycle Costing Manual for the Federal Energy Management Program*; US Department of Energy, Gaithersburg, MD; **1996;** 1-210;

(54) Campanari, S. *J. Power Sources* **2001**, *92*, 26-34.

(55) Yun, J. H.; Choi, D. K.; Kim, S. H. *AICHE J.* **1999**, *45*, 751-760.

(56) Takeuchi, Y.; Shigeta, A. *J. Chem. Eng. Japan* **1991**, *24*, 411-417.

(57) Basmadjian, D. In *Little adsorption book : a practical guide for engineers and scientists;* CRC Press: Boca Raton, Fla., 1997;

(58) De Nevers, N. In *Air pollution control engineering;* McGraw-Hill chemical engineering serie; McGraw-Hill: New York, 1995;

(59) Knaebel, K., S. 'A "How To" Guide for Adsorber Design', internal company report, Adsorption Research Inc., Dublin, Ohio, 43016 **(2000)**
http://www.adsorption.com/publications/AdsorberDes2.pdf (Accessed August 8th 2009)

(60) Ng, C.; Smith, P.; Teh, A.; Brenner, S.; Gierer, C.; Strashok, C.; Jamil, A.; Nguyen, N.; Chau, A.; Sachedina, M.; Hugo, L.; Lowe, C.; Hanson, K. In *HYSYS 3.1 User Guide;* Hyprotech: Calgary, 2002; , pp 458.

(61) Campanari, S. In *In Full load and part-load performance prediction for integrated SOFC and microturbine systems;* Journal of Engineering for Gas Turbines and Power-Transactions of the Asme; ASME-AMER SOC MECHANICAL ENG: NEW YORK; THREE PARK AVE, NEW YORK, NY 10016-5990 USA, 2000; Vol. 122, pp 239-246.

(62) Kuchonthara, P.; Bhattacharya, S.; Tsutsumi, A. *J. Power Sources* **2003**, *124*, 65-75.

(63) Chan, S. H.; Ho, H. K.; Tian, Y. *Int J Hydrogen Energy* **2003***, 28*, 889-900.

(64) Riensche, E.; Achenbach, E.; Froning, D.; Haines, M. R.; Heidug, W. K.; Lokurlu, A.; von Andrian, S. In *In Clean combined-cycle SOFC power plant - cell modelling and process analysis;* Journal of Power Sources; ELSEVIER SCIENCE SA: LAUSANNE; PO BOX 564, 1001 LAUSANNE, SWITZERLAND, 2000; Vol. 86, pp 404-410.

(65) Staite, M.; Marcazzan, P.; Ghosh, D.; Stannard, J.; Chong-Ping, C. In *In Feasibility Analysis of Methanol Fuelled SOFC Systems for Remote Distributed Power Applications;* Singhal, S. C., Mizusaki J., Eds.; Solid Oxide Fuel Cells (IX); The Electrochemical Society Inc.: New Jersey, 2005 - 2007; Vol. 1, pp 216-228.

(66) Cheremisinoff, N. P. In *Handbook of Chemical Processing Equipment;* Elsevier Butterworth-Heinemann: 2000; , pp 1-535.

(67) Peters, M. S.; Timmerhaus, K. D. In *Plant design and economics for chemical engineers;* McGraw-Hill chemical engineering serie; McGraw-Hill: New York ; Montreal, 1991;

(68) Chen, Z. X.; Elnashaie, S. S. E. H. *Ind Eng Chem Res* **2005***, 44*, 4834-4840.

(69) Myers, D. B.; Ariff, G. D.; James, B. D.; Lettow, J. S.; Thomas, C. E.; Kuhn, R. C. **2002**.

(70) Cheekatamarla, P. K.; Finnerty, C. M. *J. Power Sources* **2006***, 160*, 490-499.

(71) Zogg, R.; Sriramulu, S.; Carlson, E. *ASHRAE J.* **2006***, 48*, 116-118.